Università degli Studi di Padova

Dipartimento di Scienze Biomediche

CORSO DI DOTTORATO DI RICERCA IN SCIENZE BIOMEDICHE
31° CICLO

Altered migration of forebrain inhibitory interneurons in a mouse model of intellectual disability

Coordinatore: Ch.mo Prof. Paolo Bernardi
Supervisore: Dott.ssa Claudia Lodovichi
Co-Supervisore: Ch.mo Prof. Carlo Reggiani

Dottorando : Andrea Maset

TABLE OF CONTENTS

SOMMARIO

OPHN1 è un gene sul cromosoma X associato alla disabilità intellettiva (ID) che codifica per una Rho-GTPase activating protein (RhoGAP), la quale regola il riarrangiamento conformazionale dei filamenti di actina coinvolti in numerosi processi di sviluppo quali la crescita assonale, la maturazione dendritica e la migrazione cellulare.

L'impatto della mutazione di OPHN1 sulla morfologia e funzione neuronale è stato studiato principalmente nei neuroni glutamatergici.

Gli interneuroni inibitori GABAergici esercitano un ruolo importante nel bilancio tra eccitazione e inibizione della rete neuronale. Infatti, le alterazioni nello sviluppo e nella funzionalità degli interneuroni GABAergici sono associate a numerosi disordini neurologici.

Se e come OPHN1 influisca sul circuito inibitorio rimane ancora ampiamente da comprendere.

Per rispondere a queste domande. ho studiato la neurogenesi adulta di neuroni inibitori del prosencefalo nella zona subventricolare (SVZ) in un modello murino di disabilità intellettiva, nello specifico, una linea di topi recanti una mutazione nulla per OPHN1.

Nella zona subventricolare (SVZ), lungo le pareti dei ventricolari laterali, la neurogenesi degli interneuroni dura tutta la vita. Dalla SVZ i precursori neuronali migrano lungo la via migratoria rostrale per raggiungere il bulbo olfattivo (OB) dove diventano pienamente interneuroni maturi.

Ricordiamo che, nei mammiferi, inclusi i bambini, gli interneuroni inibitori derivanti dalla SVZ migrano non solo verso il OB ma anche verso numerose aree subcorticali e corticali. Si pensa che questi interneuroni generati in età post-natale giochino un ruolo importante nello sviluppo postnatale e nella plasticità del cervello.

In un lavoro precedente abbiamo visto che la mutazione che porta alla perdita di funzione di OPHN1 non colpisce la generazione dei precursori neuronali nella zona

subventricolare. Tuttavia, il numero di cellule nate adulte che raggiungono il bulbo olfattivo è drammaticamente ridotto nei topi OPHN1$^{-/y}$. Questo risultato suggerisce che la mutazione di OPHN1 possa compromettere la migrazione neuronale.

Abbiamo indagato se e come la migrazione fosse alterata in topi OPHN1$^{-/y}$. Combinando esperimenti di birthdating (usando Brdu come marcatore delle nuove cellule) e di immunoistochimica quantitativa abbiamo studiato la distribuzione, la morfologia la direzionalità delle cellule generate in adulto lungo la via migratoria rostrale (RMS).

Abbiamo osservato che la distribuzione dei precursori neuronali lungo la via migratoria rostrale è ampiamente alterata in topi OPHN1$^{-/y}$, con la maggior parte delle nuove cellule generate bloccate nella porzione iniziale della RMS e solo poche cellule che raggiungono la porzione finale e il OB in topi OPHN1$^{-/y}$ rispetto ai controlli.

Per sviscerare il meccanismo sottostante l'alterata migrazione cellulare, abbiamo eseguito esperimenti di time-lapse imaging dei neuroblasti in migrazione su spesse sezioni sagittali del cervello mediante imaging al due fotoni. Abbiamo investigato la velocità e la direzionalità delle cellule migratorie in topi wt e OPHN1$^{-/y}$.

Abbiamo travato che la velocità della progressione neuronale è significativamente ridotta in topi OPHN1$^{-/y}$ rispetto ai controlli. Inoltre la percentuale di cellule che migrano verso l'OB (la direzionalità) è significativamente ridotta in topi OPHN1$^{-/y}$ rispetto ai controlli.

È noto che GABA modula la migrazione dei neuroblasti durante lo sviluppo.

Si pensa che il GABA, abbondantemente presente nella RMS, venga rilasciato dai neuroblasti e agisca in maniera autocrina e paracrina sui neuroblasti che esprimono i recettori $GABA_{A.}$

L'accumulo di GABA extracellulare è impedito dal sequestro di GABA grazie a cellule astrocyte-like, che circondano le catene dei precursori in migrazione.

Il GABA è il principale neurotrasmettitore inibitorio nel cervello adulto. La polarità della risposta al GABA (iperpolarizzazione contro depolarizzazione) non è univoca, ma è criticamente regolata dalla concentrazione intracellulare di cloro, che è a sua

volta modulate da specifici co-trasportatori, NKCC1 e KCC2. NKCC1, principalmente espresso in neuroni immaturi, favorisce un'alta concentrazione intracellulare di cloro portando alla depolarizzazione delle cellule in risposta GABA. KCC2, espresso abbondantemente nei neuroni maturi, favorisce una bassa concentrazione cloridrica intracellulare, di conseguenza, il GABA iperpolarizza i neuroni. Si pensa che la depolarizzazione dovuta a GABA giochi un ruolo importante in numerosi processi di sviluppo, inclusa la migrazione cellulare.

Per valutare come il GABA moduli la migrazione cellulare in topi OPHN1$^{-/y}$, abbiamo eseguito esperimenti di time-lapse imaging su precursori neuronali in condizioni basali e in presenza di GABA in topi di controllo e topi OPHN1$^{-/y}$.

Il GABA riduce la velocità di migrazione in topi wt, ma esercita un effetto opposto in topi OPHN1$^{-/y}$, facendo così aumentare la velocità di migrazione in topi OPHN1$^{-/y}$.

L'inibizione dei recettori $GABA_A$ tramite bicucullina aumenta la velocità di progressione dei neuroblasti in topi wt, mentre in topi OPHN1$^{-/y}$ la bicucullina riduce la velocità generale delle cellule che migrano dalla SVZ.

Abbiamo analizzato l'effetto di un bloccante di NCC1, la bumetanide, sulla motilità delle cellule migratorie. Come i neuroni immaturi, le cellule migratorie esprimono principalmente NCC1. In presenza del bloccante per NKCC1, la bumetanide, la velocità delle cellule appena generate diminuisce nei topi wt. Nei topi OPHN1$^{-/y}$ invece non si è osservato nessun effetto sulla motilità delle cellule migratorie.

Abbiamo investigato gli effetti dell'inibizione di KCC2 nei precursori migratori. Nei topi wt l'applicazione di un inibitore per KCC2, VU0463271, non modifica la motilità dei neuroblasti. Contrariamente, bloccando KCC2 si è visto un aumento significativo nella velocità di migrazione in topi OPHN1$^{-/y}$.

Nessuno dei due farmaci usati ha modificato la direzionalità delle cellule migratorie né nei topi wt né nei topi OPHN1$^{-/y}$.

In un lavoro precedente del nostro laboratorio è stato dimostrato che l'amministrazione cronica di un inibitore non competitivo di ROCK, fasudil, recupera il numero degli interneuroni neogenerati nel OB in topi OPHN1$^{-/y}$ rispetto ai topi controllo. Di conseguenza, Abbiamo testato l'effetto di applicazioni acute di

fasudil su fette. Interessatamente, abbiamo scoperto che l'applicazione di fasudil recupera la direzionalità ma non agisce sulla progressione delle cellule migratorie in topi OPHN1$^{-/y}$ rispetto ai controlli.

Come menzionato precedentemente, nel nostro laboratorio, abbiamo scoperto che il trattamento cronico con fasudil su topi *ad libitum* in acqua recupera il numero di nuovi interneuroni GABAergici nel OB 15 giorni dopo la loro generazione nella SVZ, quando tutte le cellule raggiungono il OB. Dato l'effetto dell'applicazione acuta di fasudil sulla direzionalità, ma non sulla velocità, nelle cellule migratorie in topi OPHN1$^{-/y}$, ci siamo chiesti se il trattamento cronico con fasudil poteva portare ad un arrivo ritardato di tutte le nuove cellule generate al OB. Per verificare questa ipotesi abbiamo quantificato il totale delle nuove cellule generate che raggiungono il OB in 9 giorni dopo la loro nascita in topi trattati sia di controllo che OPHN1$^{-/y}$. Nei controlli il numero di nuove cellule generate che raggiunge l'OB al 9 e 15 dpi è simile. Abbiamo visto che al nono giorno dopo la loro generazione nella SVZ, il numero delle nuove cellule generate che raggiungono il OB è significativamente ridotto in topi OPHN1$^{-/y}$ trattati con fasudil rispetto ai controlli. In accordo con i nostri dati *ex vivo*, l'effetto del fasudil, *in vivo,* salva la direzionalità ma non la velocità della progressione dei precursori neuronali, risultando in un arrivo ritardato rispetto ai controlli.

Combinando immunohistochimica quantitativa e time-lapse imaging tramite due-fotoni *in vivo*, abbiamo rilevato che la perdita di funzionalità di OPHN1 porta all'incapacità delle cellule precursori neuronali di migrare in maniera corretta dalla SVZ al OB. La migrazione alterata può essere ascritta ad un'inversione della polarità della risposta al GABA nei neuroblasti in migrazione nei topi OPHN1$^{-/y}$. La mutazione di *OPHN1* può alterare la motilità neuronale agendo su due meccanismi governati da due diverse vie di segnale. In aggiunta, l'alterata migrazione, che porta ad un numero ridotto di interneuroni inibitori nella zona di interesse, verosimilmente, porta allo scompenso del bilanciamento tra eccitazione e inibizione nel OB, e questo può contribuire alla patofisiologia delle ID.

SUMMARY

OPHN1 is a X-linked gene associated to intellectual disability (ID) that encodes a Rho-GTPase activating protein (RhoGAP) that regulates the conformational rearrangements of actin filaments involved in several developmental processes including axon outgrowth, dendritic maturation and cell migration.

The impact of OPHN1 mutation on neuronal morphology and function has been studied mostly in glutamatergic neurons. GABAergic inhibitory interneurons exert an important role in the excitation inhibition balance of neuronal network. Indeed alterations in development and function of GABAergic interneurons have been associated to several neurodevelopmental disorders. Whether and how OPHN1 affects inhibitory circuitry remains largely to be understood. To address this question, I have been studying adult neurogenesis of forebrain inhibitory interneurons in the subventricular zone (SVZ) in a mouse model of intellectual disability, i.e. a line of mice carrying a null mutation for OPHN1. In the subventricular zone (SVZ), along the wall of the lateral ventricles, neurogenesis of interneurons continues throughout life. From the SVZ neuronal precursors migrate along the rostral migratory stream to reach the olfactory bulb (OB) where they become fully mature interneurons. Noteworthy, in mammals, including human infants, the SVZ-derived inhibitory interneurons migrate not only to the OB but also to several subcortical and cortical areas. These postnatally generated interneurons are thought to play a prominent role in the postnatal development and plasticity of the brain.

In a previous work we found that loss-of-function mutation of OPHN1 did not affect the generation of neuronal precursors in the subventricular zone. However, the number of adult-born cells that reached the olfactory bulb was dramatically reduced in OPHN1$^{-/y}$ mice. These results suggested that OPHN1 mutation could affect neuronal migration.

We explored whether and how the migration was altered in OPHN1$^{-/y}$ mice. Combining birthdating experiments (i.e. using BrdU as a marker of new cells) and quantitative anatomy, we studied the distribution, the morphology and the directionality of the adult born cells along the rostral migratory stream (RMS). Remarkably, we found that the distribution of neuronal precursors along the RMS was deeply altered in OPHN1$^{-/y}$ mice, with most of the newly generated cells clamped in the initial portion of the RMS, and only very few cells in the final portion of the RMS and in the OB in OPHN1$^{-/y}$ mice with respect to controls.

To dissect the mechanism underlying altered cell migration, we performed time-lapse imaging of migrating neuroblasts on thick sagittal sections of the brain by means of two-photon imaging. We investigated the velocity and the directionality of migrating cells, in wt and OPHN1$^{-/y}$ mice.

We found that the speed of neuroblasts progression was significantly reduced in OPHN1$^{-/y}$ mice respect to controls. Furthermore the percentage of cells migrating toward the OB (directionality) was significantly reduced in OPHN1$^{-/y}$ with respect to controls.

GABA is known to modulate neuroblast migration during development. GABA, abundantly present in the RMS, is thought to be released from neuroblasts and act in autocrine and paracrine fashion on neuroblasts that express $GABA_A$ receptors. Accumulation of ambient GABA is prevented by GABA uptake by astrocyte-like cells, which ensheath the chains of migrating precursors.

GABA is the major inhibitory neurotransmitter in adult brain. GABA response polarity (hyperpolarization versus depolarization) is however, not univocal, but it is critically regulated by intracellular chloride concentration, that is in turn modulated by specific co-transtranporters, NKCC1 and KCC2. NKCC1, mostly expressed in immature neurons, favors high intracellular chloride concentration leading to depolarizing GABA. KCC2, widely expressed in mature neurons, favors low intracellular chloride concentration, leading to hyperpolarizing GABA. Depolarizing GABA is thought to play a prominent role in several developmental processes, including cell migration.

To assess how GABA modulates cell migration in OPHN1$^{-/y}$ mice, time-lapse imaging of neuronal precursors was performed in baseline conditions and in

presence of GABA in control and in OPHN1$^{-/y}$ mice. GABA application reduced speed of migration in wt mice, but exerted an opposite effect in OPHN1$^{-/y}$ mice, resulting in an increased speed of migration in OPHN1$^{-/y}$ mice. The inhibition of $GABA_A$ receptors upon bicuculline application increased the speed of neuroblasts progression in wt mice, while in OPHN1$^{-/y}$ mice bicuculline application reduced the overall speed of migrating SVZ-derived cells.

We explored the effect of NKCC1 blocker, bumetanide, on the motility of the migrating cells. As immature neurons, migrating cells expressed mostly NKCC1. In presence of NKCC1 blocker bumetanide, the speed of newly generated cells was reduced in wt mice. However, no effect was observed on the motility of migrating cells in OPHN1$^{-/y}$ mice.

We investigated the effects of KCC2 inhibition in migrating precursors. In wt mice, the application of the KCC2 inhibitor VU0463271 did not affect neuroblast motility. By contrast, blocking KCC2 resulted in a significant increase in the translocation speed in OPHN1$^{-/y}$ mice. These findings corroborated the hypothesis that the polarity of GABA response is altered in migrating neuroblasts along the RMS in OPHN1$^{-/y}$ mice.

Noteworthy, none of the drug used affected the directionality of the migrating cells in controls, nor in OPHN1$^{-/y}$ mice.

In a previous work in our lab, we found that chronic administration of the ROCK non-competitive inhibitor fasudil rescued the number of adult-born interneurons in the OB of OPHN1$^{-/y}$ mice with respect to littermate controls. We therefore tested the effect of acute application of fasudil on slices. Interestingly, we found that fasudil completely rescued the directionality but it did not affect the progression of migrating cells in OPHN1$^{-/y}$ versus controls.

As mentioned above, in a previous work in our lab we found that chronic treatment with fasudil administered to mice *ad libitum* in the drinking water rescued the number of newborn GABAergic interneurons in the OB 15 days after their birth in the SVZ, when all the cells reached the OB. Given the effects of acute fasudil on the directionality, but not on the speed, of migrating cells in OPHN1$^{-/y}$ mice, we asked whether chronic treatment with fasudil could result in a delayed arrival of the whole complement of newly generated cells in the OB. To verify this

hypothesis we quantified the complement of newly generated cells that reach the OB 9 days after their generation in controls and in OPHN1$^{-/y}$ treated mice. In controls the number of newly generated cells that reach the OB at 9 and 15 dpi is similar. We found that at 9 days after their generation in the SVZ, the number of newly generated cells that reached the OB was still significantly lower in OPHN1$^{-/y}$ mice treated with fasudil with respect to controls. In agreement with our data in slices, the effect of fasudil, *in vivo*, rescued the directionality, but not the speed of neuronal precursors progression, resulting in a delayed arrival respect to controls.

Combining quantitative anatomy and time-lapse two-photon imaging *in vivo*, we found that loss-of-function mutation of *OPHN1* leads to the inability of neuronal precursor cells to migrate properly from the SVZ to the OB. The hampered migration could be ascribed to a subverted GABA signalling or GABA response polarity in migrating cells in OPHN1$^{-/y}$ mice. Null mutation of *OPHN1*, could hamper neuroblasts motility acting on two different mechanisms governed by two distinct signaling pathways. In addition, the altered migration, leading to a reduced number of inhibitory interneurons in the target area, is likely to alter the excitatory/inhibitory balance in the circuitry of the OB, and this may contribute to the pathophysiology of ID.

1. INTRODUCTION

1.1. Intellectual Disability

1.1.1. Etiopathology of Intellectual Disability

Intellectual disability (ID) in the International Classification of Diseases from World Health Organization (ICD), is a condition in which the development of the mind is compromised and incomplete. ID is characterized by impaired social and adaptive skills manifested during the developmental period. (San Martin and Pagani, 2014). Learning and memory are the most affected cognitive processes. These functions are critically required to become familiar with the social and physical environment ((Bolduc and Tully, 2009); (Luckasson and Reeve, 2001)).
ID exhibits a broad clinical spectrum, that varies from mild to severe cognitive disabilities.

The severity of ID is difficult to measure, but standardized intelligence tests, designed to measure the general intelligence quotient (IQ), provide a powerful tool to assess it. These tests are integrated by scales that evaluate social adaptation (Harris, 2005).
ID is defined by an IQ below 70 indicating limited intellectual functioning, in addition to deficits in two or more adaptive behaviours that affect the execution of daily-living skills, social skills and communication (Wilmshurst and Ouvrier, 2011).
According to the Diagnostic and Statistical Manual of Mental Disorders, fifth edition (DMS V), an IQ between 55 and 70 define mild ID, moderate between 35 and 55, severe between 20 and 35, and extremely severe when lower than 20.

ID has a prevalence of 2-3% worldwide, representing one of the biggest medical and social challenges in our society (Iwase et al., 2017). ID in general can be distinguished between syndromic forms, in which ID has to be considered as one

of a large set of symptoms, and non-syndromic forms, in which the only manifestation of the pathology coincide with ID. The syndromic forms are prevalent with about 50% of ID patients that also manifest autism and/or seizures (Stevenson et al., 2012). Non-syndromic or idiopathic ID accounts for 30 – 50 % of cases (Daily et al., 2000). ID usually manifests before the eighteenth year (Stevenson et al., 2000).

Children with ID take more time to learn than a typical child. Children display a delay in learning language, in developing social skills, and in taking care of their personal needs, such as dressing or eating. Improvement of their abilities will take them longer, requiring more repetitions. People with severe ID will need intensive support and supervision throughout their entire lives (Daily et al., 2000).

Etiopathology of ID is extremely heterogeneous. Etiological factors include both environmental factors and genetic factors (Iwase et al., 2017).

Among the large variety of environmental factors, the main are:

- maternal malnutrition;
- fetal alcohol exposure;
- fetal infections;
- premature birth;
- birth trauma;
- anoxia;
- hypothyoidism

Many genetic defects and aberrations are associated to ID, including:

- single gene mutation (in example: X-fragile syndrome);
- polygenic predisposition;
- Chromosome abnormalities (in example: Down's syndrome).

Notably, a large number of such genes encode for epigenetic regulators, the function of which occurs through genome-wide post-translational modifications of histones, DNA base modification and other covalent and noncovalent chromatin changes (Kramer and van Bokhoven, 2009).

ID comprises a broad repertoire of clinically and genetically heterogeneous disorders, which are primarily characterized by various defects of the central nervous system (Luckasson and Edwards, 2002).

Currently, no cure is available for ID (Harris, 2005). Nevertheless, Studies conducted on animal models of genetic disorders shed light on the concept that pharmacology and appropriate learning paradigms can ameliorate learning disabilities and attention deficits during development (San Martin and Pagani, 2014).

The first investigations aimed at understanding the mechanism underlying ID were conducted on human post mortem tissues. In 1974 Purpura and Huttenlocher examined post-mortem brain tissues of ID patients, and identified abnormalities in dendrites and spines as a hallmark of ID ((Purpura, 1974); (Huttenlocher, 1974)).

More recently, mouse models carrying genetic mutations associated to ID provided an invaluable opportunity to dissect the mechanisms underlying cognitive dysfunctions proper of ID, allowing to analyze the cellular, morphological and functional defects of neurons and neuronal circuits. Several studies conducted in mice carrying genetic mutation associated to ID, confirmed alterations in dendritic elaboration and spines ((Node-Langlois et al., 2006); (Khelfaoui et al., 2007); (Sarowar et al., 2016); (Montani et al., 2017)). Since spines and dendrites are elective sites of synaptic contacts, their alterations is likely to lead to impairment in neuronal connectivity and synaptic plasticity, leading to reduced cognitive function (Chechlacz and Gleeson, 2003).

1.1.2. Genes associated to X-linked Intellectual Disability

Among genes associated to ID, many are linked to chromosome X (X-linked Intellectual Disability, XLID). More than 150 XLID syndromes have been characterized, among these, 81 have been correlated to a total putative number of 102 XLID genes (Stevenson et al., 2012). In the brain, the expression of proteins encoded by XLID genes is prominent in brain regions characterized by a high degree of plasticity (Boda et al., 2002). Mutations in XLID genes frequently involve loss-of-function and lead to morphological and functional alterations. The vast majority of XLID genes encode for proteins that are mainly involved in

cytoskeleton remodelling, affecting several processes, such as formation and maturation of dendritic spines. Actin dynamic also regulates the localization and activity of surface receptors and intracellular signalling molecules (Humeau et al., 2009). All together these event modulate synaptic functions and plasticity,

At least three of the XLID genes encode for proteins strictly correlated to signalling pathways under the control of the Rho-GTPases family.

OPHN1 is a gene localized on the X-chromosome that encodes for oligophrenin-1 (Billuart et al., 1998). Oligophrnin-1 is a Rho-GTPase activating protein (Rho-GAP) that acts on Rho-GTPases, in particular on Ras homology gene subfamily member A (RhoA), Ras-related C3 botulinum toxin subfamily substrate 1 (Rac1) and Cell division control protein 42 homolog (Cdc42). Rho GTPase, and therefore OPHN1, as a Rho-GAP, play a pivotal role in the regulation of several aspects of neuronal morphology, including axonal outgrowth, development of dendritic arborization and dendritic spine morphogenesis (Govek et al., 2004).

The *PAK3* gene, encodes for the homonymous protein, p21-activated kinase-3 (PAK3; (Allen et al., 1998)). PAK3 belongs to a family of serin/threonin protein kinase that controls conformational rearrangements of the actin cytoskeleton by mediating the effects of Rac1 and Cdc42 (Hofmann et al., 2004). Detailed analysis of the genome of families with cases of XLID revealed five putative mutations in the *PAK3* gene (Ma et al., 2012). In hippocampal slices, the formation of thin elongated spines (i.e. filopodia-like) is promoted by the suppression of PAK3 activity. These spines are unstable and incapable of maturation, leading to abnormal synaptic contacts and reduced synaptic plasticity (Boda et al., 2004).

αPIX is a protein encoded by the *ARHGEF6* gene (Kutsche et al., 2000). It is a GDP/GTP exchanger (Guanine nucleotide Exchange Factor, GEF) for Rac1 and Cdc42. Its primary role is involved in the regulation of dendritic spine morphology. A decreased complement of large mushroom-type spines and a concomitant increase in dendritic elaboration of elongated spines and filopodia-like protrusions has been observed upon silencing *ARHGEF6*, in hippocampal slices (Node-Langlois et al., 2006).

OPHN1, PAK3 and αPIX act to modulate, at distinct levels, Rho-GTPase signalling pathways and their regulation of the actin cytoskeleton. All together, they regulate neuronal morphogenesis (Fauchereau et al., 2003).

A link between ID and genes encoded on the X-chromosome has been proposed also for a fourth gene: *TM4SF2*. It encodes a tetraspanin family member (Tetraspanin-7; TSPAN7), that may be indirectly linked to function of Rho-GTPase through its association with subunits of the integrin receptor which are involved in functional regulation of Rho-GTPases activity (Berditchevski, 2001).

1.2. Rho-GTPases and role of Oligophrenin-1

1.2.1. Rho-GTPases

Rho-GTPases are a sub-family of the Ras superfamily of the small GTP binding proteins, implicated in basic cellular processes at nearly all brain developmental stages. The family of the Rho small GTPases is a set of highly conserved signalling GTPases that includes the Ras homology gene subfamily (Rho), composed by RhoA, RhoB and RhoC, the Ras-related C3 botulinum toxin subfamily (Rac), that includes Rac1, Rac2, Rac3 and RhoG, and the Cell division control protein 42 homolog (CDC42), formed by Cdc42, TC10/RhoQ and TCL/RhoJ.

RhoA, Rac1 and Cdc42 are predominantly expressed in the central nervous system and most studies focused on their activity (Azzarelli et al., 2014).

Rho-GTPases act as molecular switches, that oscillate between a GTP-bound (active) and a GDP-bound (inactive) state. The GTP-bound active state allows them to propagate signal transduction, through a broad repertoire of pathways, interacting with numerous downstream effector proteins. Rho-GTPases possess an intrinsic phosphatase activity that hydrolyses GTP to GDP. When bound to GDP, Rho-GTPase are in the inactive state ((Billuart et al., 1998); (Spiering and Hodgson, 2011)).

The GDP-bound/GTP bound switch is orchestrated by a complex protein-protein interaction between the Rho-GTPases and a set of proteins that favour GTP binding, GDP/GTP exchange factors (GEFs), or with proteins that facilitate GDP binding, namely Rho-GTPase activating proteins (RhoGAPs). In addition GDP dissociation inhibitor (GDI) maintain Rho-GTPase bound to GDP, therefore in their inactive state, in the cytosol.

Rho-GTPases activation takes place upon recruitment of the molecule to the membrane and is due to the release of the GDP and the binding of GTP. This nucleotide exchange is triggered by RhoGEFs. On the other hand, RhoGAPs, inactivate Rho-GTPases by accelerating the hydrolysis of the GTP-bound. Rho-GTPases exhibit an intrinsic ability, related to a Rho GAP domain, to hydrolyse GTP to GDP. The action of Rho-GTPases facilitate and accelerate this process. Rho-GTPases are maintained in the inactive state by the activity of GDI. Namely, GDI sequester GDP-bound proteins in the cytoplasm and prevent their dissociation from GDP (Matozaki et al., 2000).

The interaction between GTP-bond active Rho-GTPase and molecular effectors mediate several biological processes. Many factors can activate Rho-GTPases, such as growth factors, adhesive ligands and guidance cue receptors (i.e. Slit, netrins and semaphorins; (Hall and Lalli, 2010)).

Rho-GTPases regulate actin cytoskeleton dynamics by orchestrating the complex interactions between extracellular and intracellular signals. In this way they contribute to regulate many biological processes such as axon elongation, axon guidance, dendrites and spines formation, cellular migration and synaptic plasticity (Figure 1.1.). In other words, they regulate neuronal morphology and connectivity as well as synaptic function providing the essential basis of the fine regulation of neuronal network activity (Zamboni et al., 2018).

Rho-GTPases govern numerous aspects of the cytoskeleton assembly/disassembly, such as actin filament polymerization and severing, microtubule extension and contractility of actomyosin filaments ((Luo, 2000); (Govek et al., 2005); (Gomez and Letourneau, 2014)). For instance, neurite extension and leading edge motility required the orchestrated activity of actin polymerization, Myosin II and active association of actin binding proteins with adhesion complexes.

Different developmental stages involve specific functions of Rho-GTPases. In early stages, the strict control of cytoskeletal dynamics is pivotal for the acquisition of polarity in cell division, that is necessary for neurogenesis (Cappello, 2013).

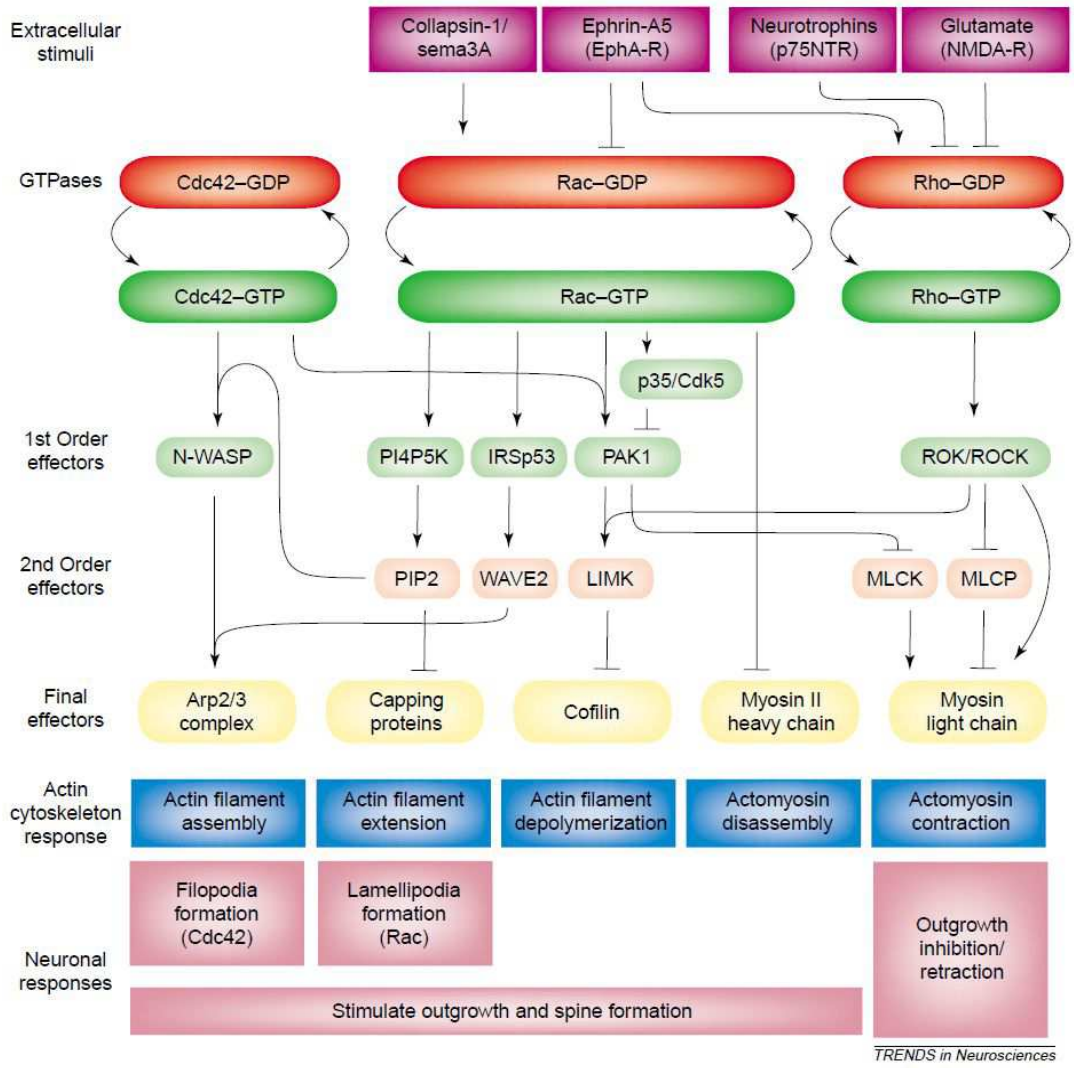

Figure 1.1.: Scheme of Rho-GTPases downstream pathways and effectors. *Abbreviations: ROCK, rho-associated, coiled-coil-containing protein kinase; LIMK, lens intrinsic membrane protein domain; MLCK, myosin light chain kinase; MLCP, myosin light chain phosphatase; N-WASP, Neuronal Wiskott–Aldrich Syndrome protein; PAK, p21-activated kinase; IRSp53, insulin receptor substrate protein53; PI4P5K, Phosphatidylinositol-4-phosphate 5-kinase; PIP2, Phosphatidylinositol 4,5-bisphosphate; p75NTR, p75 neurotrophin receptor; Cdk5, Cyclin-dependent kinase 5; sema3A, semaphorin 3A (Ramakers, 2002).*

At more advanced developmental stages, formation of axon and dendrites, axon guidance and cell migration require sophisticated cytoskeletal dynamics that are

governed by Rho-GTPases (Govek et al., 2011). These morphological events are critical for proper neuronal connectivity underlying physiological network activity.
Alterations of the spatiotemporal dynamics of Rho-GTPases, related to mutations of the proteins themselves or to mutations of GEF and/or GAP, impact on neuroblasts migration, axon targeting, dendrite elaboration, and spine formation, leading to network dysfunction underlying cognitive deficits in ID and related neurodevelopmental disorders (Zamboni et al., 2018).
Rho-GTPases direct a variety of actin-cytoskeletal dynamics, often with antagonistic mechanisms. An example is offered by the regulation of neuronal processes. Rac1 and Cdc42 generally promote elongation, branching and complexity of neuronal processes, while RhoA primarily exerts the opposite effect, i.e. inhibition of neuronal processes elaboration and elongation (Luo, 2000). It has to be highlighted that these results were obtained by *in vitro* studies and that *in vivo* experiments have often lead to different discoveries, not always in agreement, if not in open contrast, with the *in vitro* data.

In mature neurons, Rho-GTPases orchestrate actin dynamics in the postsynaptic compartment in excitatory synapses, in spines. These events critically mediate synaptic plasticity, underlying several cognitive functions, such as learning and memory (Sawada et al., 2018). In addition, dendritic spine morphology and plasticity are governed by Rho-GTPases (Woolfrey and Srivastava, 2016). RhoA activation has a negative effect on spine growth and maturation, whereas Rac1 and Cdc42 promote spine formation and maintenance (Newey et al., 2005). RhoA hyperactivation leads to reduced actin polymerization resulting in an overall decrease in the density of mature spine in mice (Sarowar et al., 2016). On the other hand, in mice with Rac1 hyperactivity, the alteration of the maturation of dendritic spines resulted in the formation of aberrant polymorphic spines (Valdez et al., 2016).
Rho-GTPases regulate also growth cone morphology and growth cone dynamic to guarantee proper elongation and targeting of neuronal processes. This fine regulation is achieved through the transduction of a wide repertoire of external guidance molecules that, through the action of Rho-GTPases, regulate cytoskeletal rearrangements. Rho-GTPases expressed at the leading edge of the process that

direct migrating neuroblasts, exert a crucial role in modulating neuronal migration (Zamboni et al., 2018). For example, mice carrying a double deletion of Rac1 and Rac3 display impaired migration and differentiation of specific population of GABAergic hippocampal and cortical interneurons (Vaghi et al., 2014).

More than 80 GEF and 70 GAP have been identified. The large number of GAPs and GEFs suggest that their regulation of Rho-GTPases can be finely tuned in space, i.e. related to specific subcellular compartments and/ or in time, i.e. could be tightly modulated at different developmental stages. Overall Rho-GTPases regulation is very complicated.

All these evidences indicate that Rho-GTPases signalling pathways regulate a wide range of morphogenetic processes, in distinct stages of development, that are essential in establishing specific neuronal circuits and define network activity. Therefore, alterations in these signalling pathways, disrupting neuronal morphology and network function, could be involved in the etiopathogenesis of ID syndromes (Ramakers, 2002).

1.2.2. The signalling pathways of Rho-GTPases

The modulation of neurite outgrowth by Rho proteins occurs in response to extracellular guidance cues such as myelin, collapsin/Sema3A and ephrin 5A (Wahl et al., 2000). Moreover, both RhoA and Rac1 are thought to act downstream of NGF, BDNF and NT-3, likely through Trk receptors (Ozdinler and Erzurumlu, 2001). Non-receptor tyrosine kinase, such as Focal Adhesion Kinase (FAK) and Src Family Kinases (SFKs) modulate actin dynamics and cell motility via Rho-GTPases activity (Rico et al., 2004). Rho-GTPases are activated also by integrin receptors and adhesion molecules, such as N-cadherin. Activated ion channels, such as α-amino-3-hydroxy-5-methyl-4-isoxazolpropionic receptor (AMPAR) and N-methyl-D-aspartate receptor (NMDAR) have been reported to influence Rho-GTPases activity (Tolias et al., 2011). At the growthcone, changes in cytosolic Ca^{2+} concentration impacts on Rho-GTPase activity and trigger actin cytoskeleton remodelling (Woo and Gomez, 2006).

RhoA bears a negative role in neuritis outgrowth, as indicated by the fact that deactivation of RhoA promotes neurite growth-cone elongation while activation of RhoA causes its collapse.

It has been hypothesized that the dual phenotype observed in translocating cells may rely on the prevailing effect of Rac1 at the leading edge, (Figure 1.2.; Spiering and Hodgson, 2011).

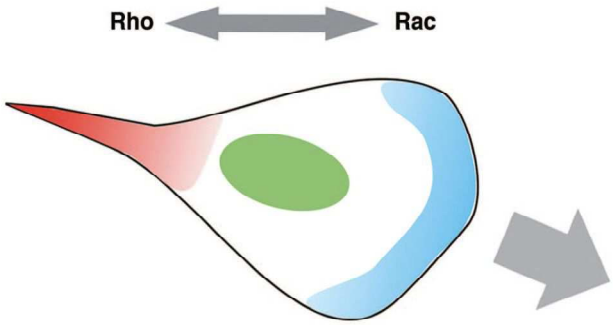

Figure 1.2.: The dual activities of Rac1 versus RhoA in migrating cells. *RhoA is primarly activated at the retracting tail (red) where it promotes tail contraction, while Rac1 is active at the front of the cell to enhance lamellipodial protrusion (blue; Spiering and Hodgson, 2011).*

The coordination of Rac1/RhoA dynamic pattern of activity takes place both spatially and temporally. It is tightly modulated and even at significantly finer time-scales within areas that undergo protrusion, retraction, ruffling or micropinocytosis. All these events depend on precisely orchestrated cytoskeletal rearrangements (Machacek et al., 2009).

RhoA has a pivotal role in governing nucleation, elongation, branching and severing of the actin filaments, mainly via the Rho-associated protein kinase-LIM domain kinase (ROCK-LIMK) pathway, that controls the actin-binding protein actin depolymerizing factor (ADF)/cofilin complex (Shamah et al., 2001). RhoA activates the immediate downstream kinase target Rho-associated protein kinase (ROCK). ROCK directly phosphorylate several actin cytoskeleton modulators, including myosin light chain (MLC) phosphatase, that stimulates actin contractility, and LIM kinase (LIMK) that regulate the phosphoregulation of ADF/cofilin. ADF/cofilin plays an important role in controlling actin severing, nucleation and capping at the tip of growing neuronal processes (Narumiya et al., 2009).

Cofilin-mediated actin nucleation is a fundamental regulatory machinery that impacts severing of preexisting actin fibers. This mechanism controls the extension of the leading edge. Direct phosphorylation of Cofilin at the Ser3 operated by LIMK provide an important regulation of the entire machinery (Bernstein and Bamburg, 2010).

ROCK has two distinct isoforms ROCK1 and ROCK2 that differentially control specific pathways downstream of RhoA. Cell polarity, required for cell migration, and synaptogenesis are initiated by the coordinate activities of the two ROCK isoforms. ROCK1 stabilizes actomyosin filament bundles formation that results in front-back and dendritic spine polarity. Contractile forces and Rac1 activity at the leading edge and at the spine head are controlled by ROCK 2. Moreover, ROCK2 specifically directs ADF/cofilin-mediated actin remodelling that underlies maturation of adhesions and the postsynaptic density (PSD) of dendritic spines (Newell-Litwa et al., 2015).

Rac1 and Cdc42 govern ADF/cofilin complex through the p21-activated kinase (PAK)-LIMK pathway to govern, (Zamboni et al., 2016). Rac1 and Cdc42 control actin dynamic also via WAS protein family member (WAVE) and neuronal Wiskott–Aldrich syndrome protein (N-WASP; (Hall and Lalli, 2010)). In addition, RhoA and Cdc42 cooperate in regulating actomyosin contractility through the ROCK-myosin light chain (MCL) pathway and the PAK-MCL kinase (MLCK) pathway, respectively (Govek et al., 2005).

The actin cytoskeleton is necessary for growth-cone motility, neurite pathfinding and branching (Tanaka and Sabry, 1995), as well as for the formation and motility of dendritic spines (Fischer et al., 1998). Neurite elongation, however, is mostly dependent on tubulin polymerization. Rho-GTPases play a role also in the control of microtubule extension through the activity of Rac1 and Cdc42 that operate via PAK kinases on downstream targets (Tivodar et al., 2015). In addition, Rac1 and Cdc42 control the formation of the leading process of migrating neuroblasts, and therefore their migration, activating the downstream c-Jun N-terminal kinase (JNK)-microtubule pathway (Choi et al., 2015). On the other hand, RhoA acts to increase the stability of microtubules (Wittmann and Waterman-Storer, 2001).

Rho-GTPases transduction pathways converge and diverge at different levels: for example, they all induce actin polymerization via LIMK activation, while actomyosin contractility is stimulated by RhoA but inhibited by Rac1 and Cdc42 that have an inhibitory effect on the MLCK (Govek et al., 2005).
Noteworthy, all signalling pathways converge on the same pool of local monomeric and filamentous actin, providing a precise spatial integration of several cues, that mediate adaptive changes in cell morphology by directing the cytoskeleton dynamics ((Gonzalez-Billault et al., 2012); (Wojnacki et al., 2014); (Coles and Bradke, 2015)).

1.2.3. Oligophrenin-1

Oligophrenin-1 is a protein of 802 aminoacids, with a relative molecular mass of 91 KDa. It is encoded by *OPHN1* gene, localized on the long arm of the X-chromosome (position Xq21) (Billuart et al.1998).
Two different domains of oligophrenin-1 have been revealed by primary sequence analysis: a Pleckstrin homology domain (aminoacids 266-370) and a central Rho-GAP domain (Rho-GTPase activating protein domain; aminoacids 384-561), followed by three carboxyl-terminal proline-rich sequences (amino acids 567-585, 629-639, and 735-748), which are putative SH3-binding sites (Billuart et al., 1998; Fauchereau et al., 2003). Chelly and colleagues in 1998 identified different mutations of *OPHN1* (X;12 balanced translocation or frameshift deletion), establishing the involvement of the gene in XLID (Billuart et al., 1998).
The Rho-GAP domain has a stimulatory activity on the intrinsic GTPase activity of Rho-GTPases, increasing the speed of hydrolysis of the GTP bound to the Rho proteins.

Oligophrenin-1 is widely expressed both during development and in adulthood in brain areas characterized by high synaptic plasticity, such as the cortex, the hippocampus and the olfactory bulb. Oligophrenin-1 is expressed both in neurons and in glial cells, where it colocalized with F-actin, notably at the tip of growing neuritis. This interaction seems to be determined by a novel

uncharacterized domain in the carboxyl-terminal end of oligophrenin-1 (Fauchereau et al., 2003). In mature neurons, oligophrenin-1 has been identify both pre-synatpically and post-synaptically and this suggests a putative involvement in synaptic formation and function (Zanni et al., 2005).

In vitro analysis showed that oligophrenin-1, a Rho-GTPases activating protein (GAP), specifically stimulates GTP hydrolysis of members of the Rho subfamily. In this way it negatively regulates Rho-GTPase activity. In vitro assays indicated that OPHN1 interact with Cdc42, RhoA and Rac1 with no obvious specificity (Fuacherau et al., 2003). Inactivation of a RhoGAP protein might cause constitutive activation of GTPase targets (Figure 1.3.), which is known to affect cell migration and outgrowth of axons and dendrites in vivo (Billuart et al., 1998). This eventually leads to network dysfunction, suggesting an association between defects in a signalling pathway that depends on Rho-GTPases and cognitive impairments.

Using RNA interference (RNAi) and antisense RNA, Van Aelst and colleagues found that in CA1 neurons in rat hippocampal slices, downregulation of oligophrenin-1 resulted in a striking decrease in dendritic spine density (Govek et al., 2004).

Loss of oligophrenin-1 function seems to have only a small effect on mature dendritic spines, but significantly increases the density and the proportion of immature spines, i.e. filopodia, in $OPHN^{-/y}$ mice (Khelfaoui et al., 2007).

Noteworthy, observations from animal models and *in vitro* studies are often controversial.

Oligophrenin-1 also interacts with Homer1b/c, a postsynaptic adaptor protein that links glutamate receptors to multiple intracellular targets and influence dendritic spine morphogenesis and synaptic transmission ((Fagni et al., 2002); (Xiao et al., 2000)).

The association between oligophrenin-1 and Homer may provide a connection between glutamate receptor signalling and actin cytoskeletal rearrangements necessary for morphological spine changes (Govek et al., 2004).

Mutations of *OPHN1* gene expression, in cultured rat hippocampal neurons at specific developmental stages and in selective population of neurons, allowed Van Aelst and colleagues to show that oligophrenin-1 plays a key role in activity-

dependent maturation and plasticity of excitatory synapses (Nadif Kasri et al., 2009). The synaptic activity and NMDA receptor activation are critical for localization and function of OPHN1 in excitatory synapses. Concomitantly, oligophrenin-1 also regulated the stability of AMPA receptors in a RhoGAP-dependent manner.

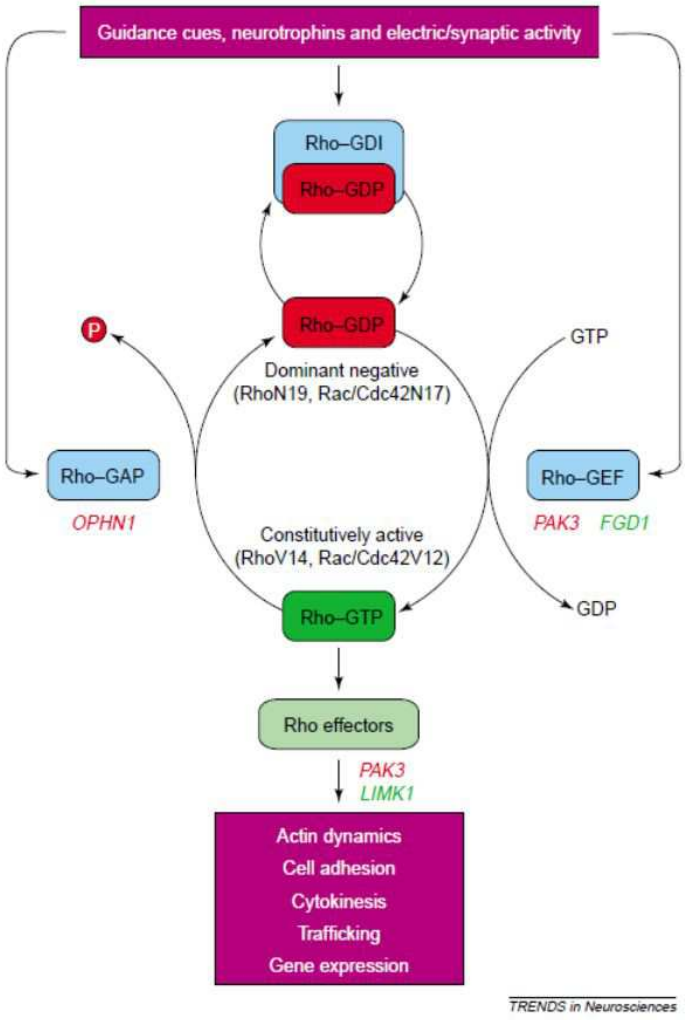

Figure 1.3.: Rho-GTPases activation/inactivation cycle. *Abbreviations: FGD, faciogenital dysplasia; GAP, GTPase-activating proteins; GDI, guanine dissociation proteins; GEF, guanine nucleotide exchange factors; LIMK, lens intrinsic membrane protein domain; PAK, p21-activated kinase (Ramakers, 2002).*

Loss of structural morphology and density of spines and synapses appears to be triggered by hampered glutamatergic synapse maturation that in turn seems to be due to defective oligophrenin-1 signalling (Nakano-Kobayashi et al., 2009).

By 2-hybrid screening of a brain cDNA library, using SH3 binding domain of OPHN1 as bait, it was found that proteins involved in clathrin-mediated endocytosis (CME), such as amphiphysin II, endophilin B1, endophilin B2, and CIN85, interacted with oligophrenin-1. GST pull-down assays confirmed the interactions through the oligophrenin-1 proline-SH3 binding sites. The interaction between proteins involved in CME and oligophrenin-1 promoted the concentration of OPHN1 to endocytic sites where it repress the inhibitory function of ROCK1 on endocytosis, due to it downregulation effect on the RhoA/ROCK1 signaling pathway. Disruption of oligophrenin-1 signalling (or null mutation in OPHN1) in mice reduced endocytosis of synaptic vesicles and postsynaptic AMPA receptor internalization, resulting in impaired NMDA-dependent long-term depression (LTD) in the hippocampus (Khelfaoui et al., 2009). Oligophrenin-1 seems to play a crucial role in mediating mGluR-LTD, and its interaction with Endo2/3 is critical for this event ((Nadif Kasri et al., 2011); (Nakano-Kobayashi et al., 2009)).

In dendrites of CA1 neurons, mGluR activation rapidly promotes the upregulation of oligophrenin-1. In addition, it has been shown that in mice expressing a truncated form of oligophrenin-1, CA1 pyramidal neurons exhibit an abnormally higher density of dendritic filopodia and immature dendritic spines (Meziane et al., 2016).

Moreover, mice carrying a null-mutation of *OPHN1* show hyperactivity and impairments in spatial learning and memory (Khelafaoui et al., 2007).

The geometry of the dendritic arborization is designed to integrate the diverse synaptic inputs, that in turn regulate neuronal network connectivity, synaptic activity and plasticity. These processes are crucial for neuronal information processing. Alterations in dendritic tree architecture and spines are a hallmark of ID (Purpura, 1974) and are thought to play a critical role in cognitive impairments (Newey et al., 2005).

The vast majority of the studies have been conducted to dissect the role of OPHN1 in modulating the maturation and function of excitatory glutamatergic neurons.

A growing body of evidence indicated that alterations in the development and function of inhibitory interneurons may play a key role in the etiopathogenesis of

neurodevelopmental disorders. ((Marin, 2012); (Le Magueresse and Monyer, 2013); (Deidda et al., 2014))

The impact of OPHN1 on inhibitory interneurons remained elusive. Lodovichi and colleagues investigated the role of OPHN1 on inhibitory interneurons, by analyzing development and function of forebrain GABAergic interneurons in a mouse model carrying a null mutation of OPHN1 (Redolfi et al., 2016).

They found that that OPHN1 mutation leads to alteration in the morphology of dendritic spines and in the functional properties of the granule cells (GCs), the main GABAergic inhibitory interneuron population of the OB.

granule cells of the OB exhibit a significant higher proportion and density of filopodia-like spines (Redolfi et al., 2016). These filopodia-like spines can establish synaptic contacts, although some features of miniature inhibitory post synaptic currents (mIPSC) and spontaneous IPSC (sIPSC) on their target cells (i.e. mitral cells, MCs) were altered. In particular, loss-of-function of oligophrenin-1 produces an increased frequency and amplitude of mIPSC, probably due to a higher amount of release of GABA per site, consistent with the finding that the expression of the vesicular GABA transporter (v-GAT) on the filopodia-like spines of the granule cells was increased in mice carrying a null mutation of *OPHN1*. (Redolfi et al., 2016).

Oligophrenin-1 specifically stimulates GTP hydrolysis of members of the Rho subfamily, acting as a negative regulator of RhoA, Rac1 and Cdc42.

By enhancing their GTPase activity, GAP proteins, such as oligophrenin-1, inactivate small Rho-GTPases. Inactivation of RhoGAP proteins is likely to induce overactivation of their GTPase targets. In particular loss-of-function of oligophrenin-1 could lead to overactivation of the ROCK and PKA pathway. The RhoA/ROCK pathway has been shown to be overactivated in $OPHN^{-/y}$ mice, leading to increase phosphorylation of ROCK's target, such as the myosin phosphatase target subunit 1 (MYPT1; Khelfaoui et al., 2009).

Loss-of-function mutation of oligophrenin-1, disrupts its modulatory role, leading to an increase in RhoA/ROCKs activity.

Such activation is known to affect cell migration, axon guidance and outgrowth and dendrite maturation (Luo et al., 1997).

Altered regulation of these downstream pathways could induce a reduction in the motility of the growth cone, a reduction in the neuritis elongation and in the dendritic ramification through an increase in actin contractility in the cytoskeleton.
An increased RhoA activity may induce a disruption of the precise organization of the actin filaments at the tip of the growth cone and in the filopodia in the leading process of migrating cells, resulting in an impairment of the neuronal precursors pathfinding ability.
On the other hand, activation of Rac1 and Cdc42 could result in a reduction in formation of mature spines, resulting in a lower synaptic connectivity (Ramakers, 2002). The actions of RhoA and Rac1 on neurite outgrowth and branching are often antagonistic because of their opposite effects on downstream effectors (Kozma et al., 1997).
Therefore loss-of-function of oligophrenin-1 disrupts signalling transduction pathways involved in a wide range of processes, such as axon guidance and outgrowth, dendrite maturation and cell migration.

1.2.4. OPHN1$^{-/y}$ mice: a mouse model of intellectual disability

In order to understand oligophrenin-1 function *in vivo*, Billuart and colleagues generated a mouse model carrying a null mutation for *OPHN1* gene (OPHN1$^{-/y}$ mice; Khelfaoui et al., 2007).
The mutation disrupts the Open Reading Frame (ORF) of *OPHN1* gene, the portion of the gene that encodes for a protein.
The open reading frame of *OPHN1* is 2406 base and begins with a consensus sequence for translation initiation (ACCAUGG) that precede a methionine codon.
In this case Billuart and colleagues inserted 100 base pairs (bp) in the exon 9 of the gene, inducing the presence of a premature STOP codon after the BAR domain (Bin, Amphiphysin, RVS), at the N-terminal, before the PH domain (Pleckstin Homology Domain) and the GAP domain (Khelafaoui et al., 2007).
The transduction of the mutated gene results in a truncated protein that it is not functional.

OPHN1$^{-/y}$ mice recapitulate some features of the pathology in humans, such as the lateral ventricles enlargement, although the morphology of the cerebellum is normal in mutant mice, while humans exhibit cerebellm hypoplasia. The loss-of-function of oligophrenin-1 in mice also recapitulates some behavioral, social and cognitive impairments of the human phenotypes. Indeed OPHN1$^{-/y}$ mice exhibit behavioral defects in spatial memory together with impairments in social behavior, lateralization and novelty drive hyperactivity (Khelfaoui et al., 2007).
In cultured hippocampal neurons, inactivation of oligophrenin-1 function increases the density and proportion of immature spines.
Oligophrenin-1 controls the maturation of dendritic spines either by maintaining the density of mature spines or by limiting the extension of new filopodia. Altogether, these observations suggest that cognitive impairment related to OPHN1 loss-of-function mutation could be associated with both presynaptic and postsynaptic alterations (Khelafaoui et al., 2007).

1.3. The olfactory system

The olfactory system (OS) is deputed to perception of odors. It is the most ancient sensory modality and it is evolutionary highly conserved, from fruit flies to humans. The OS is able to detect and discriminate thousands of different odors present in the environment, even in very low concentration.
Odor information, detected in the olfactory epithelium by olfactory sensory neurons, is conveyed by OSN axons to the olfactory bulb. The output neurons of the OB, i.e. mitral cells and tufted cells form a bundles, the lateral olfactory tract that projects to several higher brain regions, indicated as olfactory cortex. Namely the term “olfactory cortex” indicates the brain regions that receive direct projections from the mitral and tufted cells of the OB. In humans and most mammals the olfactory cortex comprises: the anterior olfactory nucleus, the olfactory tubercule, the piriform cortex, the lateral enthorinal cortex, the anterior cortical nucleus of the amygdala. The piriform cortex receives substantial projections from the ventral tegmental area, the substantia nigra, the locus

coeruleus. It is reciprocally connected to the orbito-frontal cortex, insular cortex, the hippocampus and amygdala.
Reaching several forebrain regions, odor information can affect cognitive, emotional and visceral behaviours (Shepherd, 2004).

Indeed, the olfactory system is a useful model to study not only perception but also cognitive functions, due to its connections with the hippocampus and related areas.
Another unique aspect of the olfactory system is its high degree of plasticity, related to the constant regeneration of several types of neurons, such as the olfactory sensory neurons in the epithelium and the interneurons in of the OB, that originate from the neurogenic niche around the subventricular zone (see below for details). The latter offers a window into a continuous developmental process, from which forebrain GABergic inhibitory interneurons development can be thoroughly dissected.
Below I will describe briefly the olfactory areas relevant to the present work.

1.3.1. The olfactory bulb

The olfactory bulb (OB) is an outgrowth of the forebrain and it is the first retransmission station of the olfactory system. The OB is composed by two different ovoid symmetrical structures, located above the nasal cavities. The OB is a well layered laminar structure subdivided, from the outer part to the inner one, in: olfactory nerve layer (ONL), glomerular layer (GL), external plexiform layer (EPL), mitral cell layer (MCL), internal plexiform layer (IPL) and granule cell layer (GCL) (Figure 1.4.; Shepherd, 2004).
The neuronal elements of the OB can be summarized into three categories: inputs, outputs and intrinsic.

The inputs consist of the axons of the olfactory sensory neurons (OSNs) that form the ONL. **Olfactory sensory neurons** constantly regenerate. They derive from stem cells in the olfactory epithelium. Axons of the OSNs expressing the same odorant receptor converge in specific zones of the OB to form glomeruli,

giving rise to the sensory map. **Glomeruli** are spherical structures of neuropil with a diameter of 80-160 μm located in the GL of the olfactory bulb. They are formed by axons of OSNs that participate in glutamatergic synapses with the postsynaptic cells, namely MCs, TCs and periglomerular cells. Each glomerulus is surrounded by a heterogeneous population of juxtaglomerular neurons (including periglomerular, short axon, and external tufted cells) and glial cells (Wachowiak and Shipley, 2006).

The OB also receives centrifugal inputs from the brain, in particular from the olfactory cortex, the anterior olfactory nucleus, the horizontal limb of the diagonal band, the locus coeruleus and the raphe nucleus.

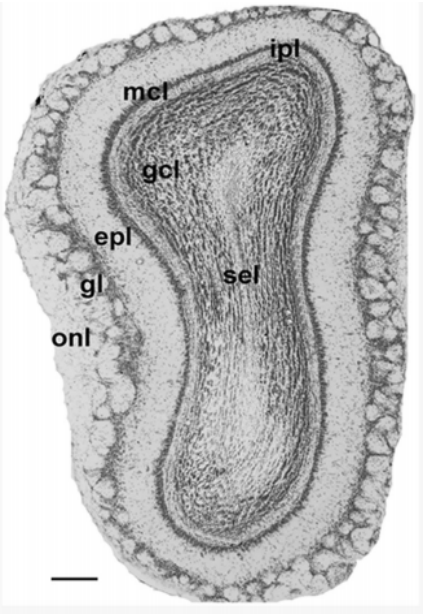

Figure 1.4.: Neutral red staining of a coronal section of the olfactory bulb. *The well layered structure of the bulb present from the outer to the inner part: olfactory nerve layer (onl); glomerular layer (gl); external plexiform layer (epl); mitral cell layer (mcl); internal plexiform layer (ipl); granule cell layer (gcl); subependymal layer (sel) (Smail et al., 2016).*

Post-synaptic neurons of the olfactory bulb are the mitral cells (MCs) and the tufted cells (TCs), that originate the efferent pathway of the olfactory bulb, forming the lateral olfactory tract (LOT).

The mitral cells are excitatory glutamatergic neurons. Their cell bodies (15-30 μm in diameter) are locate in the MCL, a thin sheet 200-400 μm below the GL. MCs extend a single apical dendrite, through the EPL and terminates within a

glomerulus in a tufted branch. The tuft has a diameter of 30-150 μm, and extend throughout most of the glomerulus. Each MC also gives rise to several secondary dendrites which terminate in the EPL and make dendro-dendritic synapses with the granule cells. mitral cells dendrites are aspiny. The mitral cells axons exiting the OB coalesce to form the lateral olfactory tract (LOT). The output axons in the LOT extend numerous collateral branches that reach the layer Ia of the olfactory cortex (Shepherd, 2004). One type of collateral is also projected from the axon within the OB (Ojima et al., 1984).

The tufted cells are similar to mitral cells but located more superficially in the EPL. According to the position of their cell body, they have been subdivided in three main groups: middle tufted cells, external tufted cells and internal tufted cells. The middle tufted cells represent the main population of tufted cells. The soma of these cells has a diameter of 15-20 μm, and extrude several thin basal dendrites (300-600 μm) and a primary dendrite (200-300 μm) that terminate in a relatively confined tuft of branches in the glomerulus. The axons of middle tufted cells funnel into the LOT to reach the olfactory cortex. The external tufted cells have the cell body located around glomeruli. Their axons project in specific loci of the internal plaxiform layer, where they link glomeruli receiving input from OSNs expressing the same odorant receptor, constituting a topographically ordered intrabulbar association system ((Belluscio et al., 2002); (Lodovichi et al., 2003)).

The interneurons of the bulb are represented by the periglomerular cells, short-axon cells and the granule cells.

The periglomerular cells (PGCs) present a short bushy dendrite that arborizes to an extent of 50-100 μm within a glomerulus. The dendritic branches intermingle with the dendrites of mitral cells and tufted cells. The periglomerular cells axons distribute laterally within the extra-glomerular region, extending as far as five glomeruli away. periglomerular cells are morphologically homogeneous, but differ in their biochemical features. They can secrete different neurotransmitters: γ-aminobutirric acid (GABA), nitric oxide, NADPH, dopamine, and neuropeptide Y. Many periglomerular cells are characterized by dual transmission of dopamine and GABA (Maher and Westbrook, 2008). periglomerular cells are thought to play a modulatory role on the incoming sensory information.

The short-axons cells (also called juxtaglomerular cells) are glutamatergic cells with axons that reach glomeruli further away than the periglomerular cells and dendrites that branch in the interglomerular spaces.

Granule cells are axonless GABAergic interneurons. They represent the major population of inhibitory interneurons of the OB (Ribak et al., 1977).

The somas of the granule cells are small (6-8 μm in diameter) and occupy the GCL, immediately below the IPL. They reside the central part of the olfactory bulb, where cell bodies are cluster together in horizontal sheets. They extend their dendritic arborisation through the IPL and EPL (Shepherd, 2004).

The dendrites of the granule cells are spiny and are divided in basal, proximal and distal dendritic domains. All these domains receives different input and output synapses, that define distinct function of the different dendritic domains in the neuronal circuits of the OB.

The basal domain result from deep branched processes that diffuse for some extension in the GCL (Shipley and Ennis, 1996). Together with the proximal dendrites, receive axo-dendritic input synapses from axon collaterals of the mitral cells and tufted cells and from centrifugal fibers from higher cortical areas (Kelsch et al., 2010).

The apical dendrite is subdivided in an unbranched segment emerging from the soma (proximal domain) followed by a branched segment (distal domain; Figure 1.5.).

The proximal dendrite is the portion of the apical dendrite near the soma, represented by the 15% of the total length of the apical dendrite. The distal dendrites form bidirectional dendro-dendritic synapses: they are intercepted by glutamatergic inputs from the lateral dendrites of mitral cells and tufted cells and release GABA that act on $GABA_A$ receptors located on the lateral dendrites of mitral cells and tufted cells. The dendro-dendritic synapses on the distal dendrites are the exclusive output of the granule cells, and are responsible for local inhibition of the projection neurons of the OB ((Kelsch et al., 2007); Figure 1.6.).

On the basis of morphological and molecular criteria, granule cells can be divided in: superficial, intermediate and deep granule cells ((Mori et al., 1983); (Greer, 1987); (Imamura et al., 2006)). Peripheral dendrites of superficial granule

cells ramify mainly in the superficial EPL, among the dendrites of tufted cells. Intermediate granule cells have dendrites that colonize all levels of the EPL (Shepherd et al., 2007). Deep granule cells have their dendritic arborization confined into the deep EPL, where they make synapses predominantly with the secondary dendrite of mitral cells.

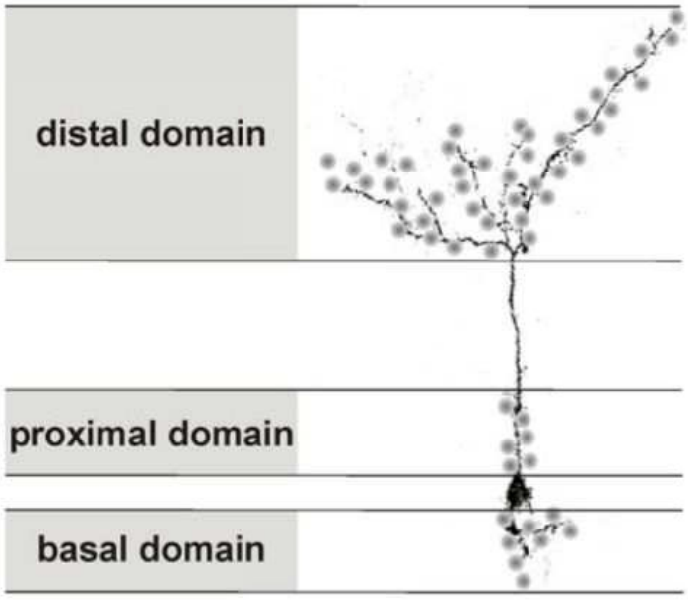

Figure1.5.: Schematic representation of the different domains of a GC. *(Kelsch et al., 2009)*

Another small population of inhibitory cells in the OB is represented by Blanes cells, large (20-25 μm in diameter) stellate-shaped interneurons with a short axon located in the GCL. Blanes cells are GABAergic cells, the action of which is still largely obscure. However, recent studies indicate that Blanes cells provide inhibition to granule cells by acting onto monosynaptic connection. The modulation of tonic feedfoward inhibition driven by Blanes cells activity seems to allow the encoding of short-term olfactory information (Pressler and Strowbridge, 2006).

periglomerular cells and granule cells constantly regenerate during the entire life of the animal. They originate from the subventricular zone (SVZ), surrounding the lateral ventricles, and from there they migrate tangentially along the rostral migratory stream (RMS) to reach the OB.

Once they reached the bulb they begin to migrate radially and they undergo a maturation process to become mature interneurons. Approximately two weeks after their generation, granule cells develop input excitatory synapses in their proximal

dendritic domain and only after several weeks, they establish output synaptic contacts on the lateral dendrites, that represent the dendro-dendiric synapses with mitral cells and tufted cells described above ((Whitman and Greer, 2007); (Kelsch et al., 2008); (Kelsch et al., 2010)). The latter are the only output inhibitory synapses formed by the granule cells on their targets, the site where they exert inhibition on their targets.

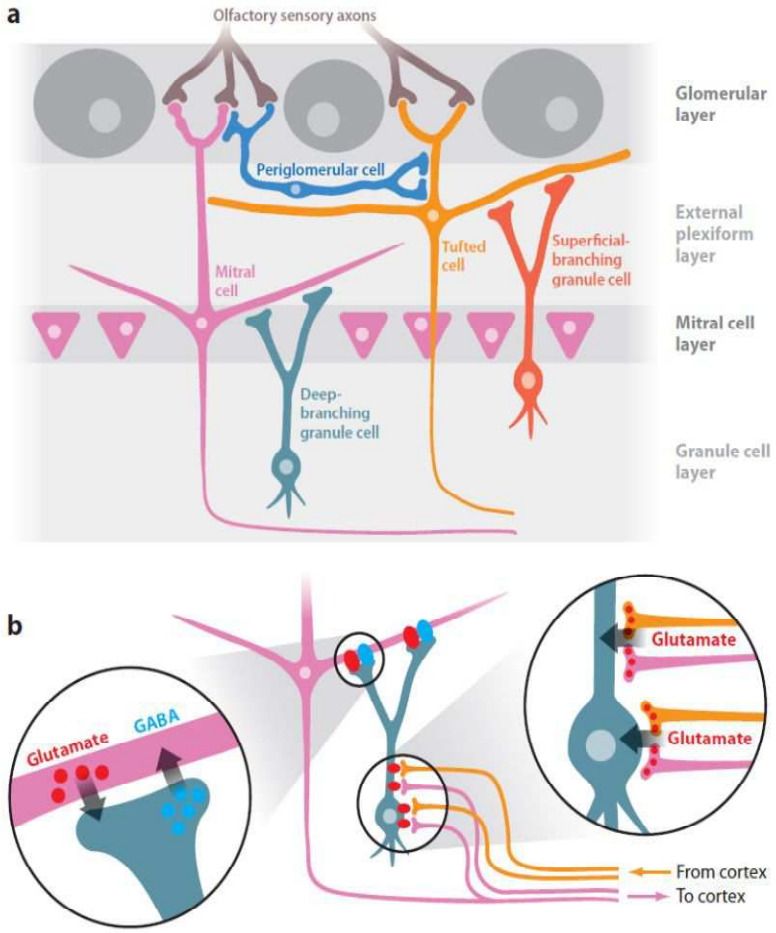

Figure 1.6.: The olfactory neuronal circuit. *(a) Synaptic organization of the olfactory bulb. (b) Dendro-dendritic synapses of granule cells (Kelsch et al., 2010).*

This sequential development of granule cell synapses, first the input synapses followed by several weeks by the output synapses, is thought to limit the disruption that integration of new cell could cause to the already existing circuits.

Inhibitory synapses are a fundamental component of the neuronal circuit: they play a critical role in shaping neuronal firing, in balancing excitation and inhibition of neuronal networks, and in coordinating correlated activity of ensemble of neurons.

1.3.2. Role of granule cells in shaping olfactory information

In the olfactory epithelium specific sets of odorant receptors expressed on the dendrites of peripheral OSNs are activated by odors. Sensory information is then transmitted to the OB. Within each glomerulus, OSN terminals excite the apical dendritic tufts of mitral cells and tufted cells (Bourne and Schoppa, 2017). mitral cells and tufted cells axons project through the IPL and GCL and collect within the LOT to actively propagate the incoming sensory information to several cortical and subcortical areas, such as the anterior olfactory nucleus, the primary olfactory cortex, and the piriform cortex. Other areas interested by bulbar innervations are the olfactory tubercle, that integrates chemical information and auditory signals, the amygdala and hypothalamus generate and integrate instinctive behaviors ((Shepherd, 2004); (Urban and Castro, 2010); (Mori and Sakano, 2011)).
In the mammalian brain, neuronal information processing critically depends on synaptic inhibition. In the OB, shaping incoming sensory information necessarily requires the pivotal activity of granule cells. Granule cells play a key role in optimizing olfactory discrimination and odor representation ((Mori and Shepherd, 1994); (Tan et al., 2010); (Adam et al., 2014)). Granule cells synaptic inhibition provides lateral inhibition that suppress the firing of adjacent unspecific mitral cells and tufted cells ((Cang and Isaacson, 2003); (Luo and Katz, 2001)). In this manner the perception of distinct odors can be tuned through the activation of the proper mitral cells and tufted cells narrowing the incoming sensory information ((Yokoi et al., 1995), (Fantana et al., 2008)).
Granule cells activity seems also fundamental to attenuate action potential propagation within mitral cells' lateral dendrites (Lowe, 2002) via graded recurrent inhibition that comes from granule cells spines and acts onto mitral cells dendrites following mitral cells excitation ((Isaacson and Strowbridge, 1998); (Schoppa et al., 1998)).

Granule cells has also a fundamental role in odor learning processes, by enhancing predisposition for long term potentiation (LTP) in the ascending connections from the OB to the piriform cortex (PC). Learning is thus enforced by reciprocal bulbar-cortical connections that undergo unique long-term modifications.

Potentiation of cortical projection to the granule cells enhances the inhibitory tone onto granule cell targets (i.e. mitral cells). The modulation of bulbar inhibition driven by LTP of cortical feedback inputs is required for proper encoding of sensory information. ((Gao and Strowbridge, 2009); (Cohen et al., 2011)).

Adult-born GABAergic interneurons and high cognitive functions of the bulbar circuitry have been propose to display a casual relationship. Many *in vivo* studies indicate that enhancement of postnatal neurogenesis in the olfactory system facilitate olfactory learning and memory. By contrast, defects in SVZ proliferation in adult mice dramatically impairs the execution of memory tasks ((Cohen et al., 2011); (Breton-Provencher et al., 2009); (Mandairon et al., 2011); (Alonso et al., 2012)).

The OB exhibits several oscillatory phenomena that span a wide range of frequency bands, in particular theta (4-10Hz), beta (15-40 Hz) and gamma (40-100 Hz) oscillations ((Adrian, 1942); (Kay et al., 2009); (Kay, 2014)). Interneurons play a key role in oscillatory phenomena not only in the OB but also in cortical and subcortical areas ((Bartos et al., 2002); (Buzsaki and Draguhn, 2004), (Dupret et al., 2008)). In particular, several findings strongly indicate that the gamma oscillation in the OB originate from reciprocal mitral cell–granule cell dendro-dendritic interactions ((Lagier et al., 2004); (Lagier et al., 2007), (Lepousez and Lledo, 2013); (Kay, 2014)). Gamma oscillation in the OB, as in other cortical and subcortical areas, contribute to several cognitive functions, in particular learning and memory ((Bartos et al., 2002); (Buzsaki and Wang, 2012)) .

The OB receives centrifugal projections from the piriform cortex, but also from several modulatory system, such as serotonin, noradrenaline and acetylcoline neuromodulators ((Li and Matsunami, 2011); (Markopoulos et al., 2012); (Boyd et al., 2012)).

These centrifugal axons form synapses electively on the basal and proximal dendrites of GCs (see above, paragraph 1.3.1), influencing the inhibitory circuitry of the OB and its role in shaping olfactory information. GCs therefore, integrate the incoming sensory stimuli (down-top sensory information) to the status of the individual (top-down neuronal information).

1.4. Neurogenesis in the Subventricular Zone

Neurogenesis is the combination of events that culminate with the production of newly generated neurons. Newborn neurons completely integrate in neuronal network as the result of a complex series of events including migration, maturation, target identification and synapse formation. These processes characterize the development from precursors to mature neurons.

The process of neurogenesis typically is present during embryonic and perinatal developmental stages, however, it persists in adulthood in two areas of the adult brain that retain the ability to generate new cells: the subgranular zone (SGZ) of the dentate gyrus in the hippocampus, that gives rise to excitatory glutamatergic neurons and the subventricular zone (SVZ) around the lateral ventricles that generate mainly inhibitory GABAergic interneurons.

Adult neurogenesis is evolutionarily highly conserved in all vertebrates, from fishes to mammals, including humans (Curtis et al., 2007).

The SVZ is a thin layer located in the medial and lateral walls of the lateral ventricles (LVs). It represents the largest germinal region in the adult mammalian brain (Mirzadeh et al., 2008). In this region, each day, thousands of neuronal progenitors constantly generate giving rise to adult-born precursors that colonize mostly the olfactory bulb (OB), but also other structures, such as the striatum and the neocortex (Inta et al., 2008).

The maintenance of the self-renewing, multipotent, state of the neuronal stem cells is achieved creating and supporting a specific microenvironment, that is the SVZ itself. Various factors contribute in the formation of the germinal niche, such as basic fibroblast growth factor (FGF2), Notch1, sonic hedgehog (SHH) and ciliary neurotrophic factor (CNTF), which all play important roles in neuronal stem cells maintenance and self-renewal (Chojnacki et al., 2003).

This vast repertoire of factors is not only involved in the maintenance of the niche, but also plays a critical role in the determination of the heterogeneity of the stem cells that compose the SVZ: in other words, several distinct neuron subtypes are generated in the SVZ. The composition of the germinal niche, therefore, contribute in determining the neuronal fate of precursor cells. The vast majority of SVZ-

derived neurons in the OB is represented by GABAergic granule cells (95%), while less than 3% of adult-born neurons maturate into periglomerular cells (Lledo et al., 2006). A small population of SVZ stem cells gives origin to juxtaglomerular glutamatergic cells (Brill et al., 2009).

Interestingly, not only neuronal precursors in the SVZ are regionally heterogeneous, but stem cells rising in different region of the ventricle walls generate distinct OB interneurons subtypes that are located in specific region of the OB (Lim and Alvarez-Buylla, 2016). For instance, the ventral portion of the SVZ is the site where deep granule cells and calbindin-positive periglomerular cells originate, whereas in the dorsal region of the SVZ superficial granule cells and TH-positive periglomerular cells are produced (Alvarez-Buylla et al., 2008). It is likely that the generation of a diversity of interneurons with unique morphological, chemical and physiological properties reside in the unique combinations of transcription factors locally provided by these subregions. The typical combination of transcription factors that affect the generation of a specific subpopulation may also contribute in the precise orchestration of the integration of adult-born interneurons into different OB circuits (Lledo et al., 2008).

1.4.1. Cellular composition of the Subventricular Zone

The SVZ is composed by four cell types (Figure 1.7.): astrocytes (expressing glial fibrillary protein, GFAP, and nestin), also called B-type cells; transit-amplifying cells (expressing nestin and distal-less homeobox 2, Dlx2), also called C-type cells; newly generated neurons called neuroblasts, or A-type cells (expressing doublecortin, DCX, polysialylated neural cell adhesion molecule, PSA-NCAM, and neuron-specific class III β-tubulin, Tuj1); ependymal cells (Alvarez-Buylla and Garcia-Verdugo, 2002).

Neuronal progenitors (B-type cells) in the SVZ resemble morphologically astrocytes and express astrocytic markers ((Doetsch et al., 1999); (Doetsch, 2003)). They express GFAP, as well as glutamate/aspartate transporter (GLAST) and brain lipid-binding protein (BLBP). From a morphological point of view, SVZ astrocytes

have end-feet on blood vessels, which is a common feature of gray matter astrocytes, but they also can directly contact the ventricular lumen, which represent a remarkable feature among brain astrocytes (Lim and Alvarez-Buylla, 2016).

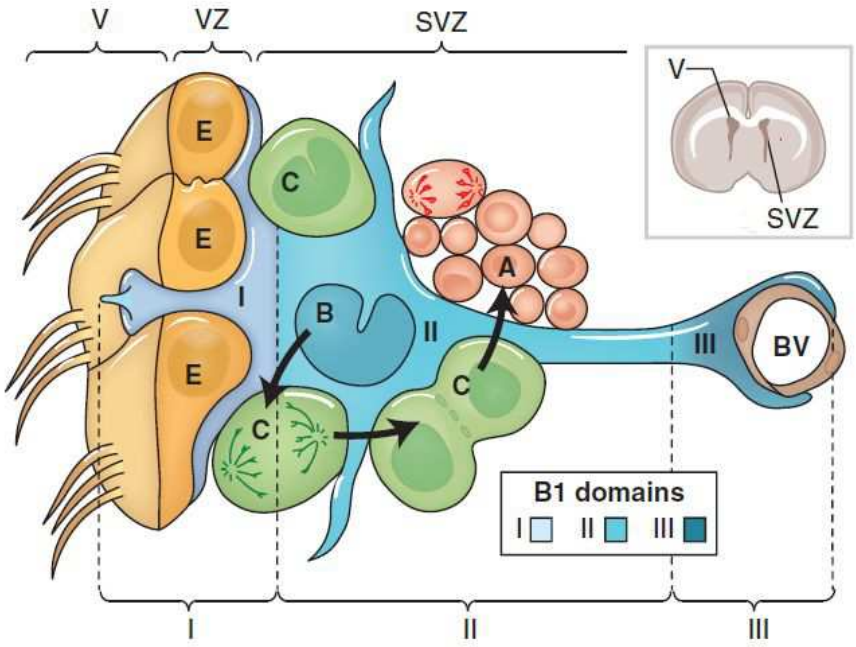

Figure 1.7.: Cellular composition of the subventricular zone (SVZ). *SVZ stem cells are represented by specialized astrocytes, also called B-type cells (blue). These can divide asymmetrically in transit amplifying cells, or C-type cells, that are rapidly dividing, transit ampliyfing cells (green), that generate A-type cells (red), the migratory neuroblasts. On the left ependymal cells are shown in yellow; on the right blood vessels in brown. (Modified from Lim and Alvarez-Buylla, 2016)*

B-type cells can exist both in a quiescent or in an active state (Codega et al., 2014). During their active state, cells continuously and slowly proliferate. B-type cells undergo asymmetric division for self-renewal and for generating C-type cells (Ortega et al., 2014). Postnatal B-type cells represent a residual pool of stem cells that derived from embryonic neuronal stem cells. During embryonic development a large population of stem cells undergoes division, but then enters a quiescent state until reactivated in postnatal life (Lim and Alvarez-Buylla, 2016). B-type cells seem to maintain intrinsic neurogenic competence and after birth they are reactivated by cell-extrinsic signals to guarantee postnatal generation of neurons. Most of the adult SVZ-derived cells differentiate into olfactory interneurons, but a minor population of cells in the SVZ eventually develop as non-neurogenic astrocytes and become mature astrocytes; In addition, the SVZ also host a small

number of oligodendrocyte precursors, which migrate into the corpus callosum (Menn et al., 2006).

B-type cells extend a thin cellular process between ependymal cells, contributing in the formation of the ventricular epithelium and helping in the maintenance of the architectural integrity of the ependimal cell layer (Doetsch et al., 1999; Mirzadeh et al., 2008). This integrity appears to be critical for the germinal function of the SVZ and for the proliferation of B-type cells themselves. The contact between B-type cells and Cerebro-Spinal Fluid (CSF) may play a role in the transduction of signalling molecules, exerting a key function in the regulation of the adult neurogenesis (Lim and Alvarez-Buylla, 2016). Indeed, several factors in the CSF were shown to regulate proliferation of newly generated cells.

C-type cells undergo fast proliferation, giving rise to a high complement of neuroblasts though symmetrical division (Ponti et al., 2013). One of the most studied regulator of the proliferation and differentiation of C-type cells is the Wnt-β-Catenin signaling (Adachi et al., 2007). β-Catenin signaling increases the pool of transit-amplifying cells promoting their proliferation and resulting in an overall increase in the number of adult-born interneurons in the OB (Kaneko and Sawamoto, 2009).

A-type cells are committed to the neuronal lineage. Neuroblasts form elongated cellular aggregates called chains, which are ensheated and supported by astrocyte-like cells, to progress through the brain parenchyma (Lois et al., 1996).

1.4.2. Factors that regulate neuronal stem cells proliferation

All the steps of cell proliferation and differentiation are finely regulated in the SVZ. Stem cells self-renewal, lineage commitment and the generation of divers neuronal population are tightly regulated by a vast set of transcription factors. In the SVZ, B-type cells express sex-determining region-Y (SOX2), a member of the SOX family of transcription factors (Ellis et al., 2004), that positively stimulates B-type cells self-renewal and maintenance (Shimozaki et al., 2012).

The proliferation of B-type cells appears to be regulated by insulin-like growth

factor 2 (IGF-2) that has been found in the CSF (Lehtinen et al., 2011).

Moreover, the basic helix-loop-helix (bHLH) transcription factor Achaete-schute homolog1 (ASCL1) is involved in the specification of both neuronal and glial lineages in C-type and a subset of B-type express ((Parras et al., 2004); (Kohwi et al., 2005)). In the adult mouse, SVZ-derived neuronal precursors express Dlx1/2 homeobox transcription factors (Batista-Brito et al., 2008). Mice carrying a null mutation for Dlx1/2 show severe impairments in the neurogenesis of both granule cells and periglomerular cells in the OB (Bulfone et al., 1998).

Adult neurogenesis in the SVZ is also modulated by several growth factors. Fibroblast growth factor 2 (FGF-2) and transforming growth factor α that are secreted by local astrocytes (TGF-α; (Zheng et al., 2004)) have been shown to provide proliferative signals for the SVZ niche, stimulating neurogenesis and they also impact onto neuronal differentiation (Anderson et al., 2001). Ciliary neurotrophic factor (CNTF) seems to increase Notch1 expression that in turn has a positive effect in stem cells proliferation, likely increasing neuronal progenitors self-renewal (Chojnacki et al., 2003). SVZ neuronal stem cells proliferation has been shown to be promoted by heparin-binding EGF (HB-EGF) administration into the ventricle as well as via vascular endothelial growth factor (VEGF) ventricular infusion (Jin et al., 2002). Furthermore, another trophic factor that has been reported to stimulate SVZ proliferation and OB neurogenesis is BDNF (Zigova et al., 1998). On the other hand, neurotrophin-3 (NT-3) signaling in neuronal progenitors causes the rapid phosphorylation of endothelial nitric oxide synthase (NOS), leading to the production of nitric oxide (NO), which reduces stem cells proliferation acting as a cytostatic factor (Delgado et al., 2014). Moreover, platelet-derived growth factor (PDGF) signaling in the SVZ contribute in guaranteeing the proper balance between neuronal and oligodendrocyte production that is essential in sustaining adult neurogenesis (Chojnacki et al., 2011).

In addition, a large variety of morphogens and mitotic factors modulate the maintenance of adult neurogenesis in the SVZ: in quiescent B-type cells active Sonic Hedgehog (SHH) has been detected in the ventral SVZ, while in stem cells in the dorsal SVZ SHH pathway seems to be silent. This different regulation could give, at least in part, an epigenetic explanation to the different B-type identities

which appear restricted to specific regions. For instance, in the SVZ the regional specification of neuronal precursors may be underlined by different level of SHH signaling (Ihrie et al., 2011). A contribution to the regulation of the germinal niche is provided by the bone morphogenetic protein (BMP). BMP signalling favours astrocytes differentiation at the expense of neurogenesis and oligodendrogenesis (Gross et al., 1996). To counterbalance BMP effects ependymal cells locally secrete NOGGING, a BMP antagonist, thus promoting neurogenesis in the SVZ and contributing to the neurogenic niche (Lim et al., 2000).

The Wnt family of secreted signalling molecules impacts onto every step of neurogenesis in the SVZ, from stem cell maintenance, to cell proliferation and differentiation, from cell migration to axon guidance (Ille and Sommer, 2005). Both canonical and non-canonical signalling pathways of Wnt proteins affect adult neurogenesis in the SVZ, defining Wnt proteins as key extrinsic factors for promoting the proliferation of B-type cells and OB neurogenesis (Adachi et al., 2007), as well as enhancing neuroblasts proliferation (Ikeda et al., 2010).

The Notch receptor is a large transmembrane protein. Notch1 and two of its ligands, Jagged1 and Delta1, are expressed in the adult SVZ (Givogri et al., 2006). In the SVZ, Notch signaling contribute in the maintenance of the stem cells pool by preventing neuronal differentiation (Gaiano and Fishell, 2002). Notch1 signaling may be activated in B-type cells by accumulation of adult-born neuroblasts expressing Jagged1 or Delta1, that leads to the suppression of differentiation and the potentiation of self-renewal, creating a feedback signal to ensure the stability of the germinal niche (Katoh and Katoh, 2006).

Also Eph receptors and their ephrin ligands control SVZ neurogenesis through a feedback mechanism (Holmberg et al., 2005). A-type and C-type cells express EphrinA2, while B-type and ependymal cells express the EphA7 receptor. B-type cells expressing EphA7 may negatively regulate the proliferation of A-type and C-type cells via reverse signaling through ephrinA2, since disruption of the interaction between ephrinA2 and EphA7 has been shown to stimulate SVZ proliferation, (Holmberg et al., 2005).

Also blood vessels that penetrate into the SVZ contribute in regulating adult neurogenesis. All SVZ cell types are in extensive contact with the vascular basal

lamina which is rich in laminin and collagen-1. The maintenance of B-type cells and neurogenesis is supported by the basal lamina by modulating the concentration of cytokines and growth factors derived from local cells, (Alvarez-Buylla and Lim, 2004).

Furthermore, blood-derived factors seem to regulate SVZ neurogenesis (Leventhal et al., 1999). Indeed, B-type cells frequently contact endothelial cells via a specialized basal end-foot, and clusters of B-type and actively dividing C-type cells are associated with blood vessels that are more leaky (Tavazoie et al., 2008).

A variety of different neurotransmitters, both originating locally or in other regions of the brain, has a role in the regulation of SVZ neurogenesis. Serotonin (5-HT) regulates cell proliferation acting on serotoninergic G-protein coupled receptor 5HT2C receptors expressed in the SVZ ((Banasr et al., 2004); (Tong et al., 2014)).

Dopamine is also involved in SVZ adult neurogenesis regulation. The SVZ receives dopaminergic innervation from the midbrain, and C-type cells are the predominant population of cells expressing D2 recptors and D3 receptors (Kim et al., 2010). Consistently, dopaminergic denervation results in decresed SVZ proliferation (Hoglinger et al., 2004).

By contrast, acetylcholine innervation of the SVZ stimulates neuroblasts production (Paez-Gonzalez et al., 2014).

Moreover, nitric oxide (NO) has been proposed to act to restrict adult neurogenesis, since disruption of NO synthase (NOS) in nitrergic neurons in close proximity to the SVZ leads to increased neurogenesis (Moreno-Lopez et al., 2004).

Also GABA secreted by SVZ cells is a regulator of adult neurogenesis. The effects of GABA activity in the SVZ will be extensively described below (paragraph 1.8.1.)

1.5. The migration along the Rostral Migratory Stream

In the SVZ, A-type cells coalesce into elongated clusters, forming chains of cells that begin to migrate tangentially along the rostral migratory stream (RMS) to reach the OB (Figure 1.8.; Lois et al., 1996). The tight association of neuroblasts into

chains is the result of the connection between transmembrane glycoproteins (i.e. cadherins, integrins) and the extracellular matrix (ECM). Neuroblasts within chains crawl onto each other, forming discontinuous adherent junctions, as they use each other as a substrate to progress along the RMS (Kaneko et al., 2017).

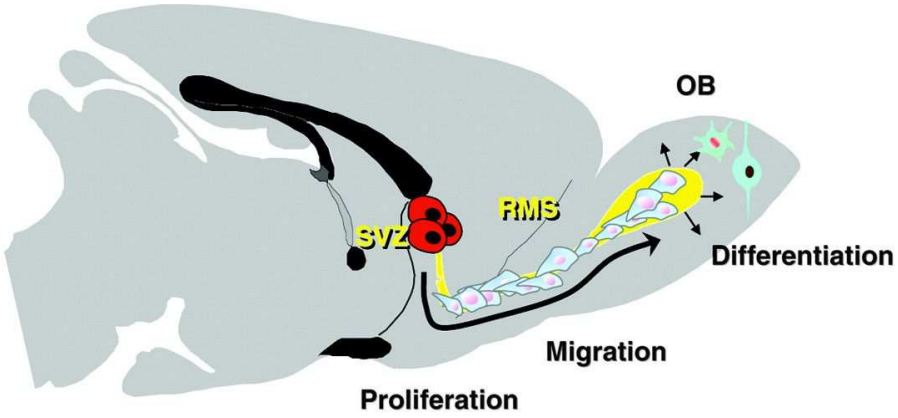

Figure 1.8.: Neurogenesis process from the subventricular zone to the olfactory bulb. *A sagittal view of a rodent brain showing the sites of proliferation (SVZ), the route of migration (RMS) and the final destination and differentiation (OB) of newly generated inhibitory interneurons. (Modified from (Abrous et al., 2005)).*

Neuroblasts' chains are supported along the entire pathway of migration by tubular structures made by specialized astrocytes. This glial scaffold and the presence of chemotactic factors, both attractive and repulsive secreted by the surrounding cells, allow them to progress along the RMS, performing their typical tangential migration pattern (Lledo et al., 2006).

The migration process results from intricate pathways depending both on cell-autonomous factors and extrinsic regulation provided by the local environment ((Lemasson et al., 2005; Lledo and Saghatelyan, 2005); (Lledo et al., 2006); (Belvindrah et al., 2011)).

At the cellular level, the migration is mainly due to continuous rearrangements of the actin cytoskeleton, located in filopodia, that explore the extracellurar environment to detect molecular signals, such as myelin, collapsin/Sema3A, ephrin 5A, ephrin-B, Slits/Robo, ambient GABA.

1.5.1. Mechanisms of progression along the rostral migratory stream

Along their migration neuronal precursors display typical morphological features that reflect cytoskeletal dynamics going on in the cell this is not clear. Migrating neuroblasts have bipolar morphology, with a long leading process and a short trailing process. Neuroblasts translocation occurs in a saltatory manner that comprehends: 1) leading-process extension; 2) swelling formation and centrosomal migration; 3) somal translocation (Figure 1.9.; (Schaar and McConnell, 2005)). Embryonic bipolar-shaped migrating neuroblasts exhibit this saltatory manner of progression that then persists in the postnatal brain (Tsai et al., 2007).

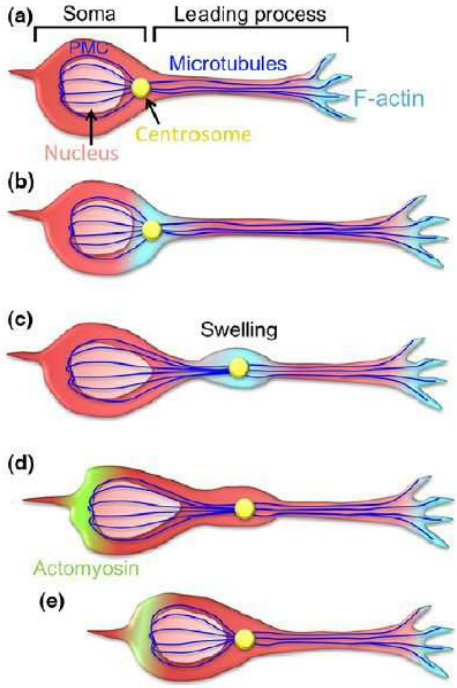

Figure 1.9.: The saltatory nature of neuroblasts' translocation. *(a) Basic morphology of a migrating neuroblast; (b) extension of the leading process; (c) swelling formation and centrosome translocation; (d, e) somal translocation. Microtubules are indicated in dark blue, areas enriched in F-actin in light blue, centrosome in yellow and the areas of acto-myosin contraction in green. (Modified from Kaneko et al., 2017).*

For migrating cells is critical to determine the directionality of progression. The proper directionality of migration is reached by the dynamics of the leading-process (Martini et al., 2009). In neuronal precursors, filamentous F-actin accumulates at the tip of leading process during extension (Shinohara et al., 2012). Small Rho-GTPases and their downstream effectors modulate F-actin dynamics and

accumulation. Microtubules are also involved in the elongation of the leading process. Destabilization of microtubule with pharmacological agents, such as nodocodazole, abolishes the extension of the leading process (Schaar and Mc Connell, 2005).

Swelling is a transient enlargement of the cytosol in the proximal part of the leading edge, near the soma. The swelling contains intracellular organelles such as the centrosome, Golgi apparatus and mitochondria (Bellion et al., 2005). The centrosome acts as a microtubule-organizing center and governs the microtubule networks (Tsai et al., 2007). The fine orchestration of microtubules operated by the centrosome is essential in migrating neuroblasts to complete soma progression, since after the swelling forms, the centrosome translocates into it, then trailing the soma after it (Schaar and McConnell, 2005).

1.5.2. Intrinsic factors regulating neuronal precursors migration

The complex process of cell migration requires a highly tuned regulation that coordinates all the steps that allow neuroblast progression. Several cell-autonomous factors cooperate to achieve this very precise regulation of the mechanism of translocation in SVZ-derived cells along the RMS. For the formation and extension of the leading-process, both actin and microtubule dynamics appear to have a key role, and the coordinated activity results ultimately in the saltatory pattern of migration (Kaneko et al., 2017). It is worth noting that to achieve the saltatory movement, the cytoskeletal machinery need to be precisely regulated in the spatiotemporal dimension, in the migrating neuroblasts.

During leading-process extension, at the tip of the leading-process has been detected high Rac1 activity (Hikita et al., 2014). Proper formation and extension of the leading process requires Rac1 and Vav3, a guanine nucleotide exchange factor (GEF) that can activate Rac1 (Khodosevich et al., 2009).

Drebrin is an F-actin binding protein that is thought to link microtubule to F-actin in filopodia. Cyclin-dependent kinase 5 phosphorylation of Drebrin is thought to stabilize this interaction (Worth et al., 2013), allowing proper dynamic of the

leading process.

The swelling formation and centrosomal migration is controlled by local RhoA signalling (Shinohara et al., 2012). Depending on the migration phase, RhoA is activated at the swelling or at the proximal leading-process, where it enhances the frequency of swelling formation. RhoA activation is limited by Gem-interacting protein (Gmip), a RhoA-specific GAP, which contributes in conferring to migration its saltatory nature (Ota et al., 2014).

RhoA signalling also regulate actomyosin dynamics that is required for somal translocation. During somal translocation F-actin accumulation has been observed in the proximal part of the leading-process and at the rear of the cell, concomitantly with Myosin II activation (Schaar and McConnell, 2005; Shinoara et al., 2012). Furthermore, application on migrating neuroblasts of the Rho-associated protein kinase (ROCK) inhibitor, Y27632, or of the myosin II inhibitor, Blebbistatin, completely hampers somal translocation (Schaar and McConnell, 2005; Shinoara et al., 2012), supporting the idea that actomyosin contractions mediated by RhoA signalling governs somal translocation in migrating neuronal precursors (Kaneko et al., 2017).

In coordination with actomyosin contractions, doublecortin (DCX) was shown to be required for nuclear translocation (but not for the centrosome position) and maintenance of bipolar morphology of migrating neuroblasts. DCX results a critical regulator of neuroblast progression mutation of DCX gene, in humans, result in a severe defect of neuroblast migration, named lissencephaly (Koizumi et al., 2006). In migrating neuroblasts, the soma proceeds by following the leading-process through mechanisms of nucleation/depolimerization of the microtubles (Marx et al., 2013).

Also a vast set of adhesion molecules participate in the regulation of the migration along the RMS. To progress properly, the adhesion between adjacent migrating neuroblasts must be appropriately and dynamically regulated. For instance, neuronal precursors in the RMS express the cell-adhesion molecules polysialylated-neural cell adhesion molecule, PSA-NCAM (Chazal et al., 2000), and N-chaderin (Yagita et al., 2009). It has been shown that knocking down the expression of these molecules deeply alters chains formation (Chazal et al., 2000;

Yagita et al., 2009).

Moreover, maintenance of neuroblast chains is controlled by the signalling coupled to the receptor of sphingosine 1-phosphate, a bioactive lipid that upregulates NCAM1 and β1-integrins (Alfonso et al., 2015) and to the P2Y1 purinergic receptor. The latter is a G-protein coupled receptor. When activated by extracellular ATP it enhances N-cadherin and β-catenin expression via PKC activity (Cao et al., 2015). β1 class integrins are also expressed in SVZ-derives neuronal precursors and play a role in chains formation (Belvindrah et al., 2007). Laminin, an extracellular matrix (ECM) protein, that covers neuroblast surface, has been proposed to act as a ligand for β1 integrin-mediated chain formation (Belvindrah et al., 2007).

Although neuronal precursors are closely associated with each other within chains, they do not display synchronized saltatory movements. Resting precursors undergo a dynamic morphological change that is characterized by an indentation in the cell body. Indeed, Rac1 was reported to be responsible for the formation of the indentation, that is prevented by Rac1 mutation, hampering migration of resting cells. It was proposed that the dynamic change of resting progenitors, mediated by Rac1 is functional to create a path for the active migrating cells (Hikita et al., 2014).

1.5.3. Extrinsic factors regulating neuronal precursors migration

Cell migration is affected not only by intrinsic cellular factors, but also by extracellular cues such as guidance molecules, trophic factors and ions ((Snapyan et al., 2009); (Leong and Turnley, 2011); (Turner and Sontheimer, 2014); (Capilla-Gonzalez et al., 2015)).

Directional cues provided along the migratory pathway guide the long-distance migration from the SVZ to the OB. Diffusible proteins produced in the OB such as Prokineticin-2, Netrin1 and glial cell line-derived neurotrophic factors are chemoattractant for neuroblasts, suggesting that these factors might direct neuroblasts' migration toward the OB (Murase and Horwitz, 2002). Surprisingly, neuroblasts' migration along the RMS is not affected by surgical removal of the OB

(Bagley and Belluscio, 2010), suggesting that other cues elaborated inside the RMS can direct the migration of neuroblasts.

For instance, neuroblasts are kept inside the RMS by hepatocyte growth factor (HGF) activity. HGF, expressed throughtout the migratory pathway, acts as a chemoattractant for migrating neuroblasts (Garzotto et al., 2008). SHH attracts and regulates the complement of migrating cells into the RMS (Angot et al., 2008).

Chemorepellents act from the proximal portion of the RMS and provide a contribution to regulate the directionality of migrating cells toward the OB. Slit2, that has been detected in the CSF, is produced in the choroid plexus and medial septum (Sawamoto et al., 2006). The coordinated beating of ependymal cilia establish a directional flow of CSF, leading to the formation of a concentration gradient of Slit2 in the lateral ventricles and in the surrounding tissue. This gradient promotes the exit of neuronal precursors from the SVZ to enter the RMS, thus pushing neuroblasts to migrate rostrally (Sawamoto et al., 2006).

Taken together, it is clear that the migration of neuroblasts from the SVZ to the OB is finely regulated by the orchestration of attractive and repulsive signals throughout the RMS (Kaneko et al., 2017).

ECMs, some of which produced by the specialized astrocytes, are highly expressed along the RMS. ECM, such as tenascin, proteoglycans and laminin, play a prominent role in regulating the motility of neuroblatasts toward the OB. (Saghatelyan et al., 2004). Neuroblasts, expressed also integrins, cell surface molecules that can bind to several ECM proteins suggesting that the integrin-ECM interaction can contribute in governing neuroblasts motility. The mechanism underpinning this process remain elusive (Belvindrah et al., 2007). Matrix metalloproteinase (MMP), a zinc-dependent proteolytic enzyme expressed by neuroblasts, has a key role in regulating cell progression along the RMS (Barkho et al., 2008). Indeed, blocking MMP activity hampers radial migration in the OB (Barkho et al., 2008).

Among extrinsic stimuli that govern the long-distance migration along the RMS, also some neurotransmitters play an important role. Serotoninergic axons, which originate in the raphe nuclei, project to the RMS, and contact the chains of SVZ-derived cells (Garcia-Gonzalez et al., 2017). Serotonin provided by these axons

coordinate velocity and directionality of migrating neuroblasts, acting on the ionotropic 5HT3A receptor. The activation of this receptor mediates large calcium influxes that are thought to exert a modulatory action on the speed and the directionality of neuronal precursors during their translocation (Garcìa-Gonzalez et al., 2017).

GABA, secreted by migrating neuroblasts themselves, tightly regulates neuroblast progression along the RMS. The regulatory role of GABA in the migration process will be extensively examined below (paragraph 1.8.2.).

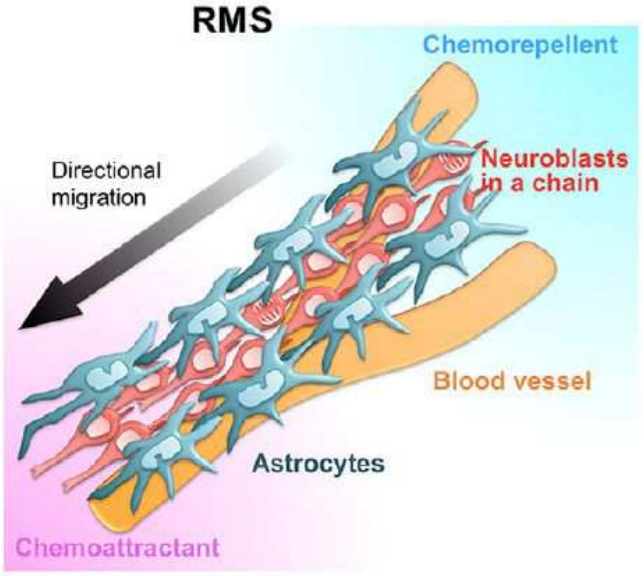

Figure 1.10.: Mechanisms that regulate the long-distance migration of neuroblasts. *The interplay between gradients of diffusible repulsive (light blue) and attractive (pink) cues guide neuroblasts (red) along the RMS. They move through a tunnel formed by specialized astrocytes (dark blue) and blood vessels (orange) run parallel to the stream. (Modified from Kaneko et al., 2017).*

Along the RMS, neuroblasts aligned in chains, are enwrapped by tubular structures formed by specialized astrocytes (Lois et al., 1996). Radial glia in the embryonic brain gives rise these astrocytes (Alves et al., 2002). The primary function of these astrocytic tunnels is to provide a scaffold that makes efficient and fast the progression of neuroblasts toward their target, i.e. the OB.

Slit-Robo signalling is critically involved in the maintenance of the tunnel-like structure. Robo is a transmembrane receptor expressed by astrocytes in the SVZ and RMS. Neuronal precursors secrete Slit1, a diffusible ligand for Robo2, that control the distribution of Robo-expressing astrocytes and their morphology, to

ensure the formation of the astocytic-tunnel that speed up the progression of neuroblasts (Kaneko et al., 2010).

Specialized astrocytes along the RMS, are also able to secrete or trap soluble factors, including GABA and BDNF. In this manner they exert a modulatory effect on neuroblast migration by creating and maintaining micro-gradients, along the migratory path, of diffusible molecules such as trophic factors, guidance molecules and neurotransmitters (Figure 1.10.; (Bolteus and Bordey, 2004); (Snapyan et al., 2009)). Furthermore, they control survival of migrating neuroblasts through ephrin/Eph signaling (Conover et al., 2000) and NMDA receptor-mediated glutamatergic signaling (Platel et al., 2010).

In addition, astrocytes control the development of the vasculature that surrounds the RMS via VEGF signalling. Blood vassels contribute in supporting the migratory path acting as a scaffold for migrating neuroblasts in the RMS (Bozoyan et al., 2012).

1.5.4. The switch to radial migration into the olfactory bulb

Once neuronal precursors reach the OB, they detached from the tangential chains and begin to migrate radially toward more superficial layers of the olfactory bulb. This change in the directionality is modulated by Reelin ((Hack et al., 2002); (Pappas et al., 2003)), TenascinR (Saghathelyan et al., 2004; (David et al., 2013)) and Prokineticin 2 (Ng et al., 2005).

Detachment of SVZ-derived cells from the chains involves also reduced expression in sphingosine 1-phosphate receptor 1, which regulates adhesion between neuroblasts (Alfonso et al., 2015). Noteworthy, the expression of Reelin and TenascinR is regulated by sensory activity (Saghathelyan et al., 2004). It has been shown that odor deprivation reduced the expression of these proteins, suggesting that sensory activity triggers radial migration. Along the radial migration they undergo a precisely orchestrated series of morphological and electrophysiological changes to become fully mature interneurons.

The final goal is the formation of correct connections within already

existing neuronal circuits ((Petreanu and Alvarez-Buylla, 2002); (Carleton et al., 2003); (Belvindrah et al., 2011)).

1.6. Development of adult-born granule cells

After completing their radial migration immature interneurons reach their layer of final destination within the OB. In the OB neuronal precursors differentiate into one of the GABAergic interneurons subtypes: granule cells and periglomerular cells expressing eventually calretinin, or calbinding, or TH (Batista-Brito et al., 2008); a small population of precursor cells differentiate into glutammatergic juxtaglomerular neurons (Brill et al., 2009). Mature adult-born interneurons in the OB exhibit dendritic patterns, synaptic targets and chemical markers expression in a layer-specific manner (Kelsch et al., 2007; Batista-Brito et al., 2008).
To analyse the morphology of the newly generated cells in respect to their date of birth, Petreanu and Alvarz-Buylla transfected neuronal precursors in the SVZ with retrovirus expressing alkaline phosphatase (Petreanu and Alvarz-Buylla, 2002), The maturation of adult-born granule cells in the OB was subdivided in five distinct and subsequent classes (Figure 1.11.):

- Class 1 (2-7 days after injection): neuroblasts in tangential migration. These cells are present almost exclusively along the RMS. In this stage cells present an elongated leading-process that emerges from a slightly stretched soma.

- Class 2 (5-7 days after injection): neuroblasts in radial migration. These cells still have a soma with stretched morphology; however, they present a longer process that often bifurcate, and emit some branches.

- Class 3 (9-13 days after injection): immature granule cells. At this time point cells show a single process that likely will become the future apical dendrite. This immature apical dendrite is still unbranched and does not extend over the mitral cell layer. Moreover, in this stage immature granule cells begin to develop basal dendrites.

- Class 4 (11-22 days after injection) granule cells continue their maturation. At

this time point interneurons present a branched dendrite without spines, which extend through the external plexiform layer.

- Class 5 (15-30 days after injection) granule cells elaborate spines. In this stage GABAergic interneurons have completed their morphological maturation and present functional spines.

The continuous arrival of newborn cells in the OB requires a mechanism of selection and elimination of part of the complement of new interneurons to avoid bulbar hypertrophy. The final goal of this process of elimination is the maintenance of a stable population of GABAergic interneurons in the OB. To accomplish this goal, half of the newborn cells are eliminated between 15 and 45 days after their generation in the SVZ. Most adult-generated neurons that survive this period of cell death will survive for several months and become indistinguishable from pre-existing neurons (Lemasson et al., 2005).

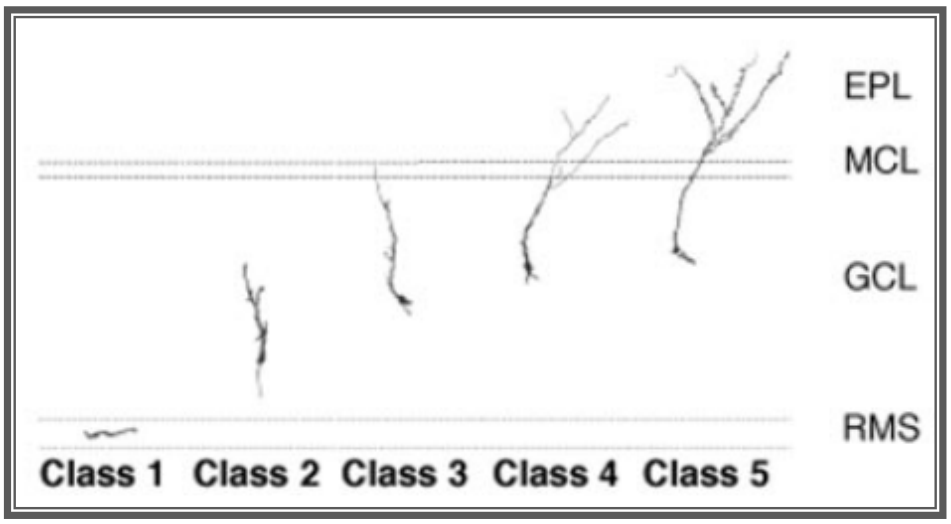

Figure 1.10.: Developmental stages of adult-generated granule cells. *Abbreviations: EPL, external plexiform layer; MCL, mitral cell layer; GCL, granule cell layer; RMS, rostral migratory stream (Petreanu and Alvarez-Buylla, 2002).*

The proliferation, differentiation, maturation and survival of the newly generated cells depends, at least in part, on sensory stimuli coming from the olfactory epithelium and on the activity of neuronal circuitry within the OB.

Both SVZ proliferation (Alonso et al., 2008) and survival of newly generated granule cells (Bovetti et al., 2009) are enhanced by long-term exposure to an

odorant-enriched environment. Similarly, active sensory experience in mice, such as an associative olfactory learning, has been shown to increase the complement of newly generated granule cells in the OB. Protracted sensory deprivation reduced the survival of newly generated cells ((Winner et al., 2002); (Yamaguchi and Mori, 2005)). Sensory experience modulate also the survival of periglomerular cells. In turn, odor learning and memory is strictly regulated by adult-generated cells ((Bardy et al., 2010); (Lazarini and Lledo, 2011); (Lepousez et al., 2013)).

1.7. The relevance of adult neurogenesis in olfaction and brain activity

The function of adult neurogenesis is still not completely understood. Although, newly generated interneurons are likely to be involved in (1.) maintain and stabilize the structural architecture of the OB, substituting loss interneurons with new ones. Furthermore, adult neurogenesis has been proposed to modulate (2.) refinement of sensory response, as well as other olfactory function, such as odorant discrimination and (3.) olfactory learning and memory ((Lledo et al., 2006); (Lazarini and Lledo, 2011); (Alonso et al., 2012)).

Changes in synaptic connectivity between neurons are the functional basis of learning and memory in the adult brain, since they allow to encode and store new memories while erasing past events and experience, which are no more useful (Fusi et al., 2005). Neurogenesis is an extreme form of synaptic plasticity that creates a constant influx of new neurons in the pre-existing circuits. In order to accommodate the new cells, the existing connections have to undergo a continuous remodelling (Sailor et al., 2017).

In addition, odor discrimination and perceptual learning are improved by the continuous recruitment of adult-born interneurons. New granule cells provide a mechanism to modulate the strength and the synchrony of firing activity of mitral cells that convey convergent sensory information, helping to divide similar but different stimuli. In turn, the survival of granule cells can be modulated by olfactory experience, improving perceptual learning (Wilson and Stevenson, 2003).

Changes in OB network activity might translate active sensory processing in perceptual learning, associative learning and memory formation, all processes related to high cognitive functions (Mandairon and Linster, 2009). Associative olfactory learning, olfactory fear conditioning, olfactory perceptual learning and long-term olfactory memory seem to demand the supply of new neurons ((Lazarini et al., 2009); (Valley et al., 2009)), suggesting a key role for adult neurogenesis in linking network plasticity and olfactory processing.

Blocking bulbar neurogenesis before and/or during odor enrichment prevents olfactory perceptual learning, suggesting that bulbar neurogenesis is directly correlated to short-term olfactory memory ((Rochefort et al., 2002); (Wilson and Stevenson, 2003)). Thus, adult-generated interneurons are required in the formation and shaping of olfactory learning and memory (Lazarini and Lledo, 2011).

Recently, it has been proposed that the generation of new neurons in the postnatal frontal lobe, including the prefrontal cortex, might be involved in evolutionarily acquired brain function in humans ((Sanai et al., 2011); (Paredes et al., 2016)). In the past few years a growing body of evidence pointed out that the postnatal SVZ-derived cells migration process occurs in all mammals, from rodents to monkeys, it takes place, also in human infants, at least for several month after birth ((Sanai et al., 2004); (Bedard and Parent, 2004)). This postnatal time window is of crucial importance in the development and in the plasticity of the human brain ((Hensch, 2004); (Paredes et al., 2016)). SVZ-derived interneurons migrate two ventral routes: the rostral migratory stream (RMS) to the OB and the medial migratory stream MMS to the frontal lobe and the medial prefrontal cortex a cortical structure fundamental for social and cognitive functions ((Sanai et al., 2011); (Wang et al., 2011); (Paredes et al., 2016)). Given the importance of postnatal GABAergic interneurons development for the functioning of the brain, the processes of neurogenesis and migration of immature neurons in infants represent a potential targets of neurological injuries affecting neonates (Sanai et al., 2011).

1.7.1. Adult neurogenesis in pathological conditions

Over the past years it has been proposed that alterations in adult neurogenesis may represent a hallmark in different neurodegenerative diseases including Parkinson's disease, Alzheimer's disease, and Huntington's disease (Winner and Winkler, 2015). Many studies showed that in several mouse models of neurodegenerative diseases impaired adult neurogenesis could be possibly linked with the onset of the pathology ((Winner et al., 2011); (Marxreiter et al., 2013); (Lazarov and Marr, 2010); (Marlatt and Lucassen, 2010); (Lazic et al., 2006)).

Only few studies have been conducted on post-mortem brains from humans patients. A significant reduction in the proliferation of progenitor cells was reported in the human SVZ of Parkinson's disease ((Hoglinger et al., 2004); (O'Keeffe et al., 2009)). In addition, post-mortem analysis of brains of Hungtinton's disease patients, revealed the proliferation of SVZ-derived stem cells, with a dilatation of the germinal niche ((Curtis et al., 2003); (Curtis et al., 2005)). However, in mouse models of Alzheimer's disease a compromised proliferation in hippocampal neuronal progenitors have been reported (Jin et al., 2004) accompanied by an altered synaptic activity and plasticity (Bossers et al., 2010).

Surprisingly, adult brain neurogenesis can be triggered by various brain insults, including stroke, neurodegenerative diseases and trauma. In these pathological conditions the loss of neurons is accompanied by the appearance of newly generated neurons in and around the damaged area (Kaneko and Sawamoto, 2009). Consistently, after neuronal death induced by ischemic stroke in mice, the arrival of ectopic migrating neuronal precursors has been observed (Liu et al., 1998).

Understanding the mechanisms that govern neuronal generation in physiological and pathological conditions, would offer a unique opportunity to improve the treatment of neurodegenerative diseases and the loss of neurons after acute damage (Kaneko and Sawamoto, 2009).

1.8. The role of GABA in regulating adult neurogenesis

GABA is the major inhibitory neurotransmitter in the mammalian central nervous system. GABA activity mainly provide inhibitory stimuli to synapses, thus exerting a pivotal role in maintaining proper balance between excitation and inhibition that is critical to preserve the excitability and the stability of neuronal networks and its normal functioning.

The polarity of the response that GABA elicits in target neurons is not univocal but critically regulated by intracellular chloride concentration, that in turn is modulated by specific cotransporters. The Na^+-K^+-$2Cl^-$ co-transporter, NKCC1, that favours intracellular high concentrations and leads to depolarizing GABA responses, because of a reversal potential for chloride that is at more depolarized level than the resting membrane potential. The K^+-Cl^- co-transporter, KCC2, activity results in low intracellular chloride, leading to hyperpolarizing GABA responses (Figure 1.11.; (Ben-Ari, 2002)).

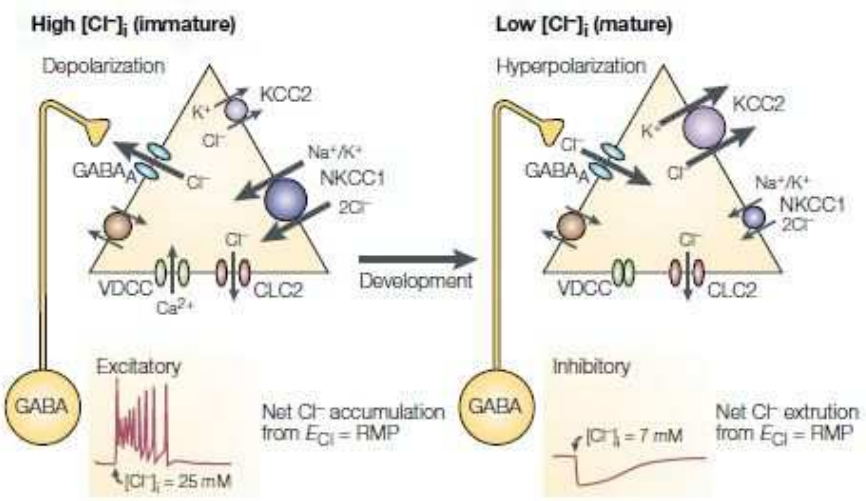

Figure 1.11.: Developmental changes in intracellular chloride are determined by downregulation of NKCC1 and upregulation of KCC2. *NKCC1 expression is predominant in immature neurons (left), maintaining relatively high* ***intracellular chloride****; in these cells $GABA_A$ receptors activation generates a depolarizing response. KCC2 is overexpressed in mature neurons (right), lowering* ***intracellular chloride****, leading to GABA hyperpolarizing response in these cells. Abbreviations: CLC2, voltage-gated chloride channels; VDCC, voltage-dependent calcium channels; E_{Cl}, chloride reversal potential; RMP, resting membrane potential (Ben-Ari, 2002).*

Therefore, the prevalent expression of one of the two chloride co-transporters, determine the shift in the action of GABA, from excitatory to inhibitory. This

switch play a key role in neuronal maturation (Ben-Ari, 2002).

The activation of $GABA_A$ receptors elicit a depolarization and an increased concentration of intracellular calcium, in immature, but not in adult, neurons in a wide range of brains structures, including the hippocampus (Gao and van den Pol, 2001), in the neocortex ((Maric et al., 2001); (Kirmse et al., 2015)), in the hypothalamus (Obrietan and van den Pol, 1999), in the spinal cord (Vinay and Clarac, 1999), in the ventral tegmental area (Ye, 2000), and in the cerebellum (Eilers et al., 2001). The activation of $GABA_A$ receptors has been shown to induce a strong positive driving force also in migrating neuroblasts along the adult RMS ((Bolteus and Bordey; 2004); (Mejia-Gervacio et al., 2011)).

Furthermore, GABA itself is thought to mediate the switch in the expression of the co-transporters, triggering the expression of KCC2 (Ben-Ari, 2002). The expression of KCC2 appears to be triggered by miniature postsynaptic currents (PSCs), which are generated by the action-potential-independent quantal release of GABA, and are essential for the establishment of functional synapses ((Wall and Usowicz, 1997); (Wollman et al., 2018)).

GABA has been proposed to exert many, sometimes conflicting, effects on neuronal proliferation, migration and differentiation in the developing brain ((Bolteus and Bordey, 2004); (Bortone and Polleux, 2009); (Dumitru et al., 2017)).

1.8.1. GABA and generation of neuronal precursors in the subventricular zone

In the postnatal SVZ, young neuroblasts spontaneously release γ-aminobutirric acid (GABA). $GABA_A$ receptors activation on precursor cells produces a depolarizing response that inhibits cell proliferation and neuronal differentiation (Fernando et al., 2011). Thus, A-type cells may use GABA to provide a negative feedback signal and to downregulate their own production. To counteract this function, B-type and C-type cells secrete the diazepam-binding inhibitor protein (DBI), which completely inhibit GABA activity onto GABA receptors, increasing the proliferation of the SVZ neuronal progenitors (Alonso et al., 2012; (Dumitru et al., 2017)).

Regulation of cell cycle progression in neuronal precursors in the SVZ seems to involve also extrasynaptically released GABA that results in enhanced survival of newly generated cells (Nguyen et al., 2003). GABA, interacts with cell cycle acting in an autocrine/paracrine fashion on SVZ-derived stem cells, triggering tonic inhibition of mitogen-activated protein kinase (MAPK) activity (Nguyen et al., 2003). Thus, GABA signalling negatively regulates stem cells proliferation in the SVZ via depolarization-induced calcium entry through voltage-gated calcium channels (VGCCs), a mechanism known to modulate gene expression ((LoTurco et al., 1995); (Ganguly et al., 2001)). On the other hand, MAPK signal transduction cascade activation is promoted by EGF, leading to increase of the neurogenic pool ((Doetsch et al., 2002); (Grant et al., 2002)). In addition, EGF controls GABA synthesis in SVZ stem cells, by limiting endogenous GABA production in these cells (Nguyen et al., 2003). Moreover, in the postnatal SVZ the inhibitory effect exerted by GABA onto precursor cells is prevented by the endogenous protein diazepam binding inhibitor (DBI) secreted by neuroblasts, providing another feedback mechanism on progenitors proliferation ((Alonso et al., 2012); (Dumitru et al., 2017)).

1.8.2. GABA and neuroblast migration along the rostral migratory stream

GABA is known to modulate progression of neuronal precursors along the RMS (Bloteus and Bordey, 2004) and in cortical areas. Tangentially migrating neuroblasts express glutamate decarboxylase (GAD) 65 and 67, enzymes that catalyze the decarboxylation of glutamate to GABA (Nguyen et al., 2003).
In precursors of cortical inhibitory interneurons, two putative mechanisms for the GABA release have been proposed: a mechanism that involve random action potential-independent fusion of GABA vesicles to the membrane (namely, action potential-independent quantal release; (Wollman et al., 2018)). Another possible mechanism might involve non-vesicular release of GABA through reversal activity of GABA transporters (Manent et al., 2005).

Along the RMS, the neurotransmitter GABA is abundantly available and

neuroblasts express $GABA_A$ and $GABA_B$ receptors (Wang et al., 2003). Specialized astrocytes that ensheat the migrating cells, prevent the accumulation of GABA in the extracellular compartment sequestering GABA via the high-affinity GABA transporter 4 (GAT4; (Borden, 1996)). These findings indicate that astrocytic processes, which surround chains of neuronal precursors, operate to maintain the tonic level of ambient GABA.

Migrating cells express NKCC1, modulating GABA response polarity, was suggested to contribute to the migration along the RMS (Mejia-gervacio et al., 2011).

It was shown that GABA, reduces the speed of migrating cells along the RMS via $GABA_A$ receptors activation, *ex vivo*, in slices that contain the entire RMS (Bolteus and Bordey, 2004). Indeed, administration of exogenous GABA, as well as inhibition of the GABA transporter GAT4, and therefore of the GABA uptake into astrocyte-like cells, lower the speed of neuroblasts' progression. By contrast, blocking $GABA_A$ receptors activity, with bicuculline, produces the opposite effect, resulting in an increase in the average speed of the migrating neuroblasts.

Calcium signalling is a key regulator of cell migration (Komuro and Rakic, 1998). In cortical inhibitory interneuron precursors, depolarizing GABA elicits calcium transients that favours neuroblast progression (Bortone and Polleux, 2009).

In the RMS, the mechanism underpinning GABA regulation of neuroblast motility remains elusive and controversial data are present in the literature. Bordey and colleagues observed that reducing extracellular calcium concentration with EGTA or lowering intracellular calcium concentration with BAPTA, result in a significant reduction of the speed of migrating cells. Furthermore, they found that blocking calcium release from inositol-3-phosphate (IP_3)-sensitive intracellular calcium stores, reduces migration rate (Bolteus and Bordey, 2004). Furthermore, it has been reported that the blockade of the L-type voltage-gated calcium channels, (VGCCs), in migrating cells does not affect the speed of migrating cells ((Bolteus and Bordey, 2004); (Darcy and Isaacson, 2009)). The latter results appear in contrast to what expected in immature neurons, where depolarizing GABA is thought to increase intracellular calcium concentration (Ben-Ari 2002). In cortical inhibitory interneurons, indeed, depolarizing GABA elicits calcium transients that modulates

the progression of inhibitory precursors (Bortone and Poleux 2009). Along the RMS, however, the link between GABA and calcium signalling remains largely to be understood.

1.8.3. Neurodevelopmental disorders involving the GABAergic system

GABAergic interneurons play a critical role in shaping the maturation of the central nervous system at various stages of development (Le Magueresse and Monyer, 2013).

GABA is known to play several effects on cell proliferation, migration, maturation in cortical and subcortical structures. According to its importance during development, altered GABA signalling is implicated in a number of neurodevelopmental disorders (Deidda et al., 2014).

Disorders of the autism spectrum have been largely correlated with alteration in the excitatory/inhibitory balance (Gillberg and Billstedt, 2000). Consistently, many mutations identified as risk factors for disorders of the autism spectrum affect genes encoding different $GABA_A$ receptor subunits (Coghlan et al., 2012). Furthermore, numerous genes related to autism spectrum disorders have been found to be mostly expressed in GABAergic interneurons (Xu et al., 2014).

Hyperexcitability of the network has been hypothesized as one of the causes that lead to the Fragile X syndrome onset, likely due to excitatory/inhibitory imbalance (Coghlan et al., 2012). The excitatory/inhibitory imbalance may rely on alterations affecting differently GABA signalling, linking deficit in GABAergic interneurons activity with Fragile X syndrome ((Deidda et al., 2014); (He et al., 2014)).

Some evidences also indicated a general alteration of GABAergic transmission as presumptive cause of Rett syndrome (Martinowich et al., 2003).

In Angelman syndrome both excitatory and inhibitory transmission seem to be decreased. However, an increase of excitatory/inhibitory ratio could be explained by the higher severity of this effect on inhibitory synapses, which might result in network hyperexcitability (Le Magueresse and Monyer, 2013).

Moreover, several data from both patients and mouse models of Down syndrome support the notion that alteration in the GABAergic signaling may underlie the cognitive component of this pathology ((Martinez-Cue et al., 2013), (Contestabile et al., 2017)).

Interestingly, multiple evidences show that GABA impinges on various cognitive aspects of schizophrenia (Ahn et al., 2011). In particular, in adult schizophrenic patients GABAergic circuits seem to be deeply perturbed (Lewis et al., 2012), suggesting that defects in the maturation of GABAergic interneurons may be a risk factor for the development of schizophrenia (Harrison and Owen, 2003).

Furthermore, an altered neuronal excitatory/inhibitory ratio, with possible implication of GABAergic signaling, has been proposed also for Tourette syndrome (Deidda et al., 2014).

Finally, defects in GABAergic transmission have been indicated as presumptive causes underlie neurofibromatosis type I, by both evidence in patients and studies in animal models of the pathology (Deidda et al., 2014).

2. OBJECTIVE

Intellectual disability (ID) is a neurodevelopmental disorder that has a heterogeneous spectrum of etiological factors, including both environmental and genetic factors.

Among the X-linked gene associated to ID, OPHN1 encodes for a RhoGAP, that regulate several developmental processes.

Most studies aimed at understanding the contribution of OPHN1 mutation in the etiopathogenesis of ID focused on the impact of OPHN1 on the development and function of glutamatergic neurons. The impact of OPHN1 on development and function of GABAergic inhibitory interneurons remained poorly understood for long time.

To unveil the role of OPHN1 on inhibitory circuitry, Lodovichi and colleagues studied the development of forebrain GABAergic interneurons generated postnatally in the subventricular zone (SVZ; Redolfi et al., 2016). Neurogenesis in the SVZ is a unique useful model to study development and function of GABAergic interneurons, since it offers a windows into a continuous developmental process, in postnatal life. It is worth noticing that SVZ postnatal neurogenesis is highly conserved among species. Several studies confirmed the presence of postnatal neurogenesis of forebrain GABAergic interneurons also in the SVZ in humans, at least in the first year of age. This developmental period is very important for human brain development, and it is thought that inhibitory interneurons, generated postnatally in the SVZ, play a key role in development and plasticity of the human brain. From the SVZ, the newly generated cells migrate to the OB, but also to several cortical (mostly prefrontal cortex) and subcortical areas. It is, therefore, likely that alterations in the proliferation, migration and maturation of SVZ derived cells could contribute to the etiopathogenesis of ID. Inhibitory interneurons has a critical role in regulating the excitation inhibition balance of neuronal networks and a growing body of evidence indicate that perturbation of their development and function have a prominent role in the pathogenesis of neurodevelopmental disorders.

In Lodovichi's lab, previous data showed that loss-of-function mutation of OPHN1 did not affect the generation of new neuronal progenitors in the SVZ. However the number of adult-born cells that reached the OB was dramatically reduced in OPHN1$^{-/y}$ mice respect to controls (Redolfi et al., 2016).

These data suggested that the migration of the SVZ-derived cells could be perturbed in OPHN1$^{-/y}$ mice. Neuronal migration is one of the fundamental process that underlies proper assembly and function of neuronal circuits, providing the correct excitatory/inhibitory balance of neuronal networks.

To verify whether and how the migration is impaired in OPHN1$^{-/y}$ mice, in this PhD projects I analyzed the migration of neuronal precursors from the SVZ, along the RMS to the OB. I analyzed this migration route because it is the best characterized. Although it has to be highlighted that the OB is not the only destination of SVZ derived interneurons, that can target also several cortical and subcortical areas.

By combining quantitative morphological analysis, to evaluate the distribution, the progression and the morphology of newborn neuronal precursors, and time-lapse imaging, to study the motility of neuroblasts *in vivo*, in physiological conditions and upon pharmacological modulation, we dissected the role of oligophrenin-1 in the migration of inhibitory interneuron precursors.

My PhD thesis was triggered by the question: Does OPHN1 mutation affect the migration of forebrain GABAergic interneurons? I addressed this question by dissecting the migration of the SVZ-derived precursors to the OB.

3. Materials and methods

3.1. Mutant mouse strains

Experiments were performed on male mice of a genetically modified line of mice: OPHN-1 knock-out (C57BL/6-ophn1; ko) mice, indicated as OPHN-$1^{-/y}$ mice. Male wt (unmodified) mice were used as controls.

OPHN-$1^{-/y}$ mice were generously provided by Pierre Billuart, and described in details previously (Khelfaoui et al. 2007).

Mice were kept in 12 hours light/12 hours dark cycles, and they were feed with water and food ad libitum.

All animal procedures were performed under a protocol approved by the ethic committee of the University of Padua.

3.2. Genotyping

Animals had to be genotyped, to assess which mice expressed the mutation of interest.

Experimental animals were male ko mice because the gene that encodes for oligophrenin-1 localize on the X-chromosome and male mice, having only one X-chromosome, present a more homogeneous expression of the gene of interest.

Female mice were rejected because, having a couple of X-chromosomes, they are subjected to the physiological inactivation of the X-chromosome. This makes more complex to control the expression of OPHN1 in the different cell types.

3.2.1. DNA extraction

We took from mice pups, before the tenth day of life, a little piece of tail and a finger (to enumerate, and so indentify, the animal). This biological sample were lysed to obtain the DNA.
In each eppendorf, containing the finger and the piece of tail, were added:

- 88 µl of autoclaved water;
- 10 µl of TRIS-HCl (Sigma-Aldrich), pH 7.5, 0.1 M;
- 2 µl of proteinase K (Invitrogen).

The lysis were performed at 57°C for 90 minutes in Thermomixer (Thermomixer comfort, Eppendorf). Eppendorfs were kept in ice and then at 99°C for 5 minutes to inactivate the proteinase K.

3.2.2. PCR

PCR (Polymerase Chain Reaction) was performed on lysed samples.
In PCR test-tubes were added:

- 4 µl of biological sample;
- 46 µl of PCR Reaction Mix (RedTaq ReadyMix, Sigma-Aldrich).

The PCR Reaction Mix was composed by:

- 25 µl of Red Taq Ready mix polymerase;
- 19.6 µl of autoclaved water;
- 0.7 µl of OPHN-1 Reverse-primer, 20 µM;
- 0.7 µ of OPHN-1 Forward-primer, 20 µM.

Test-tubes were putted in Thermocycler (Life Express, Bioer), that runs PCR cycles. PCR was also run on two positive controls (one for the ko and one for the wt) and on one negative control, to exclude contaminations of the samples.
After 3 initial minutes at 94°C, Thermocycler runs 35 cycles, organized in:

- 30 sec at 94°C;
- 45 sec at 57°C;
- 45 sec at 72°C.

At the end of the 35 cycle samples are kept at 72°C for 7 minutes, and then at 4°C.

3.2.3. Agarose gel electrophoresis

To split and visualize the different bands of DNA with the gene of interest, we ran an electrophoresis on 1 % agarose gel (Figure 3.1.).

We solubilised 1.2 g of agarose (Sigma-Aldrich) in 120 ml of TAE 1X (Buffer solution, composed by Tris-acetate, pH 8.0, and Ethylenediaminetetraacetic acid, EDTA). Then, we added 12 µl of SYBR safe DNA gel stain, 10000X (Invitrogen), a cyanine dye used as a nucleic acid stain (0.1 % of the total solution). This agarose gel was drained in a bowl and it is let cool down.

Once cold solidified, 15 µl of sample were loaded in wells in the gel. A well was loaded with the molecular weight standard (DNA ladder, Euro Clone).

The gel ran at 80 V, 400 mA until the bands split.

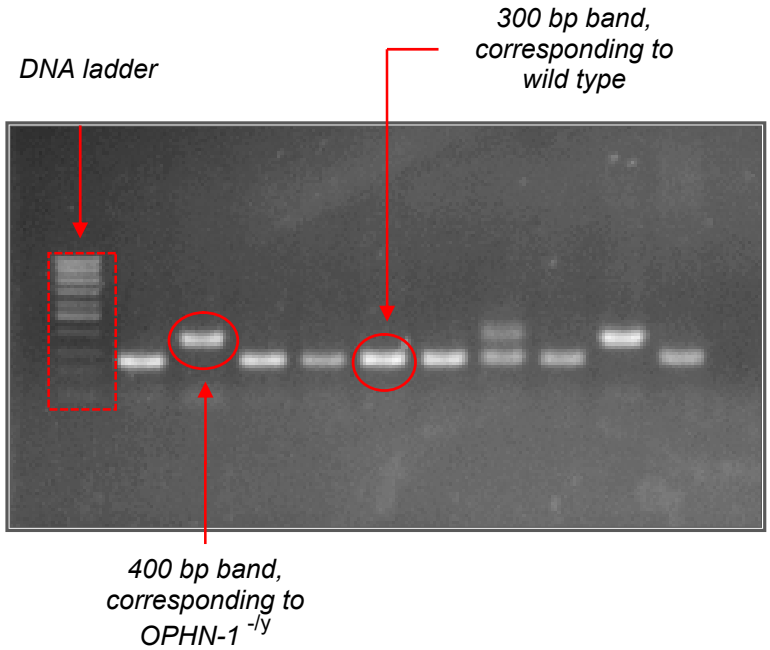

Figure 3.1: Agarose gel electrophoresis. *First well was loaded with the DNA ladder (Euro Clone), ten bands differentiated, one each 100 bp of increasing molecular weight. Higher bands (400 bp) correspond to the DNA of OPHN1$^{-/y}$ mice; lower bands (300 bp), correspond to the DNA of wt mice.*

OPHN-1 gene corresponds to the band of 300 base pair (bp) in wt mice. In ko mice the band corresponds to 400 bp, due to insertion of 100.

3.3. Quantitative morphological analysis

3.3.1. Immunohistochemistry

Animals were sacrificed with an overdose of a mixture of Zoletil 100 (a combination of Zolazepam and tiletamin, 1:1, 10 mg/kg; Vibrac) and Xilor (Xylazine 2 %, 0.06 ml/kg; Bio98). Mice were transcardially perfused with 0.9 saline, followed by 4% Paraformahaldehyde (Sigma-Aldrich) in 0.1M phosphate saline buffer (PBS). Brains were dissected and then postfixed over night. Brains were embedded in 2.5% agarose (Sigma-Aldrich) and then sectioned at vibratome (Vibratome VT1000S, Leica). To analyze cell migration along the RMS 70 μm sagittal sections were prepared.

To detect migrating neuronal precursor cells and astrocyte-like cells along the RMS floating sagittal sections were first incubated with PBS 1X supplemented with 10 % Normal Donkey Serum (NDS, Jackson laboratories) and 0.5 % Triton X-100 (blocking buffer), and then incubated over night at 4°C with a goat IgG anti DCX (neuronal precursors marker doublecortin; 1:1000, Santa Cruz Biotechnology) and a rabbit IgG anti GFAP (glial fibrillary acid protein; 1:2000, Abcam) primary antibodies. Primary antibodies were visualized, after 2 hours of incubation at RT, with Cy3 conjugate anti-goat IgG (1:500, Jackson laboratories) and AlexaFluor 488 conjugate anti-rbbit IgG (1:500, Jackson laboratories).

Sections were mounted on slides with Elvanol.

3.3.2. LV-GFP stereotaxic injection in the subventricular zone

Lentiviral vectors expressing Green Fluorescent Protein (LV-GFP) were sterotaxically injected in the SVZ to label neuronal precursor cells. Furthermore, GFP expression labels the entire cell (i.e.: soma, dentrites and dendritic spines) allowing a very detailed morphological analysis.

Animals were anesthetized with a mixture of Zoletil 100 (a combination of Zolazepam and tiletamin, 1:1, 10 mg/kg; Vibrac) and Xilor (Xylazine 2 %, 0.06 ml/kg; Bio98).

The scalp was resected, and two little hole were opened on the skull.

Injections were performed in OPHN1$^{-/y}$ mice and wt mice, as controls, using a picopump (WPI). Stereotaxic coordinates of injection, relative to Bregma (the anatomical point on the skull at which the coronal suture is intersected perpendicularly by the sagittal suture), were taken from previous studies by Petreanu and Alvarez-Buylla (2002):

- anterior = 1 mm;
- lateral = 1 mm;
- depth = 2.5 mm.

Animals were sacrificed 9 dpi with an overdose of Xilor-Zoletil 1:1 (Zoletil was diluted 1:5 in filtered physiological solution).

Mice were transcardially perfused with 0.9 saline, followed by 4% Paraformahaldehyde in 0.1M phosphate saline buffer (PBS). Brains were dissected and then postfixed over night. Brains were embedded in 2.5% agarose (Sigma-Aldrich) and then sagittally sectioned (70 µm thick sections) at vibratome (Vibratome VT1000S, Leica).

Immunostaining against DCX was performed on floating sections, with the same protocol described above, and sections were mounted on slides with Elvanol.

3.3.3. Quantification of the areas occupied by neuroblasts' populations along the rostral migratory stream

To observe the entire RMS four contiguous sagittal slices (70 μm thick) were collected from every hemisphere. Sections were immunolabeled for DCX.
Sections were analyzed at the stereomicroscope (Leica MZ16F) equipped with a PLANPO 0.63 objective, with a 3.2 X total magnification MZ16F), and images were taken with a camera (Canon Eos 1000D).
The area occupied by neuronal precursor cells was calculate in two regions of interest (ROIs): (1.) the SVZ, (2.) in the point where the RMS enters the OB. The area on these brain regions was calculated using ImageJ software (NIH); data are expressed as Median ± SEM. Mann-Whitney test was performed to assess the statistical significance of data obtained.

3.3.4. Analysis of the chains of migrating neuroblasts along the rostral migratory stream

Three contiguous sagittal slices (70 μm thick) were collected from every emisphere. Sections were immunolabeled for DCX.
Sections were analyzed using a confocal microscope (Zeiss LSM 700) equipped with a EC Plan-Neofluar 20X / 0.50 M27 objective (Zeiss).
The thickness and the length of the chains of migrating precursors were measured; in addition the points in which cells change their direction respect the main direction of the RMS were quantified. The analysis was performed using using Zen software (Zeiss). Mann-Whitney test was performed to assess the statistical significance of data obtained.

3.3.5. Evaluation of the astrocyte-like cells expansion in the rostral migratory stream

Three contiguous sagittal slices (70 µm thick) were collected from every emisphere. Sections were immunolabeled for DCX and GFAP.
Sections were analyzed using a confocal microscope (Zeiss LSM 700) equipped with a EC Plan-Neofluar 20X / 0.50 M27 objective (Zeiss). The ratio between the areas occupied by the processes of astrocyte-like cells and the total area occupied by DCX positive cells was calculated in two regions of interest (ROIs): (1.) RMS1, representing the initial portion of the RMS, near the SVZ; (2.) RMS2, representing the final portion of the RMS, near the OB. The area on these brain regions was calculated using ImageJ software (NIH); data are expressed as Median ± SEM. Mann-Whitney test was performed to assess the statistical significance of data obtained.

3.3.6. Evaluation of the neuronal precursor cells polarity during migration along the rostral migratory stream

Three contiguous sagittal slices (70 µm thick) were collected from every emisphere. Sections were immunolabeled for DCX.
Sections were analyzed using a confocal microscope (Zeiss LSM 700) equipped with a EC Plan-Neofluar 20X / 0.50 M27 objective (Zeiss).
The cell polarity were estimated categorizing neuroblasts according to the number of processes:

- type I (unipolar cells), single leading process;
- type II, bipolar cells;
- type III, multipolar cells.

Cell counts were expressed as a percentage of total number of neuroblasts.
Neuronal precursors polarity was quantified using Zen software (Zeiss); data are expressed as Median ± SEM.

Mann-Whitney test was performed to assess the statistical significance of data obtained.

3.4. Birthdating analysis

3.4.1. BrdU injection

To evaluate the number of newborn cells mice were intraperitoneally injected with synthetic nucleoside that is an analog of thymidine: 5-bromo-2'-deoxyuridine (BrdU, Sigma-Aldrich; Figure 3.2.).

BrdU is used to analyze the proliferation of cells in tissues. It is incorporated in DNA of dividing cells instead of thymidine.

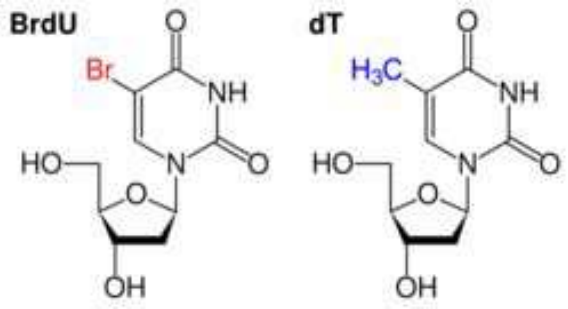

Figure 3.2.: BrdU (left) and thymidine (right) chemical structures. *A Bromine group substitutes the methyl group in the pyrimidine ring.*

BrdU injections were performed on OPHN-$1^{-/y}$ mice and control mice to analyze the number of newly generated neuronal precursors along the RMS at 7 days post-injections.

BrdU was diluted in milliQ water 10 mg/ml. Four injections of 50 mg/kg body were performed every two hours (Petreanu and Alvarez-Buylla, 2002) in male OPHN-$1^{-/y}$ mice and male wt C57B/6 mice as controls, from the same brood at 30 post natal days (p 30).

3.4.2. BrdU labelling and immunohistochemistry

To assess neurogenesis in the OB animals were sacrificed 9 days after BrdU injection (dpi) with an overdose of a mixture of Zoletil 100 (a combination of Zolazepam and tiletamin, 1:1, 10 mg/kg; Vibrac) and Xilor (Xylazine 2 %, 0.06 ml/kg; Bio98). To study the migration along the RMS animals were sacrificed 7 dpi, using the same protocol.

At 7, or 9, dpi respectively, mice were transcardially perfused with 0.9 saline, followed by 4% Paraformahaldehyde (Sigma-Aldrich) in 0.1M phosphate saline buffer (PBS). Brains were dissected and then postfixed over night. Brains were embedded in 2.5% agarose (Sigma-Aldrich) and then sectioned at vibratome (Vibratome VT1000S, Leica). To study neurogenesis in the OB 60 µm thickness coronal sections were prepared, while 70 µm sagittal sections were prepared to analyze cell migration along the RMS.

To detect BrdU labeled cells, floating coronal, or sagittal, sections were pretreated with the DNA denaturating agent HCl 2N (Sigma-Aldrich), at 37°C for 10 minutes.

To detect granule cells in the OB floating coronal sections were first incubated with PBS 1X supplemented with 10 % Normal Goat Serum (NGS, Jackson laboratories) and 0.5 % Triton X-100 (Sigma-Aldrich; blocking buffer), and then incubated over night at 4°C with a rat monoclonal anti BrdU (1:200, Abcam) and a mouse monoclonal anti NeuN (neuronal marker Neuronal Nuclear antigen; 1:200, Millipore) primary antibodies. Primary antibodies were visualized with Cy3 conjugate anti-rat IgG (1:800, Jackson laboratories) and DyLight 488 conjugate anti-mouse IgG (1:800, Jackson laboratories), after 2 hours of incubation at room temperature (RT), to double stain cells for BrdU and NeuN.

To detect migrating neuronal precursor cells along the RMS floating sagittal sections were first incubated with PBS 1X supplemented with 10 % Normal Donkey Serum (NDS, Jackson laboratories) and 0.5 % Triton X-100 (blocking buffer), and then incubated over night at 4°C with a rat monoclonal anti BrdU (1:200, Abcam) and a goat IgG anti DCX (neuronal precursors marker doublecortin; 1:1000, Santa Cruz Biotechnology) primary antibodies. Primary antibodies were visualized with DyLight 488 conjugate anti-rat IgG (1:500, Jackson

laboratories) and Cy3 conjugate anti-goat IgG (1:500, Jackson laboratories), after 2 hours of incubation at RT, to double stain cells for BrdU and DCX.
Sections were mounted on slides with Elvanol.

3.4.3. Chronic drug administration

OPHN-1$^{-/y}$ mice and controls were treated with the ROCK and PKA kinases non-competitive inhibitor Fasudil also known as HA1077 (Figure 3.3.; Selleckchem.com)
Fasudil was dissolved in daily drinking water at 0.65 mg/ml and given orally 12 or 14 days before starting the intraperitoneal injection of BrdU and for the next 9 or 7 days respectively, for a complete chronic treatment of 3 weeks.

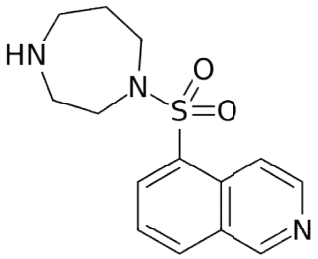

Figure 3.3.: HA1077 chemical structure.

3.4.4. Quantification of the number of newborn neuronal precursors along the rostral migratory stream

Three contiguous sagittal slices (70 µm thick) were collected from every hemisphere. Sections were immunolabeled for BrdU and DCX.
Sections were analyzed on a confocal microscope (Zeiss LSM 700) equipped with a EC Plan-Neofluar 20X / 0.50 M27 objective (Zeiss). Cell were counted using ImageJ software (NIH).
To evaluate the number of newly generated neuroblasts, cells double positive for BrdU and DCX, were counted in three different regions of interest (ROIs) in each section.

The three ROIs were, namely:

- RMS1, representing the initial portion of the RMS, near the SVZ;
- RMS2, representing the final portion of the RMS, near the OB;
- core of the OB, that is the most internal part of the bulb.

To estimate the neuronal faith of the new cells we used the percentual ratio:

$$100 * (BrdU + DCX)/_{Tot\ BrdU}$$

BrdU+DCX indicates newborn cells positive for BrdU and DCX, i.e newly generated neuronal precursor cells. *Tot BrdU* represents the total number of newly generated cells. Data are expressed as Median ± SEM.

Mann-Whitney test was performed to assess the statistical significance of data obtained.

3.4.5. Quantification of newly generated granule cells in the olfactory bulb

Every other coronal slices (60 μm thick) was collected from every bulb. Sections were immunolabeled for BrdU and NeuN.

Sections were analyzed at a confocal microscope (Leica TCS SP5) equipped with a HCPL Fluotar 20X / 0.50 NA objective (Leica). Cell were counted using ImageJ software (NIH).

To evaluate the number of newly generated granule cells in the OB, cells double positive for BrdU and NeuN, were counted in the granule cell layer of each section.

To estimate the neuronal fate of the new cells we used the percentual ratio:

$$100 * (BrdU + NeuN)/_{Tot\ BrdU}$$

BrdU+NeuN indicates newborn cells positive for BrdU and NeuN, i.e newly generated neurons. *Tot BrdU* represents the total number of newly generated cells. Data are expressed as Median ± SEM.

Mann-Whitney test was performed to assess the statistical significance of data obtained.

3.5. Analysis of the migration process *in vivo*

3.5.1. Two-photon time-lapse imaging of migrating precursors along the rostral migratory stream *in vivo*

Newly generated cells were labeled in the SVZ with LV vectors expressing GFP with the same method described above (stereotaxic injections).

Four to six day after the injection the mice were anesthetize with a mixture of Zoletil 100 (a combination of Zolazepam and tiletamin, 1:1, 10 mg/kg; Vibrac) and Xilor (Xylazine 2 %, 0.06 ml/kg; Bio98). Mice were transcardially perfused with ice-cold cutting solution (sucrose 203mM, KCl 3mM, $MgCl_2$ 2mM, $CaCl_2$ 0.5mM, $NaHCO_3$ 2mM, Na_2HPO_4 1.5mM, glucose 25mM), then rapidly decapitated. Brains were dissected then thick sagittal sections (300 µm thick sections) were cut at the vibratome (Vibratome VT1000S, Leica) in ice-cold cutting solution continuously oxygenated.

Slices containing SVZ-RMS-OB were collected and immediately immersed in ACSF (NaCl 3mM, KCl 3mM, $MgCl_2$ 1mM, $CaCl_2$ 2.5mM, $NaHCO_3$ 2mM, Na_2HPO_4 1.5mM, glucose 25mM) oxygenated at 32°C.

After one hour of recovery slices were transferred at room temperature. The best slice was selected and transferred into an imaging chamber (Ultra quiet imaging chamber RC-27LD, Warner Instruments) and continuously perfused with oxygenated ACSF at 32°C with a flow rate of 2 ml/min.

Sections were analyzed using a two-photon microscope (Scientifica 2P, Ti:Saphire based laser) equipped with a 16X/0.8NA objective (Olympus). 512x512 Z-stack were acquired at 0.86 frame/s; a Z-stack was acquired every 3 minutes and 40 total Z-stacks were acquired, allowing to follow the migration process along one single field of view for a total time of two hours for each condition.

3.5.2. Acute drug administration

Several compounds were administered to slices during time-lapse imaging experiments:

- γ-amminobutirric acid (GABA, Sigma-Aldrich);
- Bicuculline (GABAA receptors inhibitor, Sigma-Aldrich);
- Bumetanide (NKCC1 inhibitor, Sigma-Aldrich);
- VU0463271 (KCC2 inhibitor, Sigma-Aldrich);
- Fasudil (HA1077, ROCK2 and PKA inhibitor Selleckchem.com).

Drugs were suspended in ACSF or DMSO following the data sheet and then dissolved in oxygenated ACSF at 32°C and perfused continuously into the imaging chamber.

GABA was incubated for 15 minutes, bicuculline, bumetanide and VU0463271 were incubated for 1 hour, and fasudil was incubated for 30 minutes, After incubation time-lapse imaging was performed for two hours to evaluated the effect of the specific compound on the migration process along the RMS.

3.5.3. Tracking of the migrating neuroblasts along the rostral migratory stream

Because of the saltatory nature of the neuroblasts translocation, that alternate migratory phases, so phases in which they move, and pausing phases, in which they stop, motility of migrating neuroblasts was computed by using different parameters:
(1.) Average speed, considering the average translocation speed of precursors in one hour of time-lapse imaging including both migrating and pausing phases.
(2.) Instantaneous speed, that calculate cell migration speed exclusively in the translocation phase. (3.) Moving time, indicating the amount of time cells spend in the migratory phase. moreover neuronal precursors can migrate in both direction, toward and away from the bulb; for this reason we quantified also
(4.) The percentage of cells migrating towards the OB.

Neuroblasts migration along the RMS was monitored for two hours at physiological condition, then after incubation with the drug of use time-lapse imaging was repeated for other two hours.

The motility of each single was tracked using ImageJ software (NIH); data are expressed as Median ± SEM. Mann-Whitney test was performed to assess the statistical significance of data obtained.

4. RESULTS

4.1. Summary of previous results

Granule cells are the main inhibitory interneurons in the olfactory bulb (OB). They constantly generate throughout animal's life. From the subventricular zone (SVZ), neuroblasts migrate along the rostral migratory stream (RMS) to reach their final destination, the OB.

In a previous work in Lodovichi's lab, we studied whether mutation in OPHN1 could affect the development and function of forebrain GABAergic interneurons generated postnatally in the SVZ. Using 5'-bromo-2'-deoxyuridine (BrdU), a cell division marker, we estimated the number of newly generated cells in the SVZ, in OPHN1$^{-/y}$ mice and littermate controls. Mice were intraperitoneally injected with BrdU and the newly generated cells counted in the SVZ 24 hours after BrdU injection (dpi; Redolfi et al., 2016).

Data from this experiment showed that the generation of new cells in the SVZ is similar in OPHN1$^{-/y}$ mice with respect to controls.

According to Petreanu and Alvarez-Buylla (2002) by 15 dpi, the newly generated cells have reached the OB. To assess whether by this temporal point the adult-born cells have migrated to the OB also in OPHN1$^{-/y}$ mice, the BrdU positive cells were counted in the OB 15 dpi. Neurons were identified by using the neuronal marker, Neuronal Nuclei (NeuN; Redolfi et al., 2016).

The results indicated that the complement of newborn interneurons was reduced to one third in OPHN1$^{-/y}$ mice with respect to controls. Moreover, to determine whether the loss of function of OPHN1 could affect cell fate, i.e. how a particular cell develops into the final cell type, we estimated the proportion of cells double labelled for BrdU and for NeuN on the total number of cells labeled with BrdU. They found no difference in cell fate between OPHN1$^{-/y}$ mice and wt mice.

All together data obtained in Lodovichi's lab indicated that (1.) the generation of neuronal progenitors in the SVZ was not affected by OPHN1

mutation. However (2.) the complement of newly generated GABAergic interneurons in the OB was strikingly reduced 15 dpi.

The reduced number of newborn interneurons in the OB at 15 dpi could be due to: (1.) altered migration of adult-born neuronal precursors from the SVZ to the OB. According to this hypothesis only a few neuroblasts reach the OB. Alternatively, (2.) the reduced number of newly generated cells could be ascribed to perturbed integration of adult-born inhibitory interneurons in existing circuits in the OB. In the latter hypothesis the entire complement of newly generated cells arrives into the OB, but fails to integrate and therefore die. Since it is known that newborn cells begin to establish the first synapses by 14-15 days (Kelsch et al., 2010), and Lodovichi and colleagues evaluated the number of newly generated immature interneurons at this time point, it was unlikely that the failure in integration could explain such a dramatic reduction of the complement of adult-born inhibitory interneurons in the OB of OPHN1$^{-/y}$ mice.

To verify which hypothesis could explain the reduction of new cells in the OB of mutant mice, Lodovichi and colleagues quantified the complement of newborn neuronal precursors a 9 dpi, when all the new cells reached the OB and switched to radial migration (Petreanu and Alvarez-Buylla, 2002), but they have not started yet to established the first synaptic contacts. They observed that the number of adult-born interneurons is similar in the OB of wt mice at 9 or 15 days after their generation in the SVZ. However in OPHN1$^{-/y}$ mice the number of SVZ-derived neuronal precursors in the OB is already significantly reduced 9 days after their generation. Thus, the hypothesis that their decreased population is to be ascribed to a failure in integration was rejected.

Furthermore, it is well known that oligophrenin-1, as a Rho GAP, modulates the actin cytoskeleton rearrangements that are crucial for cell migration. Therefore mutation in OPHN1 could result in altered migration. Considering all these data, we hypothesized that the migration was impaired in OPHN1$^{-/y}$ mice.

To verify whether the migration process of the adult-born granule cells was hampered by loss-of-function mutation of OPHN1, in my PhD project I studied the migrating neuroblasts from the SVZ to the OB, dissecting several features of the

migration along the RMS, such as the distribution, the organization, the progression, the morphology and the motility of migrating cells.

4.2. Perturbation of the spatial organization of neuronal precursors along the rostral migratory stream in OPHN1$^{-/y}$ mice

To assess whether the migration process was disturbed by loss-of-function mutation of oligophrenin-1, we studied the distribution of migrating cells along the RMS.

To analyze the migration path from the SVZ to the OB, sagittal sections (70 µm thick) were prepared at vibratome. Slices were immunostained with antibody against doublecortin (DCX), a microtubule-associated protein expressed by neuronal precursors and immature neurons in embryonic and adult cortical structures. Neuronal precursor cells begin to express DCX while actively dividing, and their neuronal progeny continue to express DCX for 2 to 3 weeks as the cells mature into neurons. Downregulation of DCX begins after 2 weeks, and occurs at the same time that cells begin to express NeuN (Brown et al., 2003).

Four contiguous sagittal slices per hemisphere were analyzed and four animals per condition were studied.

We examined the SVZ and the RMS in control and OPHN1$^{-/y}$ mice. Six animals per condition were analyzed (Figure 4.1.). We observed that in controls newly generated precursors coalesce in organized chains that occupied a thin stripe around the walls of the lateral ventricles to converge in to the RMS. On the contrary, in OPHN1$^{-/y}$ mice neuroblasts are chaotically distributed in vast area around the lateral ventricles.

Analyzing the RMS, we found that organized chains of cells follow a stereotyped path to reach the OB in controls (Lledo et al., 2006). In OPHN1$^{-/y}$ mice the specific geometry of the RMS was deeply disrupted.

To quantify this phenomenon we measured the areas occupied by the adult-born neuronal precursors in OPHN1$^{-/y}$ mice and littermate controls. In particular we chose two regions where the perturbation of the RMS was particularly evident: the SVZ and the point where the RMS enters the OB.

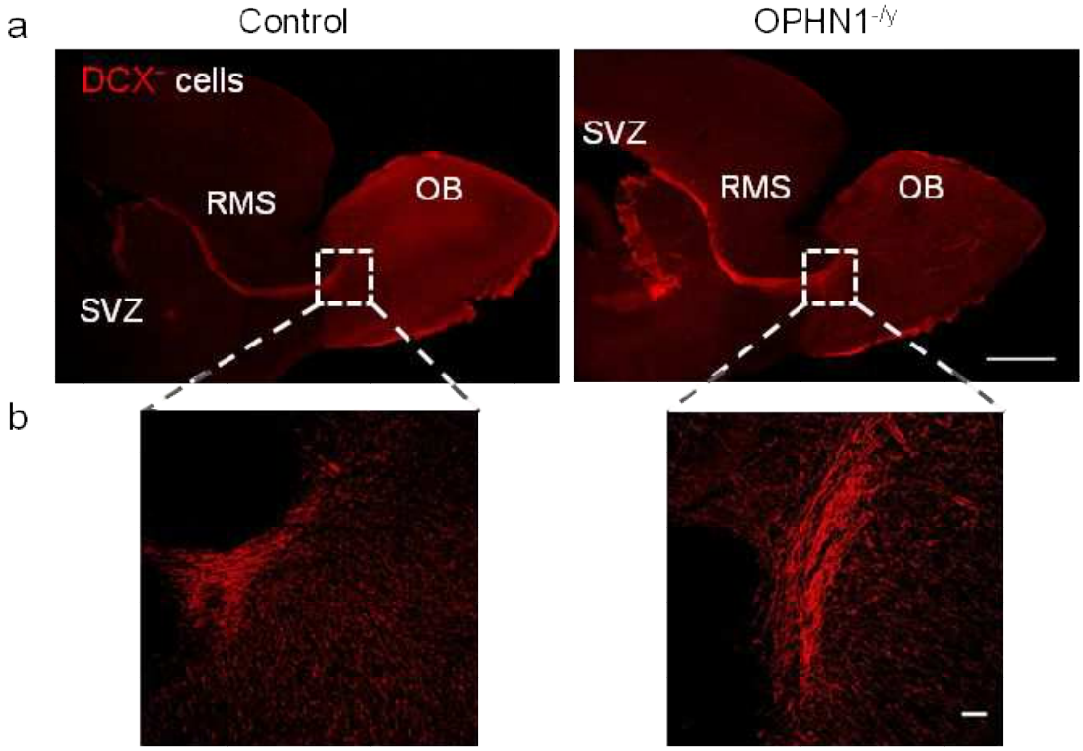

Figure 4.1.: The spatial organization of neuronal precursors is perturbed along the rostral migratory stream (RMS) in OPHN1$^{-/y}$ mice. (a) Confocal images of sagittal sections of the brain *containing the subventricular zone (SVZ), the rostral migratory stream and the olfactory bulb (OB), immunostained for doublecortin (DCX); in red: DCX^{+} cells.* ***(b) High magnification of the regions highlighted in the dotted rectangles:*** *the entry of the RMS into the OB. In OPHN1$^{-/y}$ mice (right) the spatial distribution of the neuroblasts along the RMS is disrupted with respect to wt mice (left). Bars: (a) = 1 mm; (b) = 100 µm.*

We found that the area occupied by neuroblasts in the SVZ was strikingly increased in OPHN1$^{-/y}$ mice with respect to control mice (Graph 4.1).

The area occupied by neuronal precursor cells was enlarged also in the point where the RMS enters the OB of OPHN1$^{-/y}$ mice with respect to littermate controls (Graph 4.1.).

Along all the RMS, neuroblasts distribute chaotically, in a dispersive fashion in OPHN1$^{-/y}$ mice, whereas in controls neuroblasts seem to arrange in a precise layout, occupying a more circumscribed space.

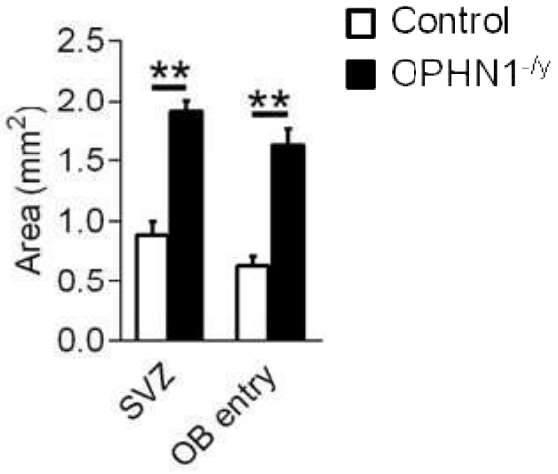

Graph 4.1.: Quantification of the areas of cells labelled with antibody against doublecortin (DCX) *in OPHN1$^{-/y}$ mice (n = 6) and wt mice (n = 6). On the left, in the subventricular zone (SVZ; OPHN1$^{-/y}$ mice S = 1.91 ± 0.10 µm^2, control mice S = 0.89 ± 0.11 µm^2; Mann-Whitney test p < 0.01). On the right, in the entry of the rostral migratory stream (RMS) into the olfactory bulb (OB; OPHN1$^{-/y}$ mice S = 1.64 ± 0.13 µm^2, control mice S = 0.64 ± 0.08 µm^2; Mann-whitney test p < 0.01).*

These data suggest that loss-of-function mutation of oligophrenin-1 results in an altered spatial organization of the newborn neuronal precursors that leads to an increase in the areas occupied by neuroblasts in the SVZ and in the OB of OPHN1$^{-/y}$ mice with respect to wt mice.

This disruption of the physiological spatial distribution of neuroblasts along the RMS may represent the first evidence that mutation in OPHN1 deeply perturbs the migration process from the SVZ to the OB.

4.3. A lower number of neuronal precursors reaches the olfactory bulb in OPHN1$^{-/y}$ mice

To investigate whether the altered architecture of the RMS reflected an impairment of the neuronal precursors migratory ability, we performed birth-dating analysis to explore the progression of neuroblasts along different segments of the

RMS. We injected BrdU intraperitoneally in OPHN1$^{-/y}$ mice and littermate controls to label neuronal progenitors that were actively dividing at the time of the injection, since they incorporated the exogenous nucleotide. We counted the number of neuroblasts that migrate along the RMS, using a double immunostaining against BrdU and DCX (Figure 4.2.).

Newborn SVZ-derived cells were counted 7 days after BrdU injection (dpi) in three spatially subsequent regions of interest (ROIs), namely:

- RMS1, representing the initial portion of the RMS, near the SVZ;
- RMS2, representing the final portion of the RMS, near the OB;
- core of the OB, that is the most internal part of the bulb.

At 7 dpi, in physiological conditions, the newly generated cells are completing their migration to the bulb (Petreanu and Alvarez-Buylla, 2002), with most of neuroblasts that are arriving in the core of the OB and some of them that already started their radial migration.

Brains were sectioned at vibratome, to obtain sagittal slices (70 μm thick). Slices were immunolabelled with antibodies against BrdU and DCX.

Three contiguous slices per hemisphere were analyzed and four animals per condition were studied.

We found that at 7 dpi the total number of newly generated neuronal precursors along the entire RMS, from the SVZ to the core of the OB, was similar in OPHN1$^{-/y}$ mice with respect to control mice (OPHN1$^{-/y}$ mice n = 880 ± 185, control mice n = 960 ± 111; p = 0.83; not shown). However their distribution along the RMS was dramatically perturbed in OPHN1$^{-/y}$ mice.

In OPHN1$^{-/y}$ mice, unlike what observed in wt mice, most of the new neuroblasts clumped in the most proximal portion of the RMS, near the SVZ. We found that the complement of newly generated neuronal precursors in RMS1 was significantly higher in OPHN1$^{-/y}$ mice with respect to littermate controls (Graph 4.2.).

By contrast the number of adult-born neuroblasts in RMS2 was strikingly lower in OPHN1$^{-/y}$ mice with respect to littermate controls (Graph 4.2.).

Furthermore the number of SVZ-derived neuronal precursors in the core of the OB was significantly reduced in OPHN1$^{-/y}$ mice than wt mice (Graph 4.2.).

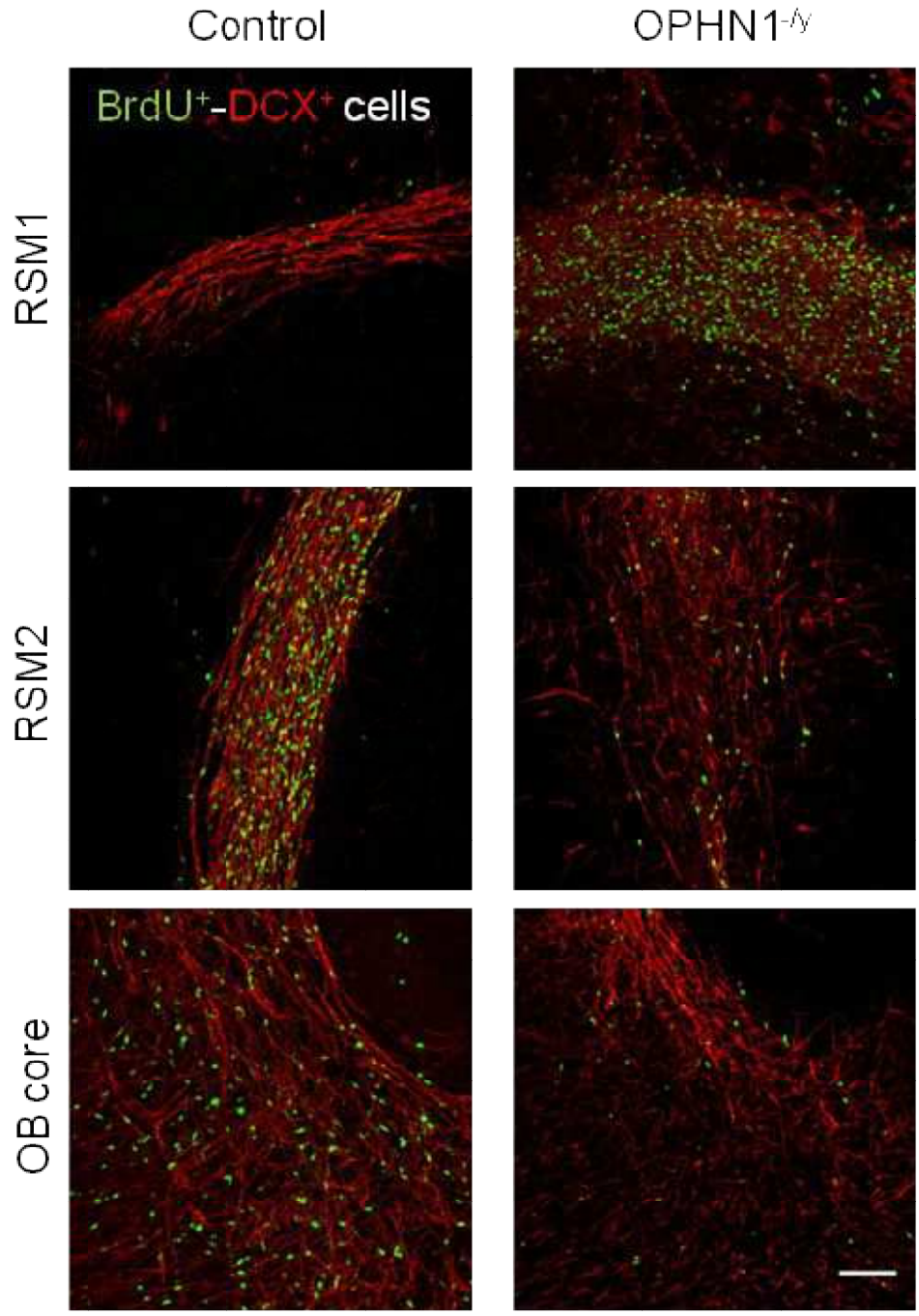

Figure 4.2.: Lower number of neuronal precursors reaches the olfactory bulb (OB) at 7 dpi in OPHN1$^{-/y}$ mice. *Examples of confocal images of the three ROIs of the rostral migratory stream (RMS) in sagittal sections of the brain: RMS1, RMS2, and the core of the OB. In red: DCX labelled cells; in green: BrdU labelled cells. In OPHN1$^{-/y}$ mice (right) at 7 dpi, the complement of newborn neuronal precursors is increased in RMS1, while is decreased in RMS2 and in the core of the OB with respect to control mice (left). Bar = 200 µm.*

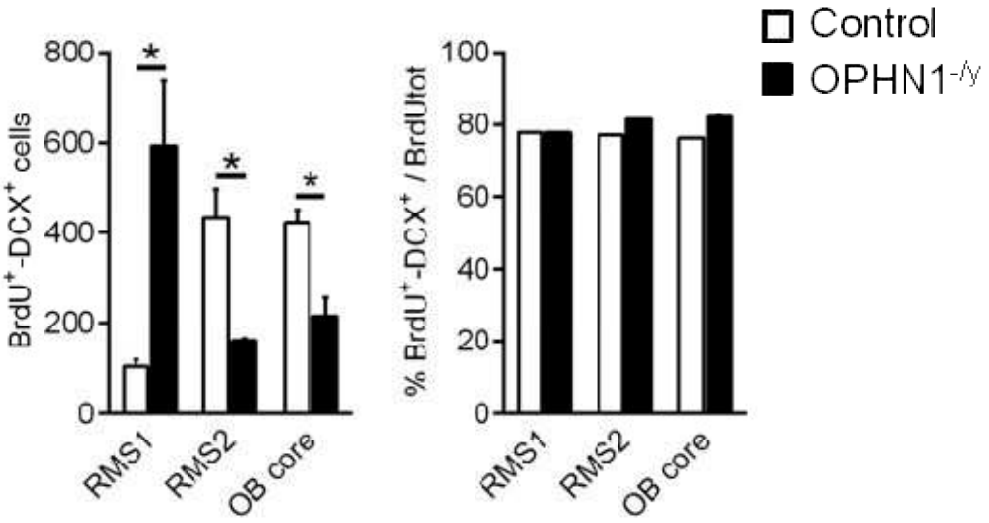

Graph 4.2.: *On the left,* ***number of newly generated neuronal precursors along the rostral migratory stream (RMS).*** *In OPHN1$^{-/y}$ mice (n = 4) and wt mice (n = 4) in the 3 ROIs (RMS1: OPHN1$^{-/y}$ mice n = 489 ± 145, control mice n = 99 ± 15; Mann-Whitney test p = 0.03; RMS2: OPHN1$^{-/y}$ mice n = 163 ± 4, control mice n = 443 ± 63; Mann-Whitney test p = 0.03; core of the OB: OPHN1$^{-/y}$ mice n = 236 ± 36, control mice n = 417 ± 32: Mann-Whitney test p = 0.03). On the right,* ***proportion of cells double labelled for bromodeoxyuridine (BrdU) and for doublecortin (DCX)*** *on the total number of cells labelled with BrdU (cell fate; percentage of BrdU-positive neuronal precursors in RMS1: 77.8% in OPHN1$^{-/y}$ mice, 77.7% in controls; Mann-Whitney test p = 0.34; in RMS2: 77.1% in OPHN1$^{-/y}$ mice, 81.5% in controls; Mann-Whitney test p = 0.29; in the core of the OB: 76.2% in OPHN1$^{-/y}$ mice, 82.2% in controls; Mann-Whitney test p = 0.06).*

Our data showed that in OPHN1$^{-/y}$ mice only a few neuroblasts could reach the distal segments of the RMS and terminate their migratory path in the OB.

To determine whether the loss of function of OPHN1 could affect cell fate, we estimated the proportion of cells double labelled for BrdU and DCX on the total number of cells labelled with BrdU. We found no difference in cell fate between OPHN1$^{-/y}$ mice and control.

These data indicated that oligophreni-1 mutation does not affect the generation but it deeply perturbs the migration process of the newly generated cells to the OB.

4.4. The geometrical organization of neuroblasts' chains is deeply perturbed in OPHN1$^{-/y}$ mice

High magnification confocal images of the RMS allowed us to visualize the chains of neuroblasts along their migration path in detail. We evaluated the geometrical organization of the chains of migrating neuronal precursors along the RMS in OPHN1$^{-/y}$ mice and littermate controls, considering the thickness of the chains, their length and the number of points in which chains changed their orientation, thus the direction of progression. Moreover we investigated the presence and the structure of the processes of astrocyte-like cells into the RMS.

To visualize the chains of migrating neuroblasts into the RMS we used an antibody against DCX, while for the scaffold astrocyte-like cells that enwrap migrating cells we used an antibody against the glial fibrillary astrocytic protein (GFAP).

Brains were sectioned at the vibratome, to obtain sagittal slices (70 μm thick). Slices were immunolabelled with antibodies against DCX and GFAP. Three contiguous slices per hemisphere were analyzed and four animals per condition were studied.

We analyzed two spatially subsequent ROIs: RMS1 and RMS2. Thickness and length of neuroblasts' chains were computed both considering the number of cells composing the chains and their dimensions in μm; the points in which chains changed their orientation corresponded to the points where all the cells composing the chain deviated the direction of their leading process. The infiltration of specialized astrocytic processes into the RMS was quantified as the ratio between the areas occupied by the single processes and the total area of the RMS:

$$\sum Sgfap / TotSdcx$$

where ∑Sgfap indicates the summation of all the single areas of astrocytic processes inside the RMS and TotSdcx represents the total area occupied by DCX-positive cells.

Analyzing the organization of the chains, we found that the specific geometry of the RMS was deeply disrupted, in OPHN1$^{-/y}$ mice with respect to controls (Figure 4.3).

We found that chains were thicker along the entire RMS. The width of the chains was computed measuring two different parameters: (1.) quantifying the number of cells adjacent along the dorso-ventral axis of the RMS (Graph 4.3a) and (2.) the dorso-ventral width of chains in micrometers (Graph 4.3b).

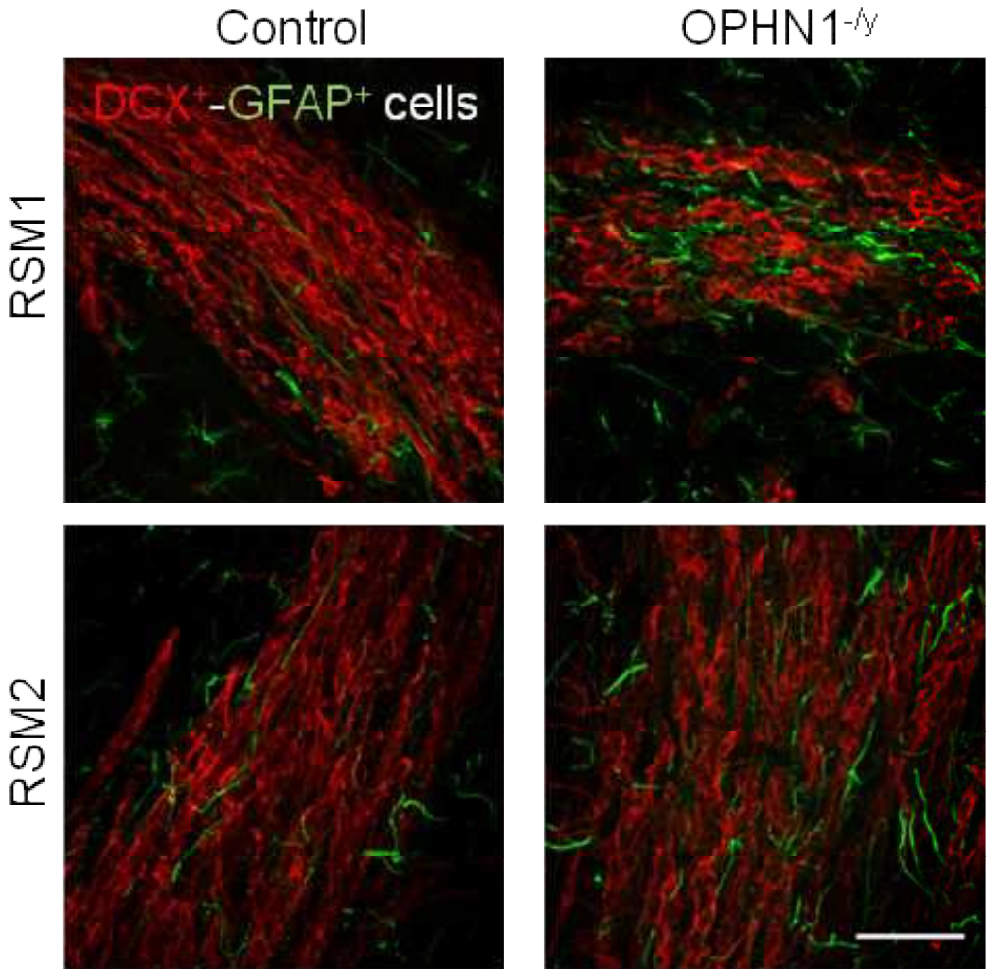

Figure 4.3.: The geometrical organization of neuroblasts' chains is deeply perturbed in OPHN1$^{-/y}$ mice. *Examples of high magnification of the rostral migratory stream (RMS) in confocal images of sagittal sections of the brain. RMS1 and RMS2. In red: doublecortin (DCX) labelled cells; in green: glial fibrillary acid protein (GFAP) labelled cells. In OPHN1$^{-/y}$ mice (right), chains appear thicker and shorter and they change direction of migration more frequently that in controls (left). Moreover astrocytic processes appears thicker and they invades the chains of migrating neuroblasts. Bar = 50 µm.*

Neuroblasts' chains were also shorter both considering the number of cells composing the chains along the antero-poterior axis of the RMS (Graph 4.3c) or measuring the relative chains' length in micrometers (Graph 4.3d). Moreover, the

number of points where the chains of neuroblasts changed direction of migration was significantly higher in OPHN1$^{-/y}$ mice than in wt controls (Graph 4.3e).

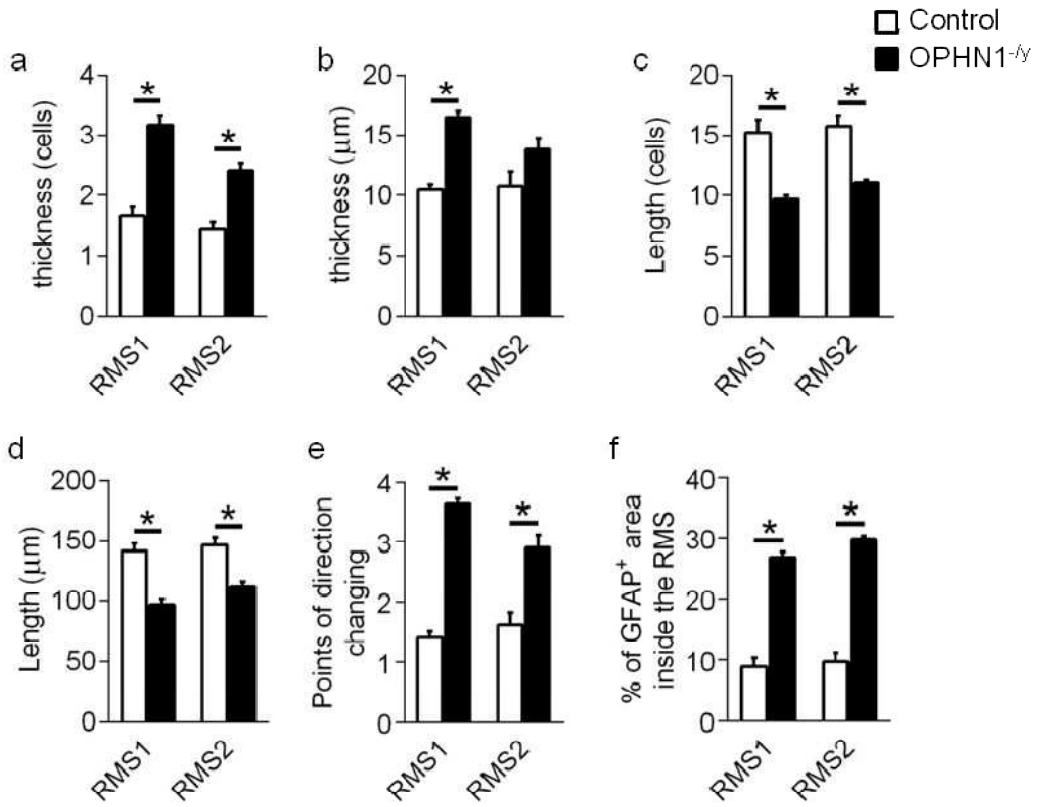

Graph 4.3.: Quantification of the geometrical arrangement of neuroblasts' chains along the rostral migratory stream (RMS) *in OPHN1$^{-/y}$ mice (n = 4) and wt mice (n = 4) in the 2 ROIs (RMS1; RMS2). (a) Chains' thickness in cell number (RMS1: OPHN1$^{-/y}$ mice n = 3.17 ± 0.16, control mice n = 1.67 ± 0.15; Mann-Whitney test p = 0.03; RMS2: OPHN1$^{-/y}$ mice n = 2.45 ± 0.12, control mice n = 1.42 ± 0.12; Mann-Whitney test p=0.03). (b) Chains' thickness in micrometers (RMS1: OPHN1$^{-/y}$ mice = 16.51 ± 0.49 µm, control mice = 10.55 ± 0.38 µm; Mann-Whitney test p = 0.03; RMS2: OPHN1$^{-/y}$ mice = 13.80 ± 0.96 µm, control mice = 10.82 ± 1.16 µm; Mann-Whitney test p = 0.15). (c) Chains' length in cell number (RMS1: OPHN1$^{-/y}$ mice n = 9.70 ± 1.07, control mice n = 15.24 ± 0.28; Mann-Whitney test p = 0.03; RMS2: OPHN1$^{-/y}$ mice n = 11.13 ± 0.22, control mice n = 15.79 ± 0.88; Mann-Whitney test p = 0.03). (d) Chains' lenght in micrometers (RMS1: OPHN1$^{-/y}$ mice = 96.84 ± 4.96 µm, control mice = 141.53 ± 6.39 µm; Mann-Whitney test p = 0.03; RMS2: OPHN1$^{-/y}$ mice = 112.11 ± 4.10 µm, control mice = 146.82 ± 6.50 µm; Mann-Whitney test p = 0.03). (e) Number of points in which chains deviate their orientation (RMS1: OPHN1$^{-/y}$ mice n = 3.63 ± 0.09, control mice n = 1.42 ± 0.10; Mann-Whitney test p = 0.03; RMS2: OPHN1$^{-/y}$ mice n = 2.90 ± 0.22, control mice n = 1.62 ± 0.21; Mann-Whitney test p = 0.03). (f) Invasion of astrocytic processes into the RMS (RMS1: OPHN1$^{-/y}$ mice % = 26.81 ± 0.89, control mice % = 8.93 ± 1.45; Mann-Whitney test p = 0.03; RMS2: OPHN1$^{-/y}$ mice % = 29.78 ± 0.12, control mice % = 9.70 ± 0.12; Mann-Whitney test p = 0.04).*

These findings could further explains the dispersion and the chaotic distribution of adult-born cells along the RMS, from the SVZ to the OB.

In wt animals, the astrocytic processes that surround the RMS and support that chains of neuronal precursors mainly run parallel to the chains of migrating neuroblasts, enwrapping them. Interestingly, in OPHN1$^{-/y}$ mice we noticed that astrocyte-like cells exhibited thicker processes, suggesting that a mechanism of gliosis was going on. Their processes invaded the chains of newly generated cells, and were intermingled between migrating neuronal precursors (Graph 4.3f). These data indicated that their role as scaffolding structures for the migrating cells could be disrupted by the mutation of OPHN1.

4.5. Alteration of the morphology of neuroblasts along the RMS in OPHN1$^{-/y}$ mice

Neuronal precursors during migration extend their leading process in response to molecular cues that drive their progression along the RMS. Neuroblast's leading process determine the direction of the migration and the soma of the cell translocate after the leading process. To fulfill this driving function, the leading-process retains a path-finding ability that play a key role in neuroblast translocation along the RMS. Exploring the surrounding environment to identify the proper path for the migration, the vast majority of neuroblasts extend a single leading process (i.e. unipolar neuroblasts). Some neuronal precursors can extend multiple processes acquiring a bipolar conformation, or, more rarely, a multipolar shape.

To investigate whether the impairment in the migration could be ascribed to the altered morphology, the latter was analyzed. Injection of lentivirus expressing GFP (LV-GFP) were performed in the SVZ to label the new cells. Immunostianing against DCX, was performed to highlight the RMS (see methods for details; Figure 4.4.).

We quantified cell polarity 7 days after LVGFP injection in the same ROIs named above (RMS1, RMS2, core of the OB; Graph 4.4.).

Neuroblasts were categorized according to the number of processes:

- type I (unipolar cells), single leading process;
- type II, bipolar cells;
- type III, multipolar cells.

Cell counts were expressed as a percentage of total number of neuroblasts.
To study the morphological aspects of the cell polarity, sagittal sections (70 µm thick) were cut at vibratome. Slices were immunolabelled with antibody against DCX.
Four contiguous slices per hemisphere were analyzed and four animals per condition were studied.

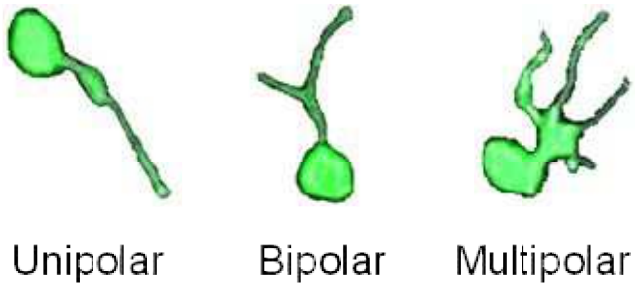

Figure 4.4.: Neuroblasts along the rostral migratory stream (RMS) has altered morphology in OPHN1$^{-/y}$ mice. *Examples of the different types of morphology of migrating neuroblasts.(On the left)Unipolar shaped neuroblasts, with one single leading process, are the typical migrating cells along the RMS. (In the middle) Some cells can exhibit a bipolar shape with the leading process that divide in two branches. (On the right) Very rarely neuroblasts can extend multiple processes acquiring a multipolar shape.*

We observed that throughout the entire pathway from the SVZ to the OB the proportion between the three populations of migrating cells was severely perturbed. We found that in RMS1, the proportion of unipolar cells was strikingly lower in OPHN1$^{-/y}$ mice with respect to controls. On the contrary the ratio of bipolar and multipolar cells was significantly increased.

RMS1		OPHN1$^{-/y}$	Controls	p-Value
	Unipolar cells	57.5% ± 1.25%	78% ± 1.25%	= 0.03
	Bipolar cells	28.5% ± 0.82%	18 ± 0.48%	= 0.03
	Multipolar cells	14.5% ± 0.65%	5 ± 0.45%	= 0.03

The reduction of the unipolar-shaped complement in favor of the bipolar/multipolar cells persists in RMS2, comparing OPHN1$^{-/y}$ mice with wt mice.

RMS2		OPHN1$^{-/y}$	Controls	p-Value
	Unipolar cells	58.5% ± 0.71%	71% ± 2.40%	= 0.03
	Bipolar cells	29.5% ± 0.48%	21 ± 1.5%	= 0.03
	Multipolar cells	13% ± 0.82%	7.5 ± 1.47 %	= 0.03

The alteration in the proportion of the three different neuroblasts' type occurred also in the core of the OB in OPHN1$^{-/y}$ mice with respect to littermate controls.

Core of the OB		OPHN1$^{-/y}$	Controls	p-Value
	Unipolar cells	58% ± 1.49%	68.5% ± 2.50%	= 0.03
	Bipolar cells	30% ± 1.55%	23 ± 1.47%	= 0.06
	Multipolar cells	13.5% ± 0.71%	9 ± 1.11%	= 0.03

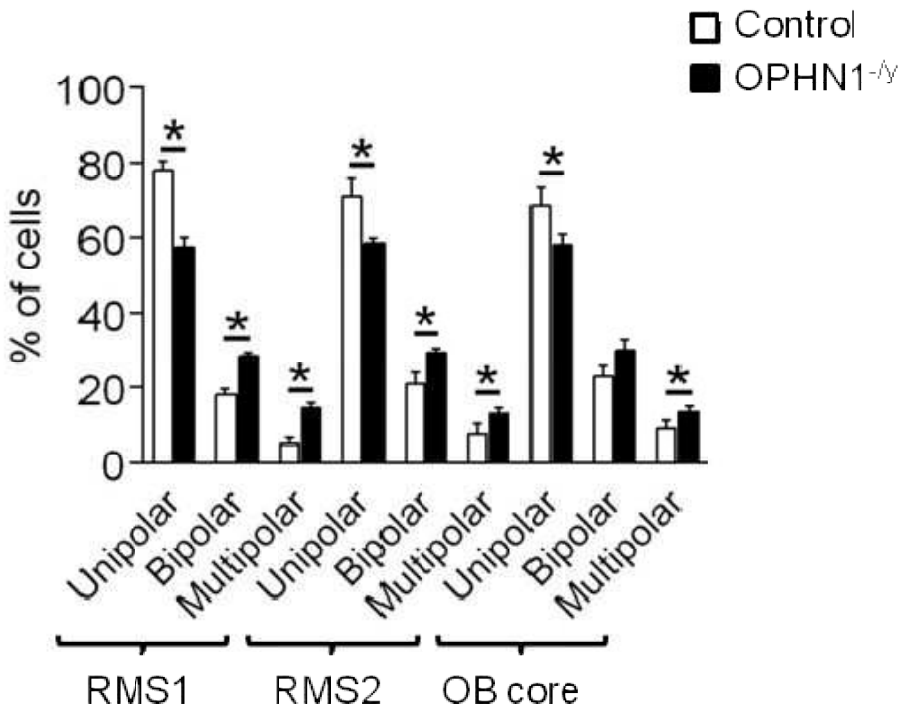

Graph 4.4.: Quantification of neuronal polarity in the three ROIs of the rostral migratory stream *(RMS1, RMS2, core of the OB and displaced neuroblasts) in OPHN1$^{-/y}$ mice (n = 4) and wt mice (n = 4). Neuroblasts are categorized according to the number of processes: unipolar cells, bipolarcells and multipolar cells. Data were analyzed using the Mann-Whitney test.*

4.6. Time-lapse imaging of migrating neuroblasts revealed reduced cell progression in OPHN1$^{-/y}$ mice

Data obtained from immunohistochemistry experiments clearly supported the hypothesis that in OPHN1$^{-/y}$ mice the migration process from the SVZ to the OB was deeply perturbed. To dissect the mechanisms underlying altered migration along the RMS we performed time-lapse imaging of GFP-labeled migrating neuroblasts in thick sagittal sections of the brain (300 μm) containing the RMS and the OB, by means of two-photon imaging. Lentiviral vectors expressing GFP were injected in the SVZ to label the newly generated cells. Slices were cut at the vibratome in oxygenated cutting solution (see methods) and imaging was performed, in six animals per condition, in oxygenated artificial cerebral-spinal fluid (ACSF) for at least two continuous hours, time during which we tracked and quantified neuroblast migration four to six days after lentiviral injection along the RMS (Figure 4.5.) in OPHN1$^{-/y}$ mice and littermate controls (Figure 4.6.).

En route to the OB, neuroblasts translocate in a saltatory manner, alternating migratory phases, in which cells move, and pausing phases, in which cells stop (Schaar and McConnell, 2005). The saltatory pattern of translocation occurs not only in the temporal but also in the spatial dimension. Indeed, neuroblasts proceed toward the OB but also in the opposite direction, although the net progression is toward the OB.

Because of the saltatory nature of neuroblasts translocation, newborn cells motility was computed by using distinct parameters: (1.) Average speed (μm/hour), considering the average translocation speed of neuroblasts in one hour of time-lapse imaging (including both migrating and pausing phases) (2.) Instantaneous speed (μm/min), that calculate migration speed exclusively in the translocation phase (3.) Moving time, indicates the amount of time cells spend in the migratory phase (4.) The directionality of migrating cells, computed as the percentage of cells migrating towards the olfactory bulb.

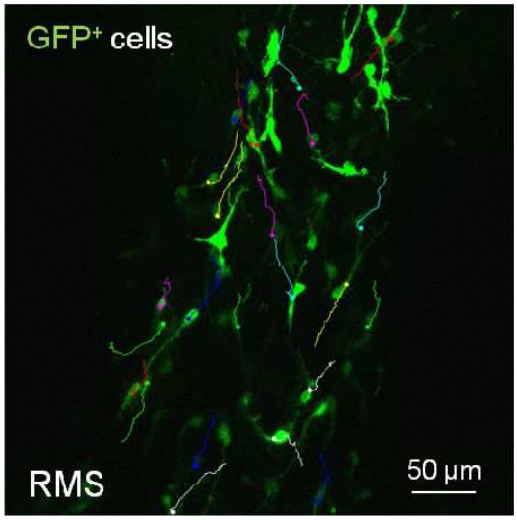

Figure 4.5.: GFP-labeled neuroblasts along the rostal migratory stream (RMS); *representative high magnification of confocal stop-frame image of GFP-labeled migrating neuroblasts along the RMS. Migrating cells tracking are overlaid: soma of the cells is indicated by dots and the path they travel is highlighted by lines; each different color represents a different cell.*

We found that in OPHN1$^{-/y}$ mice both the percentage of moving time (Graph 4.5.c) and the instantaneous speed (Graph 4.5.b) of migrating neuroblasts were significantly reduced with respect to control mice, resulting in an overall reduction of the average translocation speed of neuronal precursors (Graph 4.5.a). Furthermore, considering the complement of cells migrating towards the OB, we found a severe reduction in their percentage in OPHN1$^{-/y}$ mice compared to littermate controls (Graph 4.5.d).

By performing time-lapse imaging of migrating neuroblasts, we demonstrated that, the migration of neuronal precursors along the RMS is dramatically hampered in mice carrying a null mutation of oligophrenin-1.

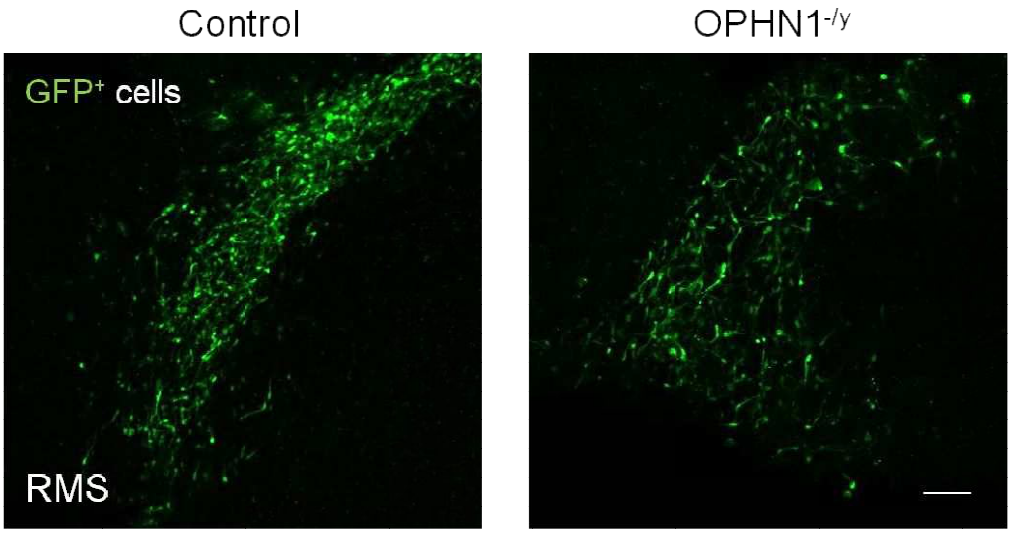

Figure 4.6.: Neuronal precursors progress less along the rostral migratory stream (RMS) in OPHN1$^{-/y}$ mice. *Representative two-photon stop-frame image of GFP-labeled migrating neuroblasts along the RMS, in OPHN1$^{-/y}$ mice (on the right) and in control mice (on the left). Bar = 100 µm.*

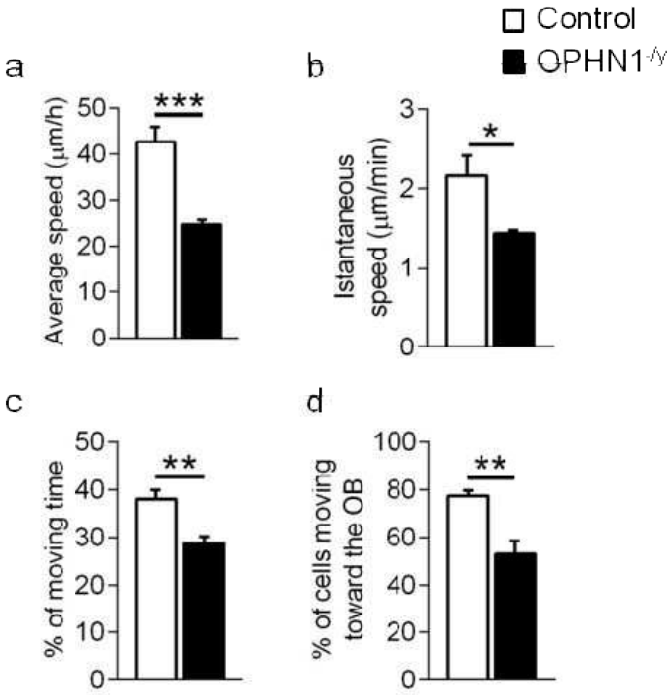

4.5.: Quantification of migrating neuronal precursors' tracking along the rostral migratory stream (RMS) *in OPHN1$^{-/y}$ mice (n = 6) and wt mice (n = 6). (a) Average translocation speed (OPHN1$^{-/y}$ mice s = 24.7 ± 0.89 µm/hour, control mice s = 42.76 ± 3.16 µm/hour; Mann-Whitney test p<0.001). (b) Instantaneous speed (OPHN1$^{-/y}$ mice s = 1.44 ± 0.04 µm/min, control mice s = 2.48 ± 0.39 µm/min; Mann-Whitney test p=0.04). (c) Percentage of moving time (OPHN1$^{-/y}$ mice % = 28.82 ± 1.40, control mice % = 38.16 ± 1.79; Mann-Whitney test p=0.01). (d) Directionality of migration (OPHN1$^{-/y}$ mice % = 53.09 ± 5.60, control mice % = 77.55 ± 0.96; Mann-Whitney test p=0.01).*

4.7. GABA reduces neuronal precursors speed in wild type mice but not in OPHN1$^{-/y}$ mice

Taken into account the modulatory role of GABA onto neuroblasts (Bolteus and Bordey, 2004), we next sought to address whether the impaired migration in OPHN1$^{-/y}$ mice could rely on altered GABA signalling. We tested several compounds able to modulate GABA signalling on migrating neuroblasts, *en route* to the OB, in OPHN1$^{-/y}$ mice and littermate controls. Time-lapse Imaging was performed using the same parameters used in the previous experiments. GFP-labeled newly generated cells were tracked for two hours at baseline condition, then slices were incubated for fifteen minutes with GABA 10 µM diluted in ACSF, and imaging was repeated for other two hours with GABA continuously perfused in the imaging chamber (Figure 4.7.). Five animals per condition were analyzed.

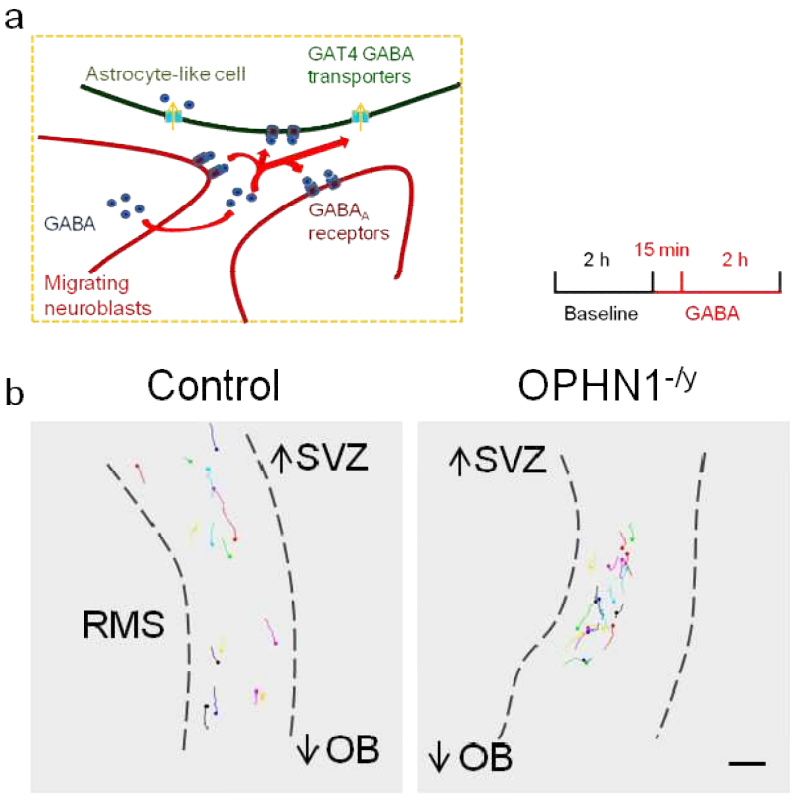

Figure 4.7.: GABA reduces neuronal precursors speed along the rostral migratory stream (RMS) in wild type mice but not in OPHN1$^{-/y}$ mice. (a) Scheme of experimental design. (b) Migrating neuroblasts' tracks *upon GABA application on slices, in OPHN1$^{-/y}$ mice (on the right) and in control mice (on the left), in two hours of imaging. Bar = 100 µm.*

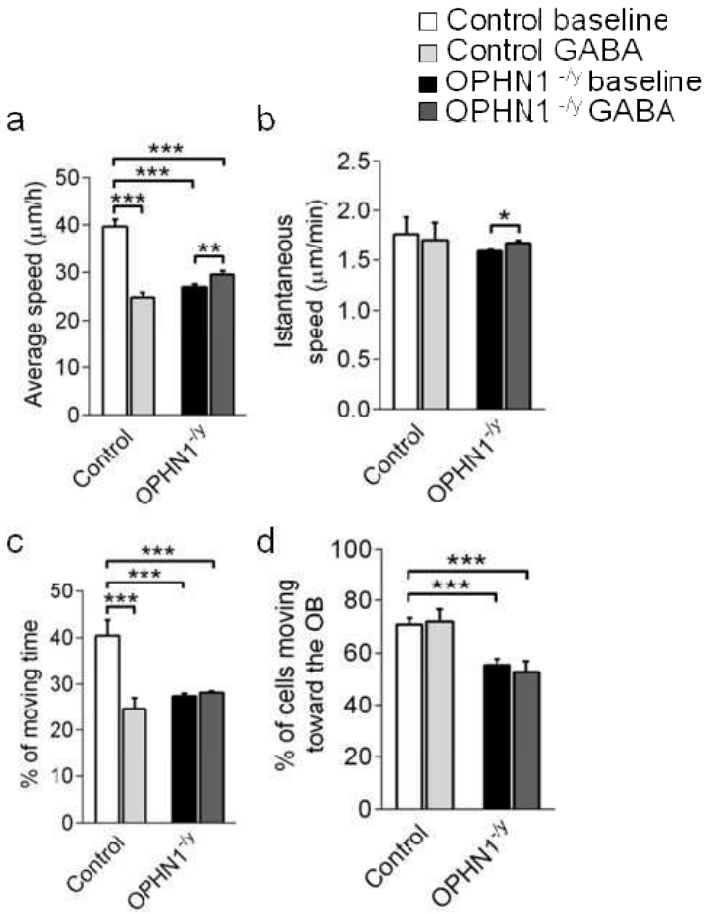

4.6.: Quantification of migrating neuronal precursors' tracking along the rostral migratory stream (RMS) upon GABA application *in OPHN1$^{-/y}$ mice (n = 5) and wt mice (n = 5). (a) Average translocation speed (wt baseline s = 39.57 ± 1.50 µm/hour, wt GABA s = 24.78 ± 1.07 µm/hour; OPHN1$^{-/y}$ baseline s = 26.96 ± 0.59 µm/hour, OPHN1$^{-/y}$ GABA s = 29.56 ± 0.76 µm/hour; Mann-Whitney test: wt baseline-wt GABA, p<0.001; OPHN1$^{-/y}$ baseline-OPHN1$^{-/y}$ GABA, p=0.02; wt baseline-OPHN1$^{-/y}$ baseline, p<0.001; wt baseline-OPHN1$^{-/y}$ GABA, p<0.001). (b) Instantaneous speed (wt baseline s = 1.69 ± 0.17 µm/min, wt GABA s = 1.65 ± 0.18 µm/min; OPHN1$^{-/y}$ baseline s = 1.65 ± 0.03 µm/min, OPHN1$^{-/y}$ GABA s = 1.76 ± 0.05 µm/min; Mann-Whitney test: wt baseline-wt GABA, p=0.75; OPHN1$^{-/y}$ baseline-OPHN1$^{-/y}$ GABA, p<0.01; wt baseline-OPHN1$^{-/y}$ baseline, p=0.12; wt baseline-OPHN1$^{-/y}$ GABA, p=0.77). (c) Percentage of moving time (wt baseline % = 40.42 ± 3.36, wt GABA % = 25.64 ± 2.31; OPHN1$^{-/y}$ baseline % = 27.19 ± 0.38, OPHN1$^{-/y}$ GABA % = 28.00 ± 0.44; Mann-Whitney test: wt baseline-wt GABA, p<0.001; OPHN1$^{-/y}$ baseline-OPHN1$^{-/y}$ GABA, p=0.29; wt baseline-OPHN1$^{-/y}$ baseline, p<0.0001; wt baseline-OPHN1$^{-/y}$ GABA, p<0.001). (d) Directionality of migration (wt baseline % = 70.84 ± 2.40, wt GABA % = 71.95 ± 4.61; p = 0.42; OPHN1$^{-/y}$ baseline % = 54.19 ± 1.66, OPHN1$^{-/y}$ GABA % = 53.65 ± 2.82; p = 0.42; Mann-Whitney test: wt baseline-wt GABA, p=0.42; OPHN1$^{-/y}$ baseline-OPHN1$^{-/y}$ GABA, p=0.75; wt baseline-OPHN1$^{-/y}$ baseline, p<0.01; wt baseline-OPHN1$^{-/y}$ GABA, p<0.01).*

In controls, exogenous GABA application significantly reduced the average translocation speed of migrating SVZ-derived cells along the RMS, confirming data obtained in previous work (Bolteus and Bordey, 2004) (Graph 4.6.a), by reducing the percentage of moving time (Graph 4.6.c); However, the instantaneous speed reached by neuroblasts was not affected by GABA application (Graph 4.6.b). Furthermore, GABA administration did not produce any effect on the directionality of migration in wt mice (Graph 4.6.d).

Remarkably, in OPHN1$^{-/y}$ mice, GABA application elicited opposite effects than in littermate controls: the average translocation speed was increased by GABA application (Graph 4.6.a), likely due to an increased instantaneous speed in migrating cells (Graph 4.6.b). Surprisingly, the percentage of moving time was not affected by tonic GABA application (Graph 4.6.c).

The results obtained with GABA application on migrating cells in OPHN1$^{-/y}$ mice strongly supported the hypothesis that loss-of-function mutation of OPHN1 leads to alterations in GABA signaling in SVZ neuronal precursors *en route* to the OB, eventually resulting in hampered progression of these cells along the migratory path.

4.8. Blocking the reuptake of GABA lowers neuroblasts translocation speed in wild type mice but not in OPHN1$^{-/y}$ mice

To further explore the effects of sustained tonic GABA activity in neuroblasts along the RMS, we decide to manipulate GABA signaling onto migrating cells by acting on scaffold astrocyte-like cells that surround the chains of neuronal precursors (Lois et al., 1996). We blocked the uptake of GABA from the extracellular compartment, inhibiting the activity of GAT4 GABA transporters that are specifically expressed in astrocytic processes along the RMS (Bolteus and Bordey, 2004). The inhibitor SNAP5114 specifically inhibits GAT4 transporter..

Time-lapse Imaging was performed using the same parameters used in the previous experiments. Briefly, GFP-labeled newborn cells were tracked for two hours at baseline condition. Slices were then incubated for one hour with

SNAP5114 50 µM diluted in ACSF, and imaging was repeated for two hours with GABA continuously perfused in the imaging chamber (Figure 4.8.). Three animals per condition were analyzed.

As expected, in control mice, blocking GAT4 transporters activation upon SNAP5114 acute application, significantly decreased average translocation speed of migrating neuronal precursors (Graph 4.7.a), consequent to a reduction in both instantaneous speed (Graph 4.7.b) and percentage of moving time (Graph 4.7.c).

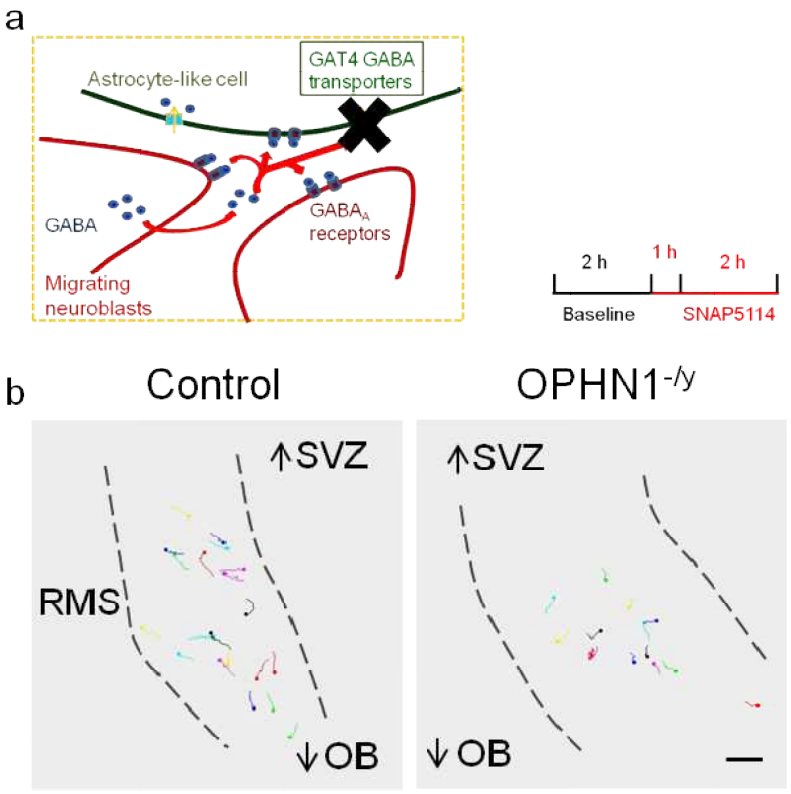

Figure 4.8.: Blocking the reuptake of GABA lowers neuroblasts translocation speed along the rostral migratory stream (RMS) in wild type mice but not in OPHN1$^{-/y}$ mice. (a) Scheme of experimental design. (b) Migrating neuroblasts' tracks *upon SNAP5114 application on slices, in OPHN1$^{-/y}$ mice (on the right) and in control mice (on the left), in two hours of imaging. Bar = 100 µm.*

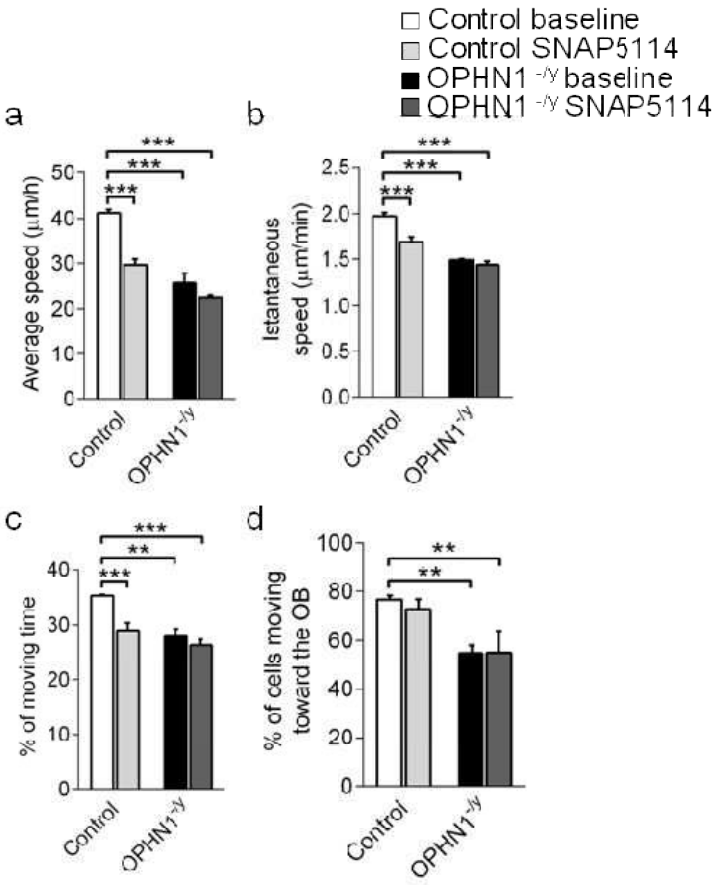

4.7.: Quantification o fmigrating neuronal precursors' tracking along the rostral migratory stream (RMS) upon SNAP5114 application *in OPHN1$^{-/y}$ mice (n = 3) and wt mice (n = 3). (a) Average translocation speed (wt baseline s = 41.16 ± 0.76 µm/hour, wt SNAP5114 s = 29.69 ± 2.10 µm/hour; OPHN1$^{-/y}$ baseline s = 25.66 ± 1.22 µm/hour, OPHN1$^{-/y}$ SNAP5114 s = 22.65 ± 0.47 µm/hour; Mann-Whitney test: wt baseline-wt SNAP5114, p<0.001; OPHN1$^{-/y}$ baseline-OPHN1$^{-/y}$ SNAP5114, p=0.08; wt baseline- OPHN1$^{-/y}$ baseline, p<0.001; wt baseline-OPHN1$^{-/y}$ SNAP5114, p<0.001). (b) Instantaneous speed (wt baseline s = 1.97 ± 0.04 µm/min, wt SNAP5114 s = 1.69 ± 0.06 µm/min; OPHN1$^{-/y}$ baseline s = 1.49 ± 0.02 µm/min, OPHN1$^{-/y}$ SNAP5114 s = 1.44 ± 0.04 µm/min; Mann-Whitney test: wt baseline-wt SNAP5114, p<0.001; OPHN1$^{-/y}$ baseline-OPHN1$^{-/y}$ SNAP5114, p=0.35; wt baseline-OPHN1$^{-/y}$ baseline, p<0.001; wt baseline-OPHN1$^{-/y}$ SNAP5114, p<0.001). (c) Percentage of moving time (wt baseline % = 35.24 ± 0.21, wt SNAP5114 % = 29.00 ± 1.34; OPHN1$^{-/y}$ baseline % = 28.16 ± 1.08, OPHN1$^{-/y}$ SNAP5114 % = 26.32 ± 1.01; Mann-Whitney test: wt baseline-wt SNAP5114, p<0.001; OPHN1$^{-/y}$ baseline-OPHN1$^{-/y}$ SNAP5114, p=0.30; wt baseline-OPHN1$^{-/y}$ baseline, p<0.01; wt baseline-OPHN1$^{-/y}$ SNAP5114, p<0.001). (d) Directionality of migration (wt baseline % = 76.67 ± 1.67, wt SNAP5114 % = 72.80 ± 3.90; OPHN1$^{-/y}$ baseline % = 54.81 ± 3.29, OPHN1$^{-/y}$ SNAP5114 % = 55.03 ± 8.84; Mann-Whitney test: wt baseline-wt SNAP5114, p=0.22; OPHN1$^{-/y}$ baseline-OPHN1$^{-/y}$ SNAP5114, p=0.68; wt baseline-OPHN1$^{-/y}$ baseline, p<0.01; wt baseline-OPHN1$^{-/y}$ SNAP5114, p<0.01).*

In OPHN1$^{-/y}$ mice, blocking GABA uptake activity in astrocytes, did not produce any effect on migrating neuroblasts. SVZ-derived cells showed similar average speed (Graph 4.7.a), as well as instantaneous speed (Graph 4.7.b) and percentage of moving time (Graph 4.7.c). In agreement with observations from immunohystochemical analysis, which revealed alterations in specialized astrocyte morphology (see Figure 4.3.), these data suggested that physiological functions of astrocyte-like cells that ensheat neuroblasts' chains may be deeply perturbed.

Directionality of migration, again, was not affected by blocking GABA reuptake in wt animals (Graph 4.7.d), nor in OPHN1$^{-/y}$ mice (Graph 4.7.d).

These data suggest that GABA signalling controlling the progression of neuroblast is deeply subverted in mutant mice

4.9. $GABA_A$ receptors inhibition enhances the speed of neuronal precursors in wild type mice with opposite effects in OPHN1$^{-/y}$ mice

GABA exerts its regulatory activity on migrating cells through $GABA_A$ receptors activation (Bolteus and Bordey, 2004), Thus, the alterations of the effects elicited by GABA on adult-generated cells along the RMS in OPHN1$^{-/y}$ mice could be ascribed to (1.) the lack of $GABA_A$ receptors, or to defects in their activity; conversely, another possible explanation could be given by (2.) a subversion of the polarity of GABA response in newborn neurons in mutant animals.

To investigate whether $GABA_A$ receptors were missing, or inactive, we employed bicuculline to block $GABA_A$ receptors in migrating neuronal precursors.

We performed time-lapse imaging on thick slices with the same parameters used in the previous experiments, tracking GFP-labeled adult-born cells migrating to the OB for two hours at baseline condition, and subsequently for two hours with bicuculline continuously perfused in the imaging chamber, after incubation for one hour with bicuculline 100 μM diluted in ACSF (Figure 4.9.). Three animals per condition were analyzed.

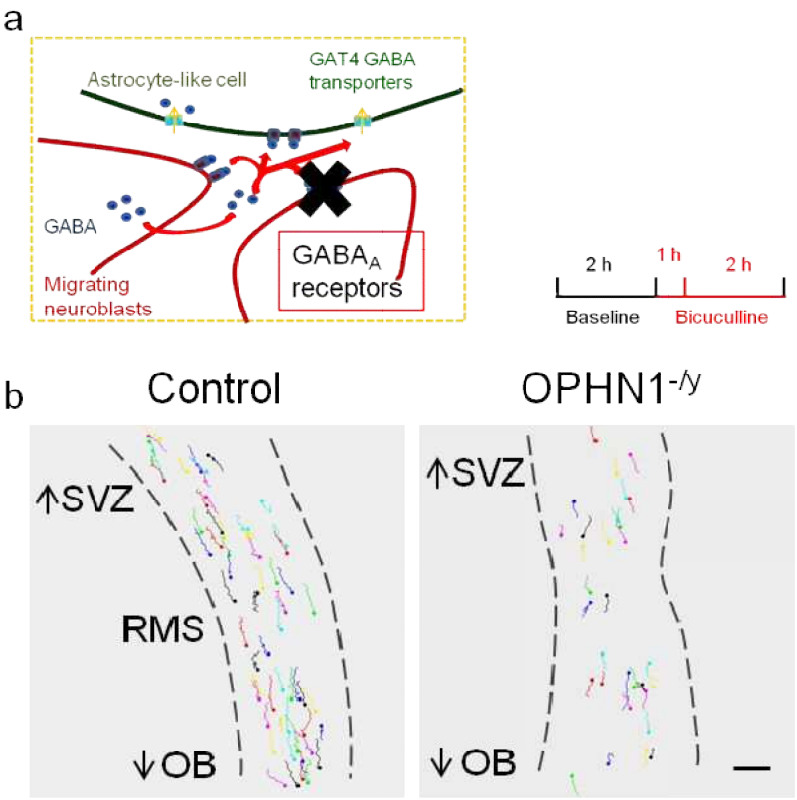

Figure 4.9.: GABA$_A$ receptors inhibition enhances the speed of neuronal precursors along the rostral migratory stream (RMS) in wild type mice with opposite effects in OPHN1$^{-/y}$ mice. (a) Scheme of experimental design. (b) Migrating neuroblasts' tracks *upon bicuculline application on slices, in OPHN1$^{-/y}$ mice (on the right) and in control mice (on the left), in two hours of imaging. Bar = 100 µm.*

In agreement with data obtained in response to GABA application, blocking the activity of GABA$_A$ receptors promptly increased the percentage of moving time and therefore the average speed in controls, (Graph 4.8.c), (Graph 4.8.a), The instantaneous speed was not affected by bicuculline treatment. (Graph 4.8.b). On the contrary, bicuculline application lowered average speed (Graph 4.8.a), affecting not only the percentage of moving time (Graph 4.8.c), but also the instantaneous speed (Graph 4.8.b) in migrating neuroblasts in OPHN1$^{-/y}$ mice.

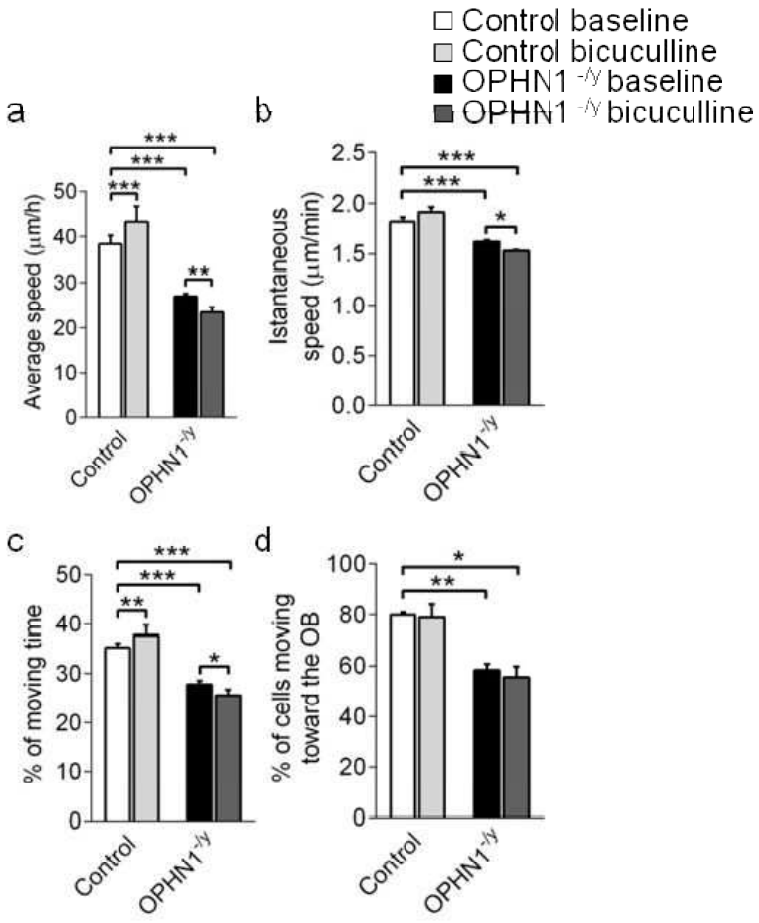

4.8.: Quantification of migrating neuronal precursors' tracking along the rostral migratory stream (RMS) upon bicuculline application *in OPHN1$^{-/y}$ mice (n = 3) and wt mice (n = 3). (a) Average translocation speed (wt baseline s = 38.33 ± 1.84 µm/hour, wt bicuculline s = 43.33 ± 3.35 µm/hour; OPHN1$^{-/y}$ baseline s = 26.96 ± 0.61 µm/hour, OPHN1$^{-/y}$ bicuculline s = 23.45 ± 1.10 µm/hour; Mann-Whitney test: wt baseline-wt bicuculline, p<0.01; OPHN1$^{-/y}$ baseline-OPHN1$^{-/y}$ bicuculline, p<0.01; wt baseline-OPHN1$^{-/y}$ baseline, p<0.001; wt baseline-OPHN1$^{-/y}$ bicuculline, p<0.001). (b) Instantaneous speed (wt baseline s = 1.82 ± 0.04 µm/min, wt bicuculline s = 1.92 ± 0.05 µm/min; OPHN1$^{-/y}$ baseline s = 1.62 ± 0.02 µm/min, OPHN1$^{-/y}$ bicuculline s = 1.53 ± 0.01 µm/min; Mann-Whitney test: wt baseline-wt bicuculline, p=0.09; OPHN1$^{-/y}$ baseline-OPHN1$^{-/y}$ bicuculline, p=0.04; wt baseline-OPHN1$^{-/y}$ baseline, p<0.001; wt baseline-OPHN1$^{-/y}$ bicuculline, p<0.001). (c) Percentage of moving time (wt baseline % = 35.24 ± 0.88, wt bicuculline % = 37.70 ± 2.04; OPHN1$^{-/y}$ baseline % = 27.79 ± 0.81, OPHN1$^{-/y}$ bicuculline % = 25.58 ± 1.17; Mann-Whitney test: wt baseline-wt bicuculline, p<0.01; OPHN1$^{-/y}$ baseline-OPHN1$^{-/y}$ bicuculline, p=0.03; wt baseline-OPHN1$^{-/y}$ baseline, p<0.001; wt baseline-OPHN1$^{-/y}$ bicuculline, p<0.001). (d) Directionality of migration (wt mice: baseline % = 81.03 ± 1.03, bicuculline % = 76.67 ± 5.24; OPHN1$^{-/y}$ mice: baseline % = 58.89 ± 2.42, bicuculline % = 51.99 ± 4.13; Mann-Whitney test: wt baseline-wt bicuculline, p=0.22; OPHN1$^{-/y}$ baseline-OPHN1$^{-/y}$ bicuculline, p=0.22; wt baseline-OPHN1$^{-/y}$ baseline, p<0.01; wt baseline-OPHN1$^{-/y}$ bicuculline, p<0.01).*

Blocking $GABA_A$ receptors, did not affect the directionality of migration along the RMS (Graph 4.8.d).

These findings suggested that loss-of function mutation of OPHN1 could lead to an altered response to GABA in neuronal precursors It is unlikely that this alteration depended on defects in $GABA_A$ receptors activity, since both GABA application and inhibition of $GABA_A$ receptors, affected the speed of neuronal precursors, in controls and $OPHN1^{-/y}$ mice.

These results may, therefore, indicate that the mechanism underlying hampered neuronal precursors migration could be ascribed, at least in part, to a subverted polarity of GABA response in mice carrying a null mutation of *OPHN1* gene.

4.10. Blocking NKCC1 activity reduced neuroblast motility along the rostral migratory stream in wild type mice but not in $OPHN1^{-/y}$ mice

The polarity of GABA response is governed by the activity of two chloride cotransporters, namely NKCC1 and KCC2, that determine the intracellular chloride concentration in neurons ($[Cl^-]_i$). In migrating neuronal precursors NKCC1 is predominantly expressed (Mejia-Gervacio et al., 2011). To understand whether impaired motility of SVZ-derived cells along the RMS in $OPHN1^{-/y}$ mice, could be ascribed to subverted GABA response polarity, we explored the effects of pharmacological blockade of chloride cotransporters activity on newly generated cells in $OPHN1^{-/y}$ mice and littermate controls.

We blocked NKCC1 activity using the specific inhibitor, bumetanide, following the same protocol used in previous experiments. Brain slices were incubated for one hours with bumetanide 10 μM diluted in ACSF, and time-lapse imaging of GFP-labeled adult-born cells was performed for two continuous hours at baseline condition and after incubation with bumetanide perfused in the imaging chamber (Figure 4.10.). Four animals per condition were analyzed.

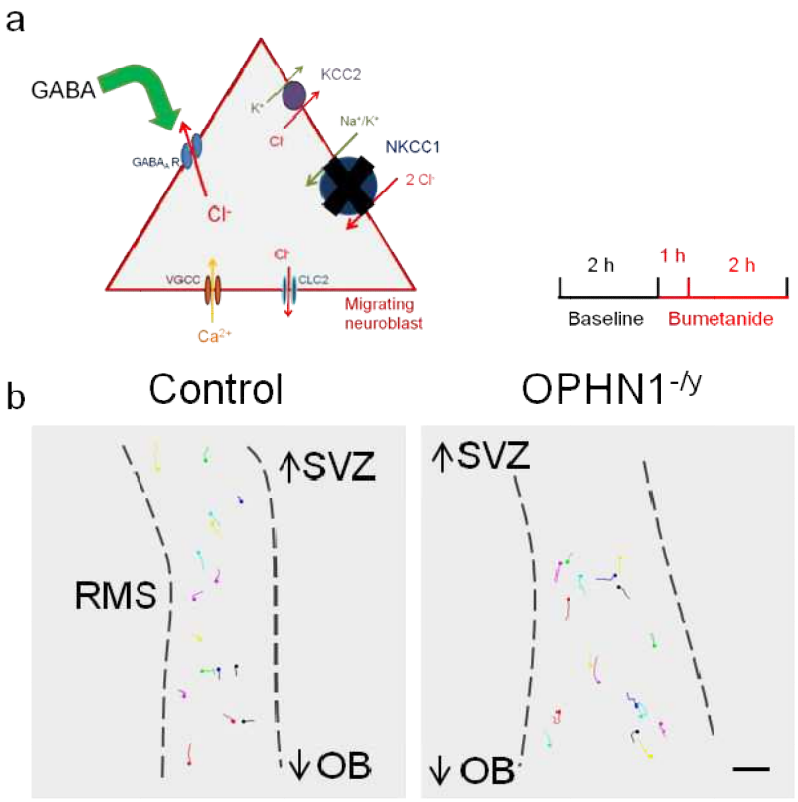

Figure 4.10.: Blocking NKCC1 activity reduce neuroblast motility along the rostral migratory stream (RMS) in wild type mice but not in OPHN1$^{-/y}$ mice. (a) Scheme of experimental design. (b) Migrating neuroblasts' tracks *upon bumetanide application on slices, in OPHN1$^{-/y}$ mice (on the right) and in control mice (on the left), in two hours of imaging. Bar = 100 µm.*

We observed that by pharmacologically blocking NKCC1 activity with bumetanide, the instantaneous speed of migrating neuroblasts (Graph 4.9.b) and the amount of time spent in their translocation phase (Graph 4.9.c) were significantly reduced in control mice, resulting in an overall reduction of the average speed (Graph 4.9.a).

The percentage of cells that migrated toward the OB did not change upon bumetanide application (Graph 4.9.d).

Surprisingly, blocking NKCC1 activity did not produce any significant effect on neuronal precursors motility in OPHN1$^{-/y}$ mice (Graph 4.9.a-b). Accordingly, the percentage of moving time was unaffected (Graph 4.9.c).

These result suggested that GABA response polarity could be subverted in OPHN1$^{-/y}$ mice.

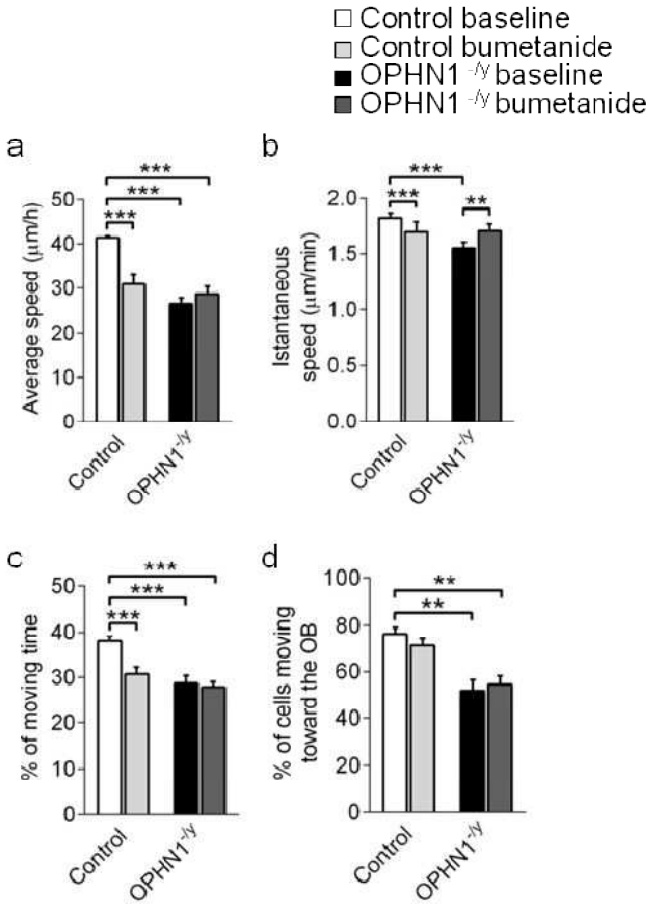

4.9.: Quantification of migrating neuronal precursors' tracking along the rostral migratory stream (RMS) upon bumetanide application *in OPHN1$^{-/y}$ mice (n = 4) and wt mice (n = 4). (a) Average translocation speed (wt baseline s = 41.33 ± 0.40 µm/hour, wt bumetanide s = 30.87 ± 2.41 µm/hour; OPHN1$^{-/y}$ baseline s = 26.47 ± 1.33 µm/hour, OPHN1$^{-/y}$ bumetanide s = 28.69 ± 1.63 µm/hour; Mann-Whitney test: wt baseline-wt bumetanide, p<0.001; OPHN1$^{-/y}$ baseline-OPHN1$^{-/y}$ bumetanide, p=0.06; wt baseline- OPHN1$^{-/y}$ baseline, p<0.001; wt baseline-OPHN1$^{-/y}$ bumetanide, p<0.001). (b) Instantaneous speed (wt baseline s = 1.82 ± 0.04 µm/min, wt bumetanide s = 1.69 ± 0.09 µm/min; OPHN1$^{-/y}$ baseline s = 1.55 ± 0.06 µm/min, OPHN1$^{-/y}$ bumetanide s = 1.70 ± 0.06 µm/min; Mann-Whitney test: wt baseline-wt bumetanide, p<0.001; OPHN1$^{-/y}$ baseline-OPHN1$^{-/y}$ bumetanide, p<0.01; wt baseline-OPHN1$^{-/y}$ baseline, p<0.001; wt baseline-OPHN1$^{-/y}$ bumetanide, p=0.28). (c) Percentage of moving time (wt baseline % = 37.99 ± 1.10, wt bumetanide % = 30.72 ± 1.51; OPHN1$^{-/y}$ baseline % = 28.72 ± 1.69, OPHN1$^{-/y}$ bumetanide % = 27.88 ± 1.20; Mann-Whitney test: wt baseline-wt bumetanide, p<0.001; OPHN1$^{-/y}$ baseline-OPHN1$^{-/y}$ bumetanide, p=0.98; wt baseline-OPHN1$^{-/y}$ baseline, p<0.001; wt baseline-OPHN1$^{-/y}$ bumetanide, p<0.001). (d) Directionality of migration (wt baseline % = 76.42 ± 2.66, wt bumetanide % = 71.19 ± 3.14; OPHN1$^{-/y}$ baseline % = 51.84 ± 4.72, OPHN1$^{-/y}$ bumetanide % = 54.51 ± 3.77; Mann-Whitney test: wt baseline-wt bumetanide, p=0.09; OPHN1$^{-/y}$ baseline-OPHN1$^{-/y}$ bumetanide, p=0.44; wt baseline-OPHN1$^{-/y}$ baseline, p<0.01; wt baseline-OPHN1$^{-/y}$ bumetanide, p<0.01).*

4.11. Blocking KCC2 activity partially restored the motility of neuronal precursors migrating to the OB in OPHN1$^{-/y}$ mice

To further dissect the polarity of the response that GABA elicits in neuronal precursors we blocked KCC2 in neuroblasts during their tangential migration.

To block KCC2 activity, we employed the specific high affinity inhibitor VU0463271 (Figure 4.11.). Imaging was performed as in the previous experiments. GFP-labeled newly generated cells were tracked for two hours at baseline condition, then slices were incubated for one hours with VU0463271 10 µM diluted in ACSF, and imaging was repeated for two hours with VU0463271 continuously perfused in the imaging chamber. Four animals per condition were analyzed.

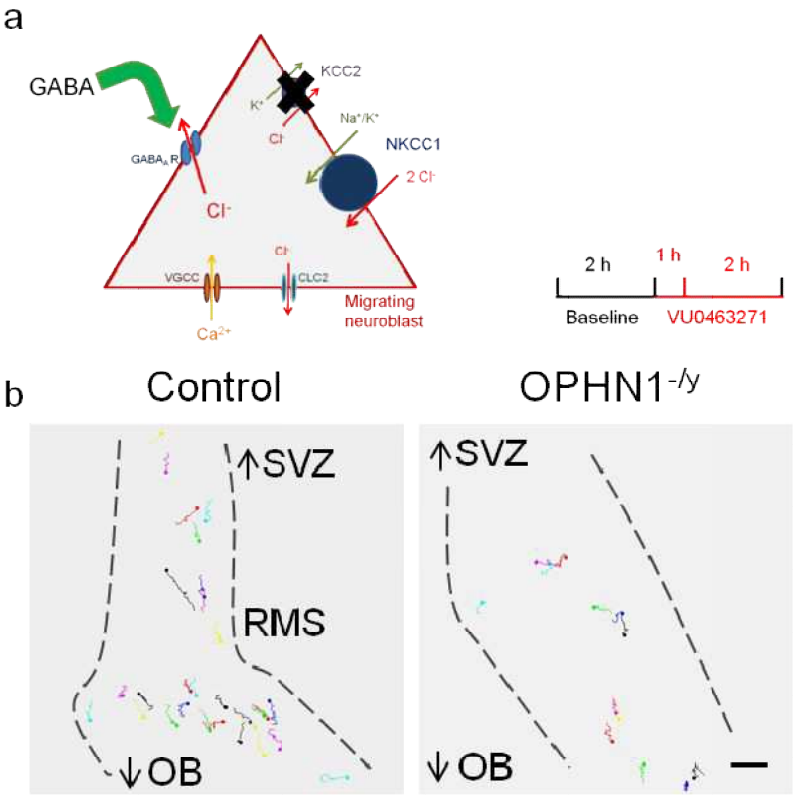

Figure 4.11.: Blocking KCC2 activity partially restore the motility of neuronal precursors migrating to the olfactory bulb (OB) in OPHN1$^{-/y}$ mice. (a) Scheme of experimental design. (b) Tracks of migrating neuroblasts along the rostral migratory stream (RMS) *upon VU0463271 application on slices, in OPHN1$^{-/y}$ mice (on the right) and in control mice (on the left), in two hours of imaging. Bar = 100 µm.*

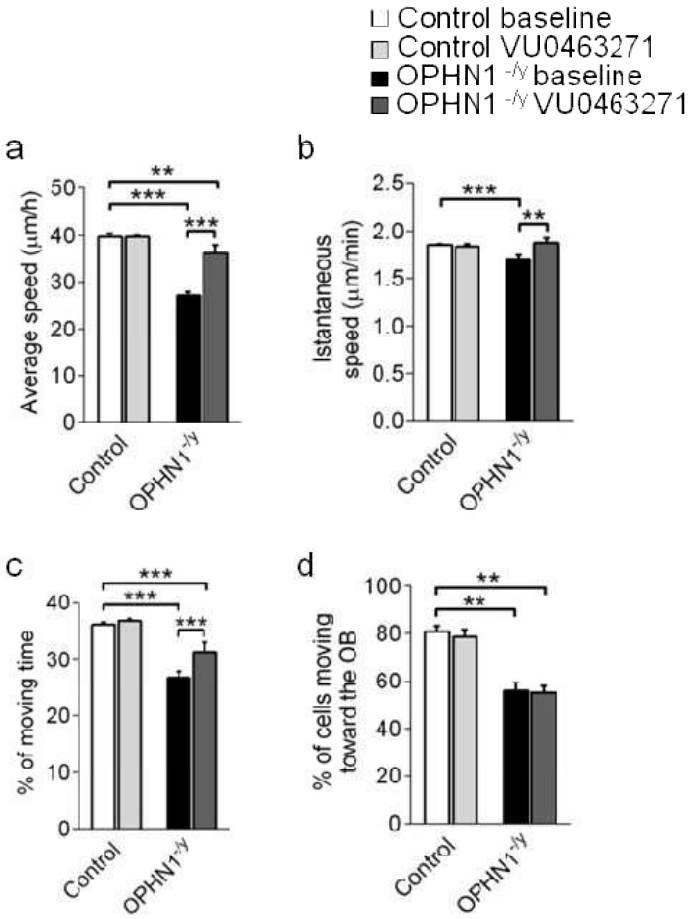

4.10.: Quantification of migrating neuronal precursors' tracking along the rostral migratory stream (RMS) upon VU0463271 application *in OPHN1$^{-/y}$ mice (n = 4) and wt mice (n = 4). (a) Average translocation speed (wt baseline s = 39.54 ± 0.80 µm/hour, wt VU0463271 s = 40.06 ± 0.54 µm/hour; OPHN1$^{-/y}$ baseline s = 27.29 ± 0.79 µm/hour, OPHN1$^{-/y}$ VU0463271 s = 35.04 ± 1.66 µm/hour; Mann-Whitney test: wt baseline-wt VU0463271, p=0.95; OPHN1$^{-/y}$ baseline-OPHN1$^{-/y}$ VU0463271, p<0.001; wt baseline-OPHN1$^{-/y}$ baseline, p<0.001; wt baseline-OPHN1$^{-/y}$ VU0463271, p<0.01). (b) Instantaneous speed (wt baseline s = 1.85 ± 0.01 µm/min, wt VU0463271 s = 1.84 ± 0.02 µm/min; OPHN1$^{-/y}$ baseline s = 1.70 ± 0.05 µm/min, OPHN1$^{-/y}$ VU0463271 s = 1.87 ± 0.05 µm/min; Mann-Whitney test: wt baseline-wt VU0463271, p=0.521; OPHN1$^{-/y}$ baseline-OPHN1$^{-/y}$ VU0463271, p<0.01; wt baseline-OPHN1$^{-/y}$ baseline, p<0.001; wt baseline-OPHN1$^{-/y}$ VU0463271, p=0.52). (c) Percentage of moving time (wt baseline % = 36.11 ± 0.34, wt VU0463271 % = 36.76 ± 0.34; OPHN1$^{-/y}$ baseline % = 26.85 ± 1.07, OPHN1$^{-/y}$ VU0463271 % = 31.34 ± 1.69; Mann-Whitney test: wt baseline-wt VU0463271, p=0.29; OPHN1$^{-/y}$ baseline-OPHN1$^{-/y}$ VU0463271, p<0.001; wt baseline-OPHN1$^{-/y}$ baseline, p<0.001; wt baseline-OPHN1$^{-/y}$ VU0463271, p<0.001). (d) Directionality of migration (wt baseline % = 80.78 ± 2.37, wt VU0463271 % = 78.63 ± 2.93; OPHN1$^{-/y}$ baseline % = 55.87 ± 3.69, OPHN1$^{-/y}$ VU0463271 % = 55.09 ± 2.82; Mann-Whitney test: wt baseline-wt VU0463271, p=0.07; OPHN1$^{-/y}$ baseline-OPHN1$^{-/y}$ VU0463271, p=0.18; wt baseline-OPHN1$^{-/y}$ baseline, p<0.01; wt baseline-OPHN1$^{-/y}$ VU0463271, p<0.01).*

KCC2 block did not exert any effect in control mice. No significant differences were reported in average translocation speed (Graph 4.10.a), instantaneous speed (Graph 4.10.b) or percentage of moving time (Graph 4.10.c).
In OPHN1$^{-/y}$ mice, blocking KCC2 activity in neuroblsts, significantly increased the average speed that was almost completely restored (Graph 4.10.a), Both instantaneous and average speed were affected (Graph 4.10.b) percentage of moving time was increased as well (Graph 4.10.c).

VU0463271 application on brain slices did not impact on the directionality of migration in control mice, nor in OPHN1$^{-/y}$ mice (Graph 4.10.d).

Overall, these findings strongly indicates that GABA response polarity in migrating cells is subverted in OPHN1$^{-/y}$ mice.

4.12. RhoA/ROCK pathway inhibition in neuronal precursors rescued the directionality of migration along the rostral migratory stream in OPHN1$^{-/y}$ mice

Mutation in OPHN1 leads to overactivation of the Rho-associated kinase (ROCK) dowstream pathway.

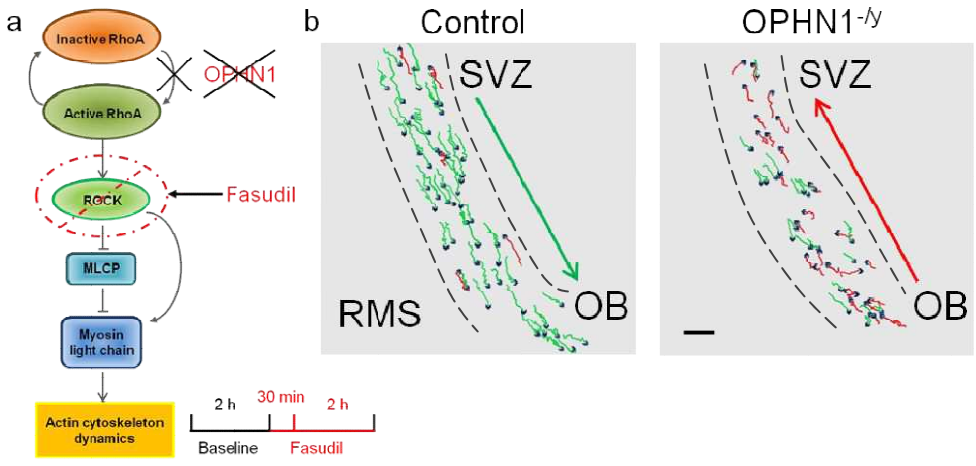

Figure 4.12.: Acute fasudil treatment in neuronal precursors rescued the directionality of migration along the rostral migratory stream (RMS) in OPHN1$^{-/y}$ mice (a) Scheme of experimental design. (b) Migrating neuroblasts' tracks *upon fasudil application on slices, in OPHN1$^{-/y}$ mice (on the right) and in control mice (on the left), in two hours of imaging; green tracks indicate cells moving toward the olfactory bulb (OB), red tracks indicate cells moving away from it, toward the subventricular zone (SVZ). Bar = 100 µm.*

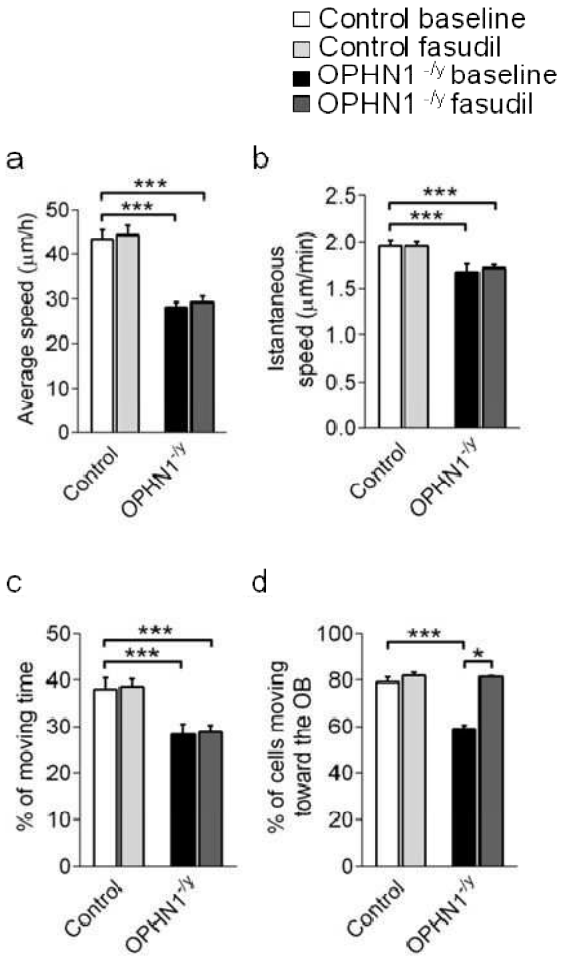

4.11.: Quantification of migrating neuronal precursors' tracking along the rostral migratory stream (RMS) upon fasudil application *in OPHN1$^{-/y}$ mice (n = 3) and wt mice (n = 3). (a) Average translocation speed (wt baseline s = 43.27 ± 2.24 µm/hour, wt fasudil s = 44.38 ± 2.13 µm/hour; OPHN1$^{-/y}$ baseline s = 28.22 ± 1.10 µm/hour, OPHN1$^{-/y}$ fasudil s = 29.30 ± 1.38 µm/hour; Mann-Whitney test: wt baseline-wt fasudil, p=0.34; OPHN1$^{-/y}$ baseline-OPHN1$^{-/y}$ fasudil, p=0.09; wt baseline- OPHN1$^{-/y}$ baseline, p<0.001; wt baseline-OPHN1$^{-/y}$ fasudil, p<0.001). (b) Instantaneous speed (wt baseline s = 1.96 ± 0.06 µm/min, wt fasudil s = 1.96 ± 0.05 µm/min; OPHN1$^{-/y}$ baseline s = 1.68 ± 0.08 µm/min, OPHN1$^{-/y}$ fasudil s = 1.72 ± 0.03 µm/min; Mann-Whitney test: wt baseline-wt fasudil, p=0.79; OPHN1$^{-/y}$ baseline-OPHN1$^{-/y}$ fasudil, p=0.08; wt baseline-OPHN1$^{-/y}$ baseline, p<0.001; wt baseline-OPHN1$^{-/y}$ fasudil, p<0.001). (c) Percentage of moving time (wt baseline % = 37.99 ± 2.46, wt fasudil % = 38.58 ± 1.58; OPHN1$^{-/y}$ baseline % = 28.30 ± 2.28, OPHN1$^{-/y}$ fasudil % = 28.22 ± 1.53; Mann-Whitney test: wt baseline-wt fasudil, p=0.33; OPHN1$^{-/y}$ baseline-OPHN1$^{-/y}$ fasudil, p=0.85; wt baseline-OPHN1$^{-/y}$ baseline, p<0.001; wt baseline-OPHN1$^{-/y}$ fasudil, p<0.001). (d) Directionality of migration (wt baseline % = 78.89 ± 2.20, wt fasudil % = 82.27 ± 1.46; OPHN1$^{-/y}$ baseline % = 60.19 ± 1.50, OPHN1$^{-/y}$ fasudil % = 81.26 ± 0.37; Mann-Whitney test: wt baseline-wt fasudil, p=0.07; OPHN1$^{-/y}$ baseline-OPHN1$^{-/y}$ fasudil, p=0.04; wt baseline-OPHN1$^{-/y}$ baseline, p=0.01; wt baseline-OPHN1$^{-/y}$ fasudil, p=0.14).*

In a previous work (Redolfi et al., 2016) inhibition of the RhoA/ROCK pathway through the ROCK non competitive inhibitor, fasudil, successfully rescued the number of adult-generated granule cells in the OB of OPHN1$^{-/y}$ mice fifteen days after their generation in the SVZ (Redolfi et al., 2016).

We, therefore, tested the impact of acute fasudil application on the RMS of OPHN1$^{-/y}$ mice and littermate controls (Figure 4.12.). We performed time-lapse imaging of GFP-labeled SVZ-derived cells following the protocol of previous experiments. We monitored cell motility for two hours at baseline condition, then slices were incubated for 30 minutes with fasudil 10 μM diluted in ACSF, and imaging was repeated for two hours with fasudil continuously perfused in the imaging chamber. Three animals per condition were analyzed.

Acute fasudil application on neuronal precursors did not affect cell speed (both average and instantaneous speed) and moving time in control mice nor in mutant mice (Graph 4.11.).

Interestingly, fasudil completely rescued the directionality of migrating cells in OPHN1$^{-/y}$ mice.

4.13. Chronic fasudil treatment did not rescue the complement of adult-born immature interneurons at 9 dpi in the OB of OPHN1$^{-/y}$ mice

The number of newly generated GABAergic interneurons is similar in the OB of control mice at nine and at fifteen days after their generation in the SVZ (Redolfi et al., 2016). Indeed, at nine days the vast majority of immature neurons reached the OB and began their radial migration through the layers of the OB (Petreanu and Alvarez-Buylla, 2002). By contrast, in mice in which OPHN1 is not functional, the complement of newborn immature granule cells in the OB is already significantly reduced nine days after their generation (Redolfi et al., 2016).

Given the effects of acute fasudil administration on the directionality but not on the speed of migrating cells, in time lapse imaging (see previous paragraph), in

mutant mice, we asked whether chronic treatment with fasudil could result in a delayed arrival of neuronal precursors in the OB.

To verify this hypothesis we performed birth-dating analysis, using a double immunostaining against BrdU and NeuN, in OPHN1$^{-/y}$ mice and littermate controls. Fasudil was administered to animals in drinking water avaiable *ad libitum* for twelve days. At this time point, BrdU was injected intraperitoneally in mice. Control mice and mutant mice were sacrificed nine days after BrdU injection (9 dpi), and during this period fasudil was continuously administered in water to mice, to reach a total treatment period of three weeks. We quantified the complement of newly generated cells that reach the OB 9 dpi, in treated controls and in OPHN1$^{-/y}$ treated mice (Figure 4.13.). Brains were sectioned at vibratome, to obtain coronal slices (60 µm thick) of the OB. Slices were immunolabelled with antibodies against BrdU and NeuN. three animals per condition were studied.

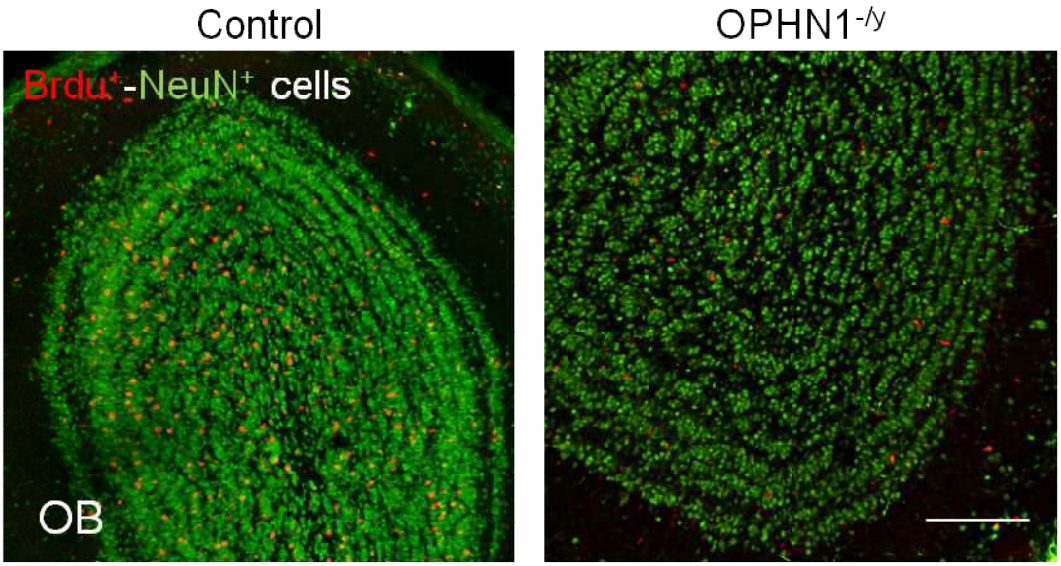

Figure 4.13.: Chronic fasudil treatment did not rescue the complement of adult-born immature interneurons at 9 dpi in the olfactory bulb (OB) of OPHN1$^{-/y}$ mice. Confocal images of coronal sections of the OB *after fasudil treatment. In red: bromodeoxyuride (BrdU) labelled cells; in green: neuronal nuclei (NeuN) labelled cells. In OPHN1$^{-/y}$ mice (right) at 9 dpi, the complement of newborn immature granule cells is significantly reduced with respect to control mice (left). Bar = 200 µm.*

Remarkably, we found that at 9 dpi chronic fasudil treatment increased significantly the complement of adult-generated immature interneurons in OPHN1$^{-/y}$ mice. Nevertheless, the number of neuroblasts that reached the OB was still strikingly lower in OPHN1$^{-/y}$ mice treated with fasudil with respect to controls (Graph 4.12.).

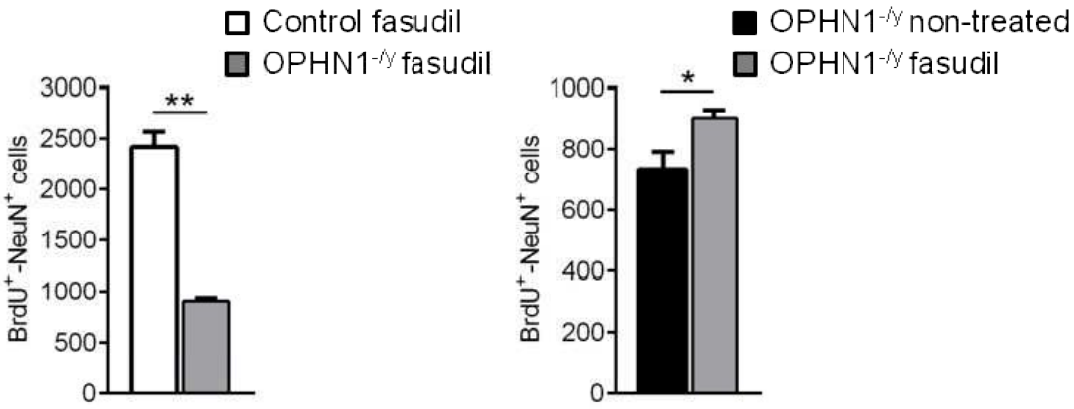

Graph 4.12.: *On the left,* ***number of newly generated granule cells in the OB.*** *In OPHN1$^{-/y}$ mice treated with fasudil (n = 3) and wt mice treated with fasudil (n = 3) (OPHN1$^{-/y}$ mice n = 902 ± 27, control mice n = 2419 ± 88; p = 0.0031; Mann-Whitney test, p = 0.0031). On the right,* ***number of newly generated granule cells in the OB.*** *In OPHN1$^{-/y}$ mice treated with fasudil (n = 3) and OPHN1$^{-/y}$ mice non-treated (n = 3) (fasudil n = 902 ± 27, non-treated n = 734 ± 29; Mann-Whitney test, p = 0.03). (Not shown: OPHN1$^{-/y}$ fasudil n = 902 ± 27, control mice non-treated n = 2407 ± 172; p = 0.01).*

5. DISCUSSION

5.1. Neuroblasts' progression along the rostral migratory stream is impaired in OPHN1$^{-/y}$ mice

In this work we found that OPHN1 mutation significantly hampers the migration of forebrain GABAergic inhibitory interneurons, generated postnatally in the subventricular zone (SVZ). These results explain the dramatically reduced number of inhibitory interneurons in target areas (Redolfi et al., 2016).

By quantitive immunohistochemical analysis and *ex vivo* time-lapse imaging of migrating neuroblasts, we dissected the impact of OPHN1 loss of function on the migration of neuronal precursors *en route* to the olfactory bulb (OB).

We found that the spatial distribution and organization of the SVZ and the rostral migratory stream (RMS) were deeply disrupted in OPHN1$^{-/y}$ mice. While in controls, neuronal precursor coalesce to form elongated and well organized chains that converge into the RMS, in OPHN1$^{-/y}$ mice neuronal precursors were arranged in a chaotic manner: the chains of precursors appeared thicker and shorter and changed direction more often than in controls.

As a result of the altered distribution of the precursors in OPHN1$^{-/y}$ mice, the area occupied by newborn cells in the SVZ and in the OB were significantly bigger in mutant mice than in controls.

Birth-dating analysis indicated that newly generated cells exhibit a deeply subverted distribution along the RMS in OPHN1$^{-/y}$ mice versus littermate controls. Namely, the complement of neuroblasts was clumped in close proximity to the SVZ at 7 days after the generation of these cells, in OPHN1$^{-/y}$ mice.
This atypical distribution of neuroblasts along the RMS could further contribute to the larger area occupied by new cells near the SVZ.

The impaired progression of neuroblasts along the RMS may depend on (1.) perturbed translation of stimuli provided by the external environment.

The finding that astrocyte-like cells, which act as scaffold for neuroblasts' chains (Lois et al., 1996), exhibited hypertrophic processes, and that were often intermingled within chains in OPHN1$^{-/y}$ mice, while in control mice they usually run parallel to neuroblasts clusters could support this hypothesis.

The presumptive gliosis in the RMS in mutant mice, could be a consequence of the alteration of the graded concentration of molecular cues and/or of signals that govern the migration toward the OB.

On the other hand, (2.) impaired adult-born precursors progression could be ascribed to a diminished motility of the migrating cells, due to abnormalities in the modulation of actin cytoskeleton dynamics, which is necessary to extend the leading-process and to trail the soma after it. Both conditions could coexists and contribute to block cell migration along the RMS.

5.2. Migrating neuronal precursors show an abnormal morphology in OPHN1$^{-/y}$ mice

The actin cytoskeleton is required for growth cone motility, neurite pathfinding and branching, cellular mechanisms that are crucial for migrating cells to organize chains, orientate their leading process and follow the RMS.

The altered remodeling of actin cytoskeleton was further supported by the altered polarity of neuronal precursors in OPHN1$^{-/y}$ mice. We used a lentiviral-vector expressing GFP to label SVZ derived cells and study their morphology during migration. In wt mice most of neuroblasts exhibited unipolar shape, with a single leading-process that drove cells along the RMS. Loss of OPHN1 function results in an increased proportion of cells that extended two or more processes in the surrounding environment.

The abnormal morphology we observed could be ascribed to (1.) neuronal precursors inability to detect and/or to translate into intracellular signaling pathway, cues that direct their progression along the migratory path. In this scenario, the emission of multiple cellular processes reflect the constant search for molecular cues able to guide neuroblasts along the RMS. Another possible explanation is (2.)

the perturbation of actin cytoskeleton dynamics, due to overactivation of RhoGTPases downstream pathways in adult-generated precursors. Could result in the extension of numerous cellular processes that cannot be retracted by migrating cells. This overactivation is consistent with the deletion of a RhoGAP, such as OPHN1. For instance, the imbalance between the activity of Rac1 (and in a lesser extent Cdc42) and RhoA is likely to lead to formation of overabundant leading-processes. Rac1 is required for the extension of the leading-edge of cellular processes (Khodosevich et al., 2009), while RhoA is necessary for the stabilization of microtubules (Govek et al., 2005) and centrosomal translocation (Shinohara et al., 2012). The failure of the fine temporal orchestration of their activity could represent the mechanism underlying disrupted cell motility. Both mechanisms can lead to a restriction of cell motility and in turn hampered progression of newly generated cells along the RMS.

5.3. Loss-of-function mutation of OPHN1 subverts the polarity of GABA response in newly generated neuroblasts

By two-photon time-lapse imaging we directly dissect the migration process. Consistent with findings from quantitative immunohistochemical analysis, in OPHN1$^{-/y}$ mice we directly observed a reduced motility of neuroblasts that resulted in a reduced average speed, instantaneous speed and reduced time of motility. In addition, we found that the directionality of migration along the RMS was severely altered in mutant mice, with more neuroblasts that were moving away from the OB than in littermate controls.

The drop of the speed of neuroblast progression, is likely the cause at the basis of the accumulation of SVZ-derived cells in the initial part of the RMS, in mutant mice. Both the instantaneous speed and the percentage of moving time was strikingly reduced in OPHN1$^{-/y}$ mice, indicating that along tangential migration neuronal precursors move slower and for a less amount of time. The reduced speed of migration can be linked with the loss of a RhoGAP function, such as OPHN1, and the consequent overactivation of the downstream signaling. Impairments of

migration have been reported in a mouse line carrying mutation of proteins associated with RhoGTPases signaling pathways (Vaghi et al., 2014; Hikita et al., 2014; Ota et al., 2014; Zamboni et al., 2018), although in these studies the altered migration was deduced by the altered position of neurons in the target areas, and not by a direct analysis of the moving cells, as we did in this PhD project.

In addition, we found that loss-of-function of OPHN1 affected also the directionality of the migration, with a significant reduction of the percentage of cells that were moving toward the OB. If the reduction of the speed of migration can be ascribed to a decreased motility of neuroblasts, likely due to perturbed actin cytoskeleton dynamics, the alteration of the directionality of migration seem to be related to actual inability of neuroblasts to find proper cues to direct their progression and/or inability to integrate and translate extracellular signals to coordinate actin cytoskeleton modifications. For instance, the chemorepellent protein Slit2 is known to push neuronal precursors to migrate rostrally (Sawamoto et al., 2006) and an erroneous translation of its signal might be involved in the altered directionality of migration.

GABA is among the main modulator of adult-born cells progression toward the OB. We found that in wt mice, application of GABA, as well as inhibition of GABA reuptake from the extracellular compartment, slowed down migrating neuronal precursors along the RMS. By contrast, inhibition of $GABA_A$ receptors activity, by bicuculline, increased the speed of neuronal precursors in the RMS, confirming data obtained in previous work (Bolteus and Bordey, 2004)

In $OPHN1^{-/y}$ mice exogenous GABA exerted opposite effects with respect to those observed in wt. GABA induced an increased in translocation speed along the RMS, while inhibition of $GABA_A$ receptors activity, with bicuculline, resulted in decreased migration speed. Noteworthy, the directionality of migration was not affected by exogenous GABA, nor by GABA reuptake inhibition, nor inhibition of $GABA_A$ receptors. $GABA_A$ receptors respond to GABA application in both $OPHN1^{-/y}$ mice and littermate controls, and in both cases their activation is inhibited by bicuculline application on brain slices, indicating that in RMS-neuroblasts of mutant mice $GABA_A$ receptors are present and functional. Hence, the opposite effect obtained with GABA signaling manipulation in RMS-

neuroblasts in OPHN1$^{-/y}$ and in wt mice suggested that the polarity of GABA responses, regulated by specific cotransporters, could be subverted in mutant mice.

These results prompted us to explore the effect of pharmacological blockade of the chloride cotransporters (i.e. NKCC1 and KCC2) on neuronal precursor motility. In wt mice, blocking NKCC1 in SVZ-derived cells, with the specific inhibitor bumetanide, reduce the speed of migration in the RMS (Mejia-Gervacio et al., 2011). On the contrary, in OPHN1$^{-/y}$ mice bumetanide was ineffective. Remarkably, blocking KCC2 activity in adult-born migrating cells with the specific inhibitor VU0463271 accelerate and almost completely rescued the progression of neuroblasts along the RMS in mutant mice. These findings strongly suggest that the alteration of GABA signaling in OPHN1$^{-/y}$ mice may be ascribed to the subverted polarity of the response to GABA, related to an altered expression of the cotransporters. The incomplete rescue of the speed in mutant mice could be ascribed to (1.) limited diffusion of KCC2 inhibitor in the tissue. Alternatively, (2.) to the presence of other factors, at the moment unknown, that contribute to regulate the speed of migration along the RMS, in OPHN1$^{-/y}$ mice.

The lack of effect upon NKCC1 blockade and the surprising increase of the speed upon KCC2 inhibition, in neuronal precursors in mutant mice together with the opposite effects to GABA manipulations, in control mice with respect to OPHN1$^{-/y}$ mice, suggest that loss-of-function mutation of OPHN1 causes a premature expression of KCC2 in SVZ-derived cells. High expression of KCC2 leads to lower intracellular concentration of chloride in migrating cells, that may contribute in hampering neuroblasts migration along the RMS.

How GABA could contribute to neuroblasts motility? GABA is thought to depolarize migrating neuroblasts, triggering an intracellular calcium increase in these cells. However, although this process was demonstrated to operate in cortical interneurons (Bortone and Polleux, 2009), whether it takes place also in SVZ-derived cells remains obscure. The link between GABA and calcium signaling in RMS-neuroblasts is elusive and data in the literature are controversial (Bolteus and Bordey, 2004; Darcy and Isaacson, 2009). We aim to address this question in future research. At the moment we have already optimized a method to perform calcium imaging *in vivo* in migrating cells by mean of two-photon imaging.

It is worth noticing that in rat embryos, premature KCC2 expression in neuronal progenitors from the ventricular zone dramatically impaired morphological maturation of neonatal cortical neurons derived from these progenitors (Cancedda et al., 2007). In line with these data, our results demonstrate that another aspect of the maturation of the brain is perturbed by premature expression of KCC2: the migration of postanatally generated inhibitory interneurons. All these data prompt us to speculate that even the altered morphology in dendrites (Khelfaoui et al., 2007; Redolfi et al., 2016) or axons (Allegra et al., 2017) in neuronal subpopulations of cortical and subcortical areas, related to null mutation of OPHN1 could be ascribed at least in part to premature expression of KCC2.

5.4. Fasudil treatment rescues the directionality of migrating neuroblasts along the rostral migratory stream in OPHN1$^{-/y}$ mice

Mutation of OPHN1 leads to overactivation of the downstream signaling pathway, namely RhoA/Rho-associated Kinase (ROCK) pathway and the related effectors, in particular the actin depolymerizing factor ADF/Cofilin complex, via lens intrinsic membrane protein kinase (LIMK) activation and the myosin light chain (MLC).

Fasudil, a non-competive inhibitor of ROCK activity, has been largely employed to rescue alterations triggered by OPHN1 mutation.

In our lab we discovered that blocking the RhoA/ROCK signaling pathway, with chronic administration of fasudil, rescued the complement of adult-born cells in the OB of OPHN1$^{-/y}$ mice fifteen day after their generation in the SVZ (Redolfi et al., 2016). However, the morphology and the electrical physiological properties were not completely rescued suggesting that some other signaling pathways controlled by RhoGTPases proteins are affected by loss of OPHN1 function.

These was observed also in other studies, were fasudil treatment was able to rescue some but not all the defects associated to null mutation of OPHN1 (Meziane et al., 2016; Allegra et al., 2017).

Interestingly, acute fasudil application in slices, completely rescued the directionality but not the speed of migrating neuronal precursors in mutant mice. These result suggested that fasudil, (1.) triggering proper actin-myosin remodeling, was able to reestablish proper morphological polarity of neuronal precursors and, therefore, their directionality.

However, (2.) since the GABA polarity remain subverted, calcium influx remained impaired and, therefore, the speed of neuroblasts along the RMS cannot be rescued by fasudil application on slices.

All these data suggested that fasudil favors the correct direction of adult-generated immature interneurons, which persist, however, to progress very low pace, in respect to controls.

This hypothesis was confirmed by experiments on chronic treatment with fasudil. At 9 days after their generation in the SVZ, the number of newly generated cells that reached the OB was still significantly lower in OPHN1$^{-/y}$ mice treated with fasudil with respect to littermate controls. Therefore upon fasudil treatment the entire complement of newborn cells reached the OB, but in a longer time.

In agreement with our data in slices, the effect of fasudil, *in vivo*, rescued the directionality, but not the speed of neuronal precursors progression in mutant mice, resulting in a delayed arrival respect to controls.

Results obtained with GABA and those with fasudil indicate that different aspect of migration are affected by diverse signaling pathways associated with the actin cytoskeleton.

OPHN1 intermediates extracellular cues with intracellular signaling cascade, which translate the external signals in information for the cell. It modulates actomyosin contraction, controlling the motility of neuronal precursors. In particular the upregulation of the MLCP and the LIMK, two enzymes downstream to RhoA/ROCK, could lead to an increased contractility of the actin cytoskeleton and to failure of the correct actin filaments rearrangement. It could also play a role in the regulation of gene expression, or in the localization of specific proteins on the cellular surface that contribute on neuroblast migration. One or more of these processes are likely to be subverted in forebrain GABAergic interneurons generated in the SVZ, in OPHN1$^{-/y}$ mice, resulting in hampered motility and morphological

polarity. Moreover, GABA could impinge on actin cytoskeleton dynamics through mechanisms largely unknown. GABA likely leads to the rising of calcium transients, which, ultimately, trigger actin cytoskeleton remodeling that is critical for neuroblasts motility.

5.5. The hampered migration of neuronal precursors, resulting in a dramatic reduction of inhibitory interneurons in the target areas, could contribute to the pathophysiology of intellectual disability

All together, our findings corroborate the hypothesis that (1.) loss-of-function mutation of OPHN1 leads to the inability of neuronal precursor to migrate properly from the SVZ to their target area. (2.) The hampered migration appears to be related to subverted polarity of GABA response in migrating neuroblasts in OPHN1$^{-/y}$ mice. The lack of GABA depolarizing action, and the consequent disruption of GABA-dependent calcium transients, is likely to affect cell motility and the speed of newly generated cells toward the OB.
Moreover, (3.) OPHN1 mutation impacts the migration process along the RMS impairing neuroblasts motility through erroneous actin cytoskeleton remodelling.
Alterations in development and function of GABAergic interneurons have been associated to several neurodevelopmental disorders (Le Magueresse and Monyer, 2013; Deidda et al., 2014). Postnatal migration of inhibitory interneurons is thought to play a prominent role in developmental plasticity and proper migration of inhibitory interneurons to their final destination is essential for excitatory/inhibitory balance of neuronal networks.

Our data demonstrated a perturbed migration in the RMS of OPHN1$^{-/y}$ mice that results in reduced number of inhibitory interneurons in target areas (Redolfi et al., 2016). (4.) This is likely to alter excitatory/inhibitory balance in neuronal networks, that could contribute to the pathophysiology of intellectual disability.

6. Conclusion

Intellectual disability is a very complex disease whose etiopathogenesis remains largely obscure. Revealing which molecular, cellular and network features are affected by gene associated to ID is critical to understand the pathophysiology of the disease and develop new effective treatments. Proper migration of inhibitory interneurons to their final destination, is critical for proper excitatory/inhibitory balance of neuronal networks, that is essential for normal brain function. In my thesis project I provided compelling evidence that the migration is perturbed in OPHN1$^{-/y}$ mice and I unraveled mechanisms associated to altered progression: namely, (1.) abnormalities in the actin cytoskeleton remodeling during migration and (2.) a subversion in the polarity of GABA response in neuronal precursors.

Our results provide a new significant insight into the causes that contribute to the pathophysiology of intellectual disability and identified new mechanisms and targets that could help to design effective therapeutic treatments.

Bibliography

Abrous, D.N., Koehl, M., and Le Moal, M. (2005). Adult neurogenesis: from precursors to network and physiology. Physiological reviews *85*, 523-569.

Adachi, K., Mirzadeh, Z., Sakaguchi, M., Yamashita, T., Nikolcheva, T., Gotoh, Y., Peltz, G., Gong, L., Kawase, T., Alvarez-Buylla, A.*, et al.* (2007). Beta-catenin signaling promotes proliferation of progenitor cells in the adult mouse subventricular zone. Stem cells *25*, 2827-2836.

Adam, Y., Livneh, Y., Miyamichi, K., Groysman, M., Luo, L., and Mizrahi, A. (2014). Functional transformations of odor inputs in the mouse olfactory bulb. Frontiers in neural circuits *8*, 129.

Adrian, E.D. (1942). Olfactory reactions in the brain of the hedgehog. The Journal of physiology *100*, 459-473.

Ahn, K., Gil, R., Seibyl, J., Sewell, R.A., and D'Souza, D.C. (2011). Probing GABA receptor function in schizophrenia with iomazenil. Neuropsychopharmacology : official publication of the American College of Neuropsychopharmacology *36*, 677-683.

Alfonso, J., Penkert, H., Duman, C., Zuccotti, A., and Monyer, H. (2015). Downregulation of Sphingosine 1-Phosphate Receptor 1 Promotes the Switch from Tangential to Radial Migration in the OB. The Journal of neuroscience : the official journal of the Society for Neuroscience *35*, 13659-13672.

Allegra, M., Spalletti, C., Vignoli, B., Azzimondi, S., Busti, I., Billuart, P., Canossa, M., and Caleo, M. (2017). Pharmacological rescue of adult hippocampal neurogenesis in a mouse model of X-linked intellectual disability. Neurobiology of disease *100*, 75-86.

Allen, K.M., Gleeson, J.G., Bagrodia, S., Partington, M.W., MacMillan, J.C., Cerione, R.A., Mulley, J.C., and Walsh, C.A. (1998). PAK3 mutation in nonsyndromic X-linked mental retardation. Nature genetics *20*, 25-30.

Alonso, M., Lepousez, G., Sebastien, W., Bardy, C., Gabellec, M.M., Torquet, N., and Lledo, P.M. (2012). Activation of adult-born neurons facilitates learning and memory. Nature neuroscience *15*, 897-904.

Alonso, M., Ortega-Perez, I., Grubb, M.S., Bourgeois, J.P., Charneau, P., and Lledo, P.M. (2008). Turning astrocytes from the rostral migratory stream into neurons: a role for the olfactory sensory organ. The Journal of neuroscience : the official journal of the Society for Neuroscience *28*, 11089-11102.

Alvarez-Buylla, A., and Garcia-Verdugo, J.M. (2002). Neurogenesis in adult subventricular zone. The Journal of neuroscience : the official journal of the Society for Neuroscience *22*, 629-634.

Alvarez-Buylla, A., Kohwi, M., Nguyen, T.M., and Merkle, F.T. (2008). The heterogeneity of adult neural stem cells and the emerging complexity of their niche. Cold Spring Harbor symposia on quantitative biology *73*, 357-365.

Alvarez-Buylla, A., and Lim, D.A. (2004). For the long run: maintaining germinal niches in the adult brain. Neuron *41*, 683-686.

Alves, J.A., Barone, P., Engelender, S., Froes, M.M., and Menezes, J.R. (2002). Initial stages of radial glia astrocytic transformation in the early postnatal anterior subventricular zone. Journal of neurobiology *52*, 251-265.

Anderson, S.A., Marin, O., Horn, C., Jennings, K., and Rubenstein, J.L. (2001). Distinct cortical migrations from the medial and lateral ganglionic eminences. Development *128*, 353-363.

Angot, E., Loulier, K., Nguyen-Ba-Charvet, K.T., Gadeau, A.P., Ruat, M., and Traiffort, E. (2008). Chemoattractive activity of sonic hedgehog in the adult subventricular zone modulates the number of neural precursors reaching the olfactory bulb. Stem cells *26*, 2311-2320.

Azzarelli, R., Kerloch, T., and Pacary, E. (2014). Regulation of cerebral cortex development by Rho GTPases: insights from in vivo studies. Frontiers in cellular neuroscience *8*, 445.

Bagley, J.A., and Belluscio, L. (2010). Dynamic imaging reveals that brain-derived neurotrophic factor can independently regulate motility and direction of neuroblasts within the rostral migratory stream. Neuroscience *169*, 1449-1461.

Banasr, M., Hery, M., Printemps, R., and Daszuta, A. (2004). Serotonin-induced increases in adult cell proliferation and neurogenesis are mediated through different and common 5-HT receptor subtypes in the dentate gyrus and the subventricular zone. Neuropsychopharmacology : official publication of the American College of Neuropsychopharmacology *29*, 450-460.

Bardy, C., Alonso, M., Bouthour, W., and Lledo, P.M. (2010). How, when, and where new inhibitory neurons release neurotransmitters in the adult olfactory bulb. The Journal of neuroscience : the official journal of the Society for Neuroscience *30*, 17023-17034.
Barkho, B.Z., Munoz, A.E., Li, X., Li, L., Cunningham, L.A., and Zhao, X. (2008). Endogenous matrix metalloproteinase (MMP)-3 and MMP-9 promote the differentiation and migration of adult neural progenitor cells in response to chemokines. Stem cells *26*, 3139-3149.
Bartos, M., Vida, I., Frotscher, M., Meyer, A., Monyer, H., Geiger, J.R., and Jonas, P. (2002). Fast synaptic inhibition promotes synchronized gamma oscillations in hippocampal interneuron networks. Proceedings of the National Academy of Sciences of the United States of America *99*, 13222-13227.
Batista-Brito, R., Close, J., Machold, R., and Fishell, G. (2008). The distinct temporal origins of olfactory bulb interneuron subtypes. The Journal of neuroscience : the official journal of the Society for Neuroscience *28*, 3966-3975.
Bedard, A., and Parent, A. (2004). Evidence of newly generated neurons in the human olfactory bulb. Brain research Developmental brain research *151*, 159-168.
Bellion, A., Baudoin, J.P., Alvarez, C., Bornens, M., and Metin, C. (2005). Nucleokinesis in tangentially migrating neurons comprises two alternating phases: forward migration of the Golgi/centrosome associated with centrosome splitting and myosin contraction at the rear. The Journal of neuroscience : the official journal of the Society for Neuroscience *25*, 5691-5699.
Belluscio, L., Lodovichi, C., Feinstein, P., Mombaerts, P., and Katz, L.C. (2002). Odorant receptors instruct functional circuitry in the mouse olfactory bulb. Nature *419*, 296-300.
Belvindrah, R., Hankel, S., Walker, J., Patton, B.L., and Muller, U. (2007). Beta1 integrins control the formation of cell chains in the adult rostral migratory stream. The Journal of neuroscience : the official journal of the Society for Neuroscience *27*, 2704-2717.
Belvindrah, R., Nissant, A., and Lledo, P.M. (2011). Abnormal neuronal migration changes the fate of developing neurons in the postnatal olfactory bulb. The Journal of neuroscience : the official journal of the Society for Neuroscience *31*, 7551-7562.
Ben-Ari, Y. (2002). Excitatory actions of gaba during development: the nature of the nurture. Nature reviews Neuroscience *3*, 728-739.
Berditchevski, F. (2001). Complexes of tetraspanins with integrins: more than meets the eye. Journal of cell science *114*, 4143-4151.
Bernstein, B.W., and Bamburg, J.R. (2010). ADF/cofilin: a functional node in cell biology. Trends in cell biology *20*, 187-195.
Billuart, P., Bienvenu, T., Ronce, N., des Portes, V., Vinet, M.C., Zemni, R., Roest Crollius, H., Carrie, A., Fauchereau, F., Cherry, M.*, et al.* (1998). Oligophrenin-1 encodes a rhoGAP protein involved in X-linked mental retardation. Nature *392*, 923-926.
Boda, B., Alberi, S., Nikonenko, I., Node-Langlois, R., Jourdain, P., Moosmayer, M., Parisi-Jourdain, L., and Muller, D. (2004). The mental retardation protein PAK3 contributes to synapse formation and plasticity in hippocampus. The Journal of neuroscience : the official journal of the Society for Neuroscience *24*, 10816-10825.
Boda, B., Mas, C., and Muller, D. (2002). Activity-dependent regulation of genes implicated in X-linked non-specific mental retardation. Neuroscience *114*, 13-17.
Bolduc, F.V., and Tully, T. (2009). Fruit flies and intellectual disability. Fly *3*, 91-104.
Bolteus, A.J., and Bordey, A. (2004). GABA release and uptake regulate neuronal precursor migration in the postnatal subventricular zone. The Journal of neuroscience : the official journal of the Society for Neuroscience *24*, 7623-7631.
Borden, L.A. (1996). GABA transporter heterogeneity: pharmacology and cellular localization. Neurochemistry international *29*, 335-356.
Bortone, D., and Polleux, F. (2009). KCC2 expression promotes the termination of cortical interneuron migration in a voltage-sensitive calcium-dependent manner. Neuron *62*, 53-71.
Bossers, K., Wirz, K.T., Meerhoff, G.F., Essing, A.H., van Dongen, J.W., Houba, P., Kruse, C.G., Verhaagen, J., and Swaab, D.F. (2010). Concerted changes in transcripts in the prefrontal cortex precede neuropathology in Alzheimer's disease. Brain : a journal of neurology *133*, 3699-3723.
Bourne, J.N., and Schoppa, N.E. (2017). Three-dimensional synaptic analyses of mitral cell and external tufted cell dendrites in rat olfactory bulb glomeruli. The Journal of comparative neurology *525*, 592-609.

Bovetti, S., Veyrac, A., Peretto, P., Fasolo, A., and De Marchis, S. (2009). Olfactory enrichment influences adult neurogenesis modulating GAD67 and plasticity-related molecules expression in newborn cells of the olfactory bulb. PloS one *4*, e6359.
Boyd, A.M., Sturgill, J.F., Poo, C., and Isaacson, J.S. (2012). Cortical feedback control of olfactory bulb circuits. Neuron *76*, 1161-1174.
Bozoyan, L., Khlghatyan, J., and Saghatelyan, A. (2012). Astrocytes control the development of the migration-promoting vasculature scaffold in the postnatal brain via VEGF signaling. The Journal of neuroscience : the official journal of the Society for Neuroscience *32*, 1687-1704.
Breton-Provencher, V., Lemasson, M., Peralta, M.R., 3rd, and Saghatelyan, A. (2009). Interneurons produced in adulthood are required for the normal functioning of the olfactory bulb network and for the execution of selected olfactory behaviors. The Journal of neuroscience : the official journal of the Society for Neuroscience *29*, 15245-15257.
Brill, M.S., Ninkovic, J., Winpenny, E., Hodge, R.D., Ozen, I., Yang, R., Lepier, A., Gascon, S., Erdelyi, F., Szabo, G.*, et al.* (2009). Adult generation of glutamatergic olfactory bulb interneurons. Nature neuroscience *12*, 1524-1533.
Bulfone, A., Wang, F., Hevner, R., Anderson, S., Cutforth, T., Chen, S., Meneses, J., Pedersen, R., Axel, R., and Rubenstein, J.L. (1998). An olfactory sensory map develops in the absence of normal projection neurons or GABAergic interneurons. Neuron *21*, 1273-1282.
Buzsaki, G., and Draguhn, A. (2004). Neuronal oscillations in cortical networks. Science *304*, 1926-1929.
Buzsaki, G., and Wang, X.J. (2012). Mechanisms of gamma oscillations. Annual review of neuroscience *35*, 203-225.
Cancedda, L., Fiumelli, H., Chen, K., and Poo, M.M. (2007). Excitatory GABA action is essential for morphological maturation of cortical neurons in vivo. The Journal of neuroscience : the official journal of the Society for Neuroscience *27*, 5224-5235.
Cang, J., and Isaacson, J.S. (2003). In vivo whole-cell recording of odor-evoked synaptic transmission in the rat olfactory bulb. The Journal of neuroscience : the official journal of the Society for Neuroscience *23*, 4108-4116.
Cao, L., Pu, J., Scott, R.H., Ching, J., and McCaig, C.D. (2015). Physiological electrical signals promote chain migration of neuroblasts by up-regulating P2Y1 purinergic receptors and enhancing cell adhesion. Stem cell reviews *11*, 75-86.
Capilla-Gonzalez, V., Lavell, E., Quinones-Hinojosa, A., and Guerrero-Cazares, H. (2015). Regulation of subventricular zone-derived cells migration in the adult brain. Advances in experimental medicine and biology *853*, 1-21.
Cappello, S. (2013). Small Rho-GTPases and cortical malformations: fine-tuning the cytoskeleton stability. Small GTPases *4*, 51-56.
Carleton, A., Petreanu, L.T., Lansford, R., Alvarez-Buylla, A., and Lledo, P.M. (2003). Becoming a new neuron in the adult olfactory bulb. Nature neuroscience *6*, 507-518.
Chazal, G., Durbec, P., Jankovski, A., Rougon, G., and Cremer, H. (2000). Consequences of neural cell adhesion molecule deficiency on cell migration in the rostral migratory stream of the mouse. The Journal of neuroscience : the official journal of the Society for Neuroscience *20*, 1446-1457.
Chechlacz, M., and Gleeson, J.G. (2003). Is mental retardation a defect of synapse structure and function? Pediatric neurology *29*, 11-17.
Choi, S., Thapa, N., Tan, X., Hedman, A.C., and Anderson, R.A. (2015). PIP kinases define PI4,5P(2)signaling specificity by association with effectors. Biochimica et biophysica acta *1851*, 711-723.
Chojnacki, A., Mak, G., and Weiss, S. (2011). PDGFRalpha expression distinguishes GFAP-expressing neural stem cells from PDGF-responsive neural precursors in the adult periventricular area. The Journal of neuroscience : the official journal of the Society for Neuroscience *31*, 9503-9512.
Chojnacki, A., Shimazaki, T., Gregg, C., Weinmaster, G., and Weiss, S. (2003). Glycoprotein 130 signaling regulates Notch1 expression and activation in the self-renewal of mammalian forebrain neural stem cells. The Journal of neuroscience : the official journal of the Society for Neuroscience *23*, 1730-1741.
Codega, P., Silva-Vargas, V., Paul, A., Maldonado-Soto, A.R., Deleo, A.M., Pastrana, E., and Doetsch, F. (2014). Prospective identification and purification of quiescent adult neural stem cells from their in vivo niche. Neuron *82*, 545-559.

Coghlan, S., Horder, J., Inkster, B., Mendez, M.A., Murphy, D.G., and Nutt, D.J. (2012). GABA system dysfunction in autism and related disorders: from synapse to symptoms. Neuroscience and biobehavioral reviews *36*, 2044-2055.
Cohen, Y., Avramoav, S., Barkai, E., and Maroun, M. (2011). Olfactory learning-induced enhancement of the predisposition for LTP induction. Learning & memory *18*, 594-597.
Coles, C.H., and Bradke, F. (2015). Coordinating neuronal actin-microtubule dynamics. Current biology : CB *25*, R677-691.
Conover, J.C., Doetsch, F., Garcia-Verdugo, J.M., Gale, N.W., Yancopoulos, G.D., and Alvarez-Buylla, A. (2000). Disruption of Eph/ephrin signaling affects migration and proliferation in the adult subventricular zone. Nature neuroscience *3*, 1091-1097.
Contestabile, A., Magara, S., and Cancedda, L. (2017). The GABAergic Hypothesis for Cognitive Disabilities in Down Syndrome. Frontiers in cellular neuroscience *11*, 54.
Curtis, M.A., Eriksson, P.S., and Faull, R.L. (2007). Progenitor cells and adult neurogenesis in neurodegenerative diseases and injuries of the basal ganglia. Clinical and experimental pharmacology & physiology *34*, 528-532.
Curtis, M.A., Penney, E.B., Pearson, A.G., van Roon-Mom, W.M., Butterworth, N.J., Dragunow, M., Connor, B., and Faull, R.L. (2003). Increased cell proliferation and neurogenesis in the adult human Huntington's disease brain. Proceedings of the National Academy of Sciences of the United States of America *100*, 9023-9027.
Curtis, M.A., Waldvogel, H.J., Synek, B., and Faull, R.L. (2005). A histochemical and immunohistochemical analysis of the subependymal layer in the normal and Huntington's disease brain. Journal of chemical neuroanatomy *30*, 55-66.
Daily, D.K., Ardinger, H.H., and Holmes, G.E. (2000). Identification and evaluation of mental retardation. American family physician *61*, 1059-1067, 1070.
Darcy, D.P., and Isaacson, J.S. (2009). L-type calcium channels govern calcium signaling in migrating newborn neurons in the postnatal olfactory bulb. The Journal of neuroscience : the official journal of the Society for Neuroscience *29*, 2510-2518.
David, L.S., Schachner, M., and Saghatelyan, A. (2013). The extracellular matrix glycoprotein tenascin-R affects adult but not developmental neurogenesis in the olfactory bulb. The Journal of neuroscience : the official journal of the Society for Neuroscience *33*, 10324-10339.
Deidda, G., Bozarth, I.F., and Cancedda, L. (2014). Modulation of GABAergic transmission in development and neurodevelopmental disorders: investigating physiology and pathology to gain therapeutic perspectives. Frontiers in cellular neuroscience *8*, 119.
Delgado, A.C., Ferron, S.R., Vicente, D., Porlan, E., Perez-Villalba, A., Trujillo, C.M., D'Ocon, P., and Farinas, I. (2014). Endothelial NT-3 delivered by vasculature and CSF promotes quiescence of subependymal neural stem cells through nitric oxide induction. Neuron *83*, 572-585.
Doetsch, F. (2003). The glial identity of neural stem cells. Nature neuroscience *6*, 1127-1134.
Doetsch, F., Caille, I., Lim, D.A., Garcia-Verdugo, J.M., and Alvarez-Buylla, A. (1999). Subventricular zone astrocytes are neural stem cells in the adult mammalian brain. Cell *97*, 703-716.
Doetsch, F., Petreanu, L., Caille, I., Garcia-Verdugo, J.M., and Alvarez-Buylla, A. (2002). EGF converts transit-amplifying neurogenic precursors in the adult brain into multipotent stem cells. Neuron *36*, 1021-1034.
Dumitru, I., Neitz, A., Alfonso, J., and Monyer, H. (2017). Diazepam Binding Inhibitor Promotes Stem Cell Expansion Controlling Environment-Dependent Neurogenesis. Neuron *94*, 125-137 e125.
Dupret, D., Pleydell-Bouverie, B., and Csicsvari, J. (2008). Inhibitory interneurons and network oscillations. Proceedings of the National Academy of Sciences of the United States of America *105*, 18079-18080.
Eilers, J., Plant, T.D., Marandi, N., and Konnerth, A. (2001). GABA-mediated Ca2+ signalling in developing rat cerebellar Purkinje neurones. The Journal of physiology *536*, 429-437.
Ellis, P., Fagan, B.M., Magness, S.T., Hutton, S., Taranova, O., Hayashi, S., McMahon, A., Rao, M., and Pevny, L. (2004). SOX2, a persistent marker for multipotential neural stem cells derived from embryonic stem cells, the embryo or the adult. Developmental neuroscience *26*, 148-165.
Fagni, L., Worley, P.F., and Ango, F. (2002). Homer as both a scaffold and transduction molecule. Science's STKE : signal transduction knowledge environment *2002*, re8.
Fantana, A.L., Soucy, E.R., and Meister, M. (2008). Rat olfactory bulb mitral cells receive sparse glomerular inputs. Neuron *59*, 802-814.
Fauchereau, F., Herbrand, U., Chafey, P., Eberth, A., Koulakoff, A., Vinet, M.C., Ahmadian, M.R., Chelly, J., and Billuart, P. (2003). The RhoGAP activity of OPHN1, a new F-actin-binding protein,

is negatively controlled by its amino-terminal domain. Molecular and cellular neurosciences *23*, 574-586.
Fernando, R.N., Eleuteri, B., Abdelhady, S., Nussenzweig, A., Andang, M., and Ernfors, P. (2011). Cell cycle restriction by histone H2AX limits proliferation of adult neural stem cells. Proceedings of the National Academy of Sciences of the United States of America *108*, 5837-5842.
Fischer, M., Kaech, S., Knutti, D., and Matus, A. (1998). Rapid actin-based plasticity in dendritic spines. Neuron *20*, 847-854.
Fusi, S., Drew, P.J., and Abbott, L.F. (2005). Cascade models of synaptically stored memories. Neuron *45*, 599-611.
Gaiano, N., and Fishell, G. (2002). The role of notch in promoting glial and neural stem cell fates. Annual review of neuroscience *25*, 471-490.
Ganguly, K., Schinder, A.F., Wong, S.T., and Poo, M. (2001). GABA itself promotes the developmental switch of neuronal GABAergic responses from excitation to inhibition. Cell *105*, 521-532.
Gao, X.B., and van den Pol, A.N. (2001). GABA, not glutamate, a primary transmitter driving action potentials in developing hypothalamic neurons. Journal of neurophysiology *85*, 425-434.
Gao, Y., and Strowbridge, B.W. (2009). Long-term plasticity of excitatory inputs to granule cells in the rat olfactory bulb. Nature neuroscience *12*, 731-733.
Garcia-Gonzalez, D., Khodosevich, K., Watanabe, Y., Rollenhagen, A., Lubke, J.H.R., and Monyer, H. (2017). Serotonergic Projections Govern Postnatal Neuroblast Migration. Neuron *94*, 534-549 e539.
Garzotto, D., Giacobini, P., Crepaldi, T., Fasolo, A., and De Marchis, S. (2008). Hepatocyte growth factor regulates migration of olfactory interneuron precursors in the rostral migratory stream through Met-Grb2 coupling. The Journal of neuroscience : the official journal of the Society for Neuroscience *28*, 5901-5909.
Gillberg, C., and Billstedt, E. (2000). Autism and Asperger syndrome: coexistence with other clinical disorders. Acta psychiatrica Scandinavica *102*, 321-330.
Givogri, M.I., de Planell, M., Galbiati, F., Superchi, D., Gritti, A., Vescovi, A., de Vellis, J., and Bongarzone, E.R. (2006). Notch signaling in astrocytes and neuroblasts of the adult subventricular zone in health and after cortical injury. Developmental neuroscience *28*, 81-91.
Gomez, T.M., and Letourneau, P.C. (2014). Actin dynamics in growth cone motility and navigation. Journal of neurochemistry *129*, 221-234.
Gonzalez-Billault, C., Munoz-Llancao, P., Henriquez, D.R., Wojnacki, J., Conde, C., and Caceres, A. (2012). The role of small GTPases in neuronal morphogenesis and polarity. Cytoskeleton *69*, 464-485.
Govek, E.E., Hatten, M.E., and Van Aelst, L. (2011). The role of Rho GTPase proteins in CNS neuronal migration. Developmental neurobiology *71*, 528-553.
Govek, E.E., Newey, S.E., Akerman, C.J., Cross, J.R., Van der Veken, L., and Van Aelst, L. (2004). The X-linked mental retardation protein oligophrenin-1 is required for dendritic spine morphogenesis. Nature neuroscience *7*, 364-372.
Govek, E.E., Newey, S.E., and Van Aelst, L. (2005). The role of the Rho GTPases in neuronal development. Genes & development *19*, 1-49.
Grant, S., Qiao, L., and Dent, P. (2002). Roles of ERBB family receptor tyrosine kinases, and downstream signaling pathways, in the control of cell growth and survival. Frontiers in bioscience : a journal and virtual library *7*, d376-389.
Greer, C.A. (1987). Golgi analyses of dendritic organization among denervated olfactory bulb granule cells. The Journal of comparative neurology *257*, 442-452.
Gross, R.E., Mehler, M.F., Mabie, P.C., Zang, Z., Santschi, L., and Kessler, J.A. (1996). Bone morphogenetic proteins promote astroglial lineage commitment by mammalian subventricular zone progenitor cells. Neuron *17*, 595-606.
Hack, I., Bancila, M., Loulier, K., Carroll, P., and Cremer, H. (2002). Reelin is a detachment signal in tangential chain-migration during postnatal neurogenesis. Nature neuroscience *5*, 939-945.
Hall, A., and Lalli, G. (2010). Rho and Ras GTPases in axon growth, guidance, and branching. Cold Spring Harbor perspectives in biology *2*, a001818.
Harrison, P.J., and Owen, M.J. (2003). Genes for schizophrenia? Recent findings and their pathophysiological implications. Lancet *361*, 417-419.

He, Q., Nomura, T., Xu, J., and Contractor, A. (2014). The developmental switch in GABA polarity is delayed in fragile X mice. The Journal of neuroscience : the official journal of the Society for Neuroscience *34*, 446-450.
Hensch, T.K. (2004). Critical period regulation. Annual review of neuroscience *27*, 549-579.
Hikita, T., Ohno, A., Sawada, M., Ota, H., and Sawamoto, K. (2014). Rac1-mediated indentation of resting neurons promotes the chain migration of new neurons in the rostral migratory stream of post-natal mouse brain. Journal of neurochemistry *128*, 790-797.
Hofmann, C., Shepelev, M., and Chernoff, J. (2004). The genetics of Pak. Journal of cell science *117*, 4343-4354.
Hoglinger, G.U., Rizk, P., Muriel, M.P., Duyckaerts, C., Oertel, W.H., Caille, I., and Hirsch, E.C. (2004). Dopamine depletion impairs precursor cell proliferation in Parkinson disease. Nature neuroscience *7*, 726-735.
Holmberg, J., Armulik, A., Senti, K.A., Edoff, K., Spalding, K., Momma, S., Cassidy, R., Flanagan, J.G., and Frisen, J. (2005). Ephrin-A2 reverse signaling negatively regulates neural progenitor proliferation and neurogenesis. Genes & development *19*, 462-471.
Humeau, Y., Gambino, F., Chelly, J., and Vitale, N. (2009). X-linked mental retardation: focus on synaptic function and plasticity. Journal of neurochemistry *109*, 1-14.
Huttenlocher, P.R. (1974). Dendritic development in neocortex of children with mental defect and infantile spasms. Neurology *24*, 203-210.
Ihrie, R.A., Shah, J.K., Harwell, C.C., Levine, J.H., Guinto, C.D., Lezameta, M., Kriegstein, A.R., and Alvarez-Buylla, A. (2011). Persistent sonic hedgehog signaling in adult brain determines neural stem cell positional identity. Neuron *71*, 250-262.
Ikeda, M., Hirota, Y., Sakaguchi, M., Yamada, O., Kida, Y.S., Ogura, T., Otsuka, T., Okano, H., and Sawamoto, K. (2010). Expression and proliferation-promoting role of Diversin in the neuronally committed precursor cells migrating in the adult mouse brain. Stem cells *28*, 2017-2026.
Ille, F., and Sommer, L. (2005). Wnt signaling: multiple functions in neural development. Cellular and molecular life sciences : CMLS *62*, 1100-1108.
Imamura, F., Nagao, H., Naritsuka, H., Murata, Y., Taniguchi, H., and Mori, K. (2006). A leucine-rich repeat membrane protein, 5T4, is expressed by a subtype of granule cells with dendritic arbors in specific strata of the mouse olfactory bulb. The Journal of comparative neurology *495*, 754-768.
Inta, D., Alfonso, J., von Engelhardt, J., Kreuzberg, M.M., Meyer, A.H., van Hooft, J.A., and Monyer, H. (2008). Neurogenesis and widespread forebrain migration of distinct GABAergic neurons from the postnatal subventricular zone. Proceedings of the National Academy of Sciences of the United States of America *105*, 20994-20999.
Isaacson, J.S., and Strowbridge, B.W. (1998). Olfactory reciprocal synapses: dendritic signaling in the CNS. Neuron *20*, 749-761.
Iwase, S., Berube, N.G., Zhou, Z., Kasri, N.N., Battaglioli, E., Scandaglia, M., and Barco, A. (2017). Epigenetic Etiology of Intellectual Disability. The Journal of neuroscience : the official journal of the Society for Neuroscience *37*, 10773-10782.
Jin, K., Peel, A.L., Mao, X.O., Xie, L., Cottrell, B.A., Henshall, D.C., and Greenberg, D.A. (2004). Increased hippocampal neurogenesis in Alzheimer's disease. Proceedings of the National Academy of Sciences of the United States of America *101*, 343-347.
Jin, K., Zhu, Y., Sun, Y., Mao, X.O., Xie, L., and Greenberg, D.A. (2002). Vascular endothelial growth factor (VEGF) stimulates neurogenesis in vitro and in vivo. Proceedings of the National Academy of Sciences of the United States of America *99*, 11946-11950.
Kaneko, N., Marin, O., Koike, M., Hirota, Y., Uchiyama, Y., Wu, J.Y., Lu, Q., Tessier-Lavigne, M., Alvarez-Buylla, A., Okano, H*., et al.* (2010). New neurons clear the path of astrocytic processes for their rapid migration in the adult brain. Neuron *67*, 213-223.
Kaneko, N., Sawada, M., and Sawamoto, K. (2017). Mechanisms of neuronal migration in the adult brain. Journal of neurochemistry *141*, 835-847.
Kaneko, N., and Sawamoto, K. (2009). Adult neurogenesis and its alteration under pathological conditions. Neuroscience research *63*, 155-164.
Katoh, M., and Katoh, M. (2006). Notch ligand, JAG1, is evolutionarily conserved target of canonical WNT signaling pathway in progenitor cells. International journal of molecular medicine *17*, 681-685.
Kay, L.M. (2014). Circuit oscillations in odor perception and memory. Progress in brain research *208*, 223-251.

Kay, L.M., Beshel, J., Brea, J., Martin, C., Rojas-Libano, D., and Kopell, N. (2009). Olfactory oscillations: the what, how and what for. Trends in neurosciences *32*, 207-214.
Kelsch, W., Lin, C.W., and Lois, C. (2008). Sequential development of synapses in dendritic domains during adult neurogenesis. Proceedings of the National Academy of Sciences of the United States of America *105*, 16803-16808.
Kelsch, W., Lin, C.W., Mosley, C.P., and Lois, C. (2009). A critical period for activity-dependent synaptic development during olfactory bulb adult neurogenesis. The Journal of neuroscience : the official journal of the Society for Neuroscience *29*, 11852-11858.
Kelsch, W., Mosley, C.P., Lin, C.W., and Lois, C. (2007). Distinct mammalian precursors are committed to generate neurons with defined dendritic projection patterns. PLoS biology *5*, e300.
Kelsch, W., Sim, S., and Lois, C. (2010). Watching synaptogenesis in the adult brain. Annual review of neuroscience *33*, 131-149.
Khelfaoui, M., Denis, C., van Galen, E., de Bock, F., Schmitt, A., Houbron, C., Morice, E., Giros, B., Ramakers, G., Fagni, L.*, et al.* (2007). Loss of X-linked mental retardation gene oligophrenin1 in mice impairs spatial memory and leads to ventricular enlargement and dendritic spine immaturity. The Journal of neuroscience : the official journal of the Society for Neuroscience *27*, 9439-9450.
Khelfaoui, M., Pavlowsky, A., Powell, A.D., Valnegri, P., Cheong, K.W., Blandin, Y., Passafaro, M., Jefferys, J.G., Chelly, J., and Billuart, P. (2009). Inhibition of RhoA pathway rescues the endocytosis defects in Oligophrenin1 mouse model of mental retardation. Human molecular genetics *18*, 2575-2583.
Khodosevich, K., Seeburg, P.H., and Monyer, H. (2009). Major signaling pathways in migrating neuroblasts. Frontiers in molecular neuroscience *2*, 7.
Kim, Y., Wang, W.Z., Comte, I., Pastrana, E., Tran, P.B., Brown, J., Miller, R.J., Doetsch, F., Molnar, Z., and Szele, F.G. (2010). Dopamine stimulation of postnatal murine subventricular zone neurogenesis via the D3 receptor. Journal of neurochemistry *114*, 750-760.
Kirmse, K., Kummer, M., Kovalchuk, Y., Witte, O.W., Garaschuk, O., and Holthoff, K. (2015). GABA depolarizes immature neurons and inhibits network activity in the neonatal neocortex in vivo. Nature communications 6:7750.
Kohwi, M., Osumi, N., Rubenstein, J.L., and Alvarez-Buylla, A. (2005). Pax6 is required for making specific subpopulations of granule and periglomerular neurons in the olfactory bulb. The Journal of neuroscience : the official journal of the Society for Neuroscience *25*, 6997-7003.
Koizumi, H., Higginbotham, H., Poon, T., Tanaka, T., Brinkman, B.C., and Gleeson, J.G. (2006). Doublecortin maintains bipolar shape and nuclear translocation during migration in the adult forebrain. Nature neuroscience *9*, 779-786.
Komuro, H., and Rakic, P. (1998). Orchestration of neuronal migration by activity of ion channels, neurotransmitter receptors, and intracellular Ca2+ fluctuations. Journal of neurobiology *37*, 110-130.
Kozma, R., Sarner, S., Ahmed, S., and Lim, L. (1997). Rho family GTPases and neuronal growth cone remodelling: relationship between increased complexity induced by Cdc42Hs, Rac1, and acetylcholine and collapse induced by RhoA and lysophosphatidic acid. Molecular and cellular biology *17*, 1201-1211.
Kramer, J.M., and van Bokhoven, H. (2009). Genetic and epigenetic defects in mental retardation. The international journal of biochemistry & cell biology *41*, 96-107.
Kutsche, K., Yntema, H., Brandt, A., Jantke, I., Nothwang, H.G., Orth, U., Boavida, M.G., David, D., Chelly, J., Fryns, J.P.*, et al.* (2000). Mutations in ARHGEF6, encoding a guanine nucleotide exchange factor for Rho GTPases, in patients with X-linked mental retardation. Nature genetics *26*, 247-250.
Lagier, S., Carleton, A., and Lledo, P.M. (2004). Interplay between local GABAergic interneurons and relay neurons generates gamma oscillations in the rat olfactory bulb. The Journal of neuroscience : the official journal of the Society for Neuroscience *24*, 4382-4392.
Lagier, S., Panzanelli, P., Russo, R.E., Nissant, A., Bathellier, B., Sassoe-Pognetto, M., Fritschy, J.M., and Lledo, P.M. (2007). GABAergic inhibition at dendrodendritic synapses tunes gamma oscillations in the olfactory bulb. Proceedings of the National Academy of Sciences of the United States of America *104*, 7259-7264.
Lazarini, F., and Lledo, P.M. (2011). Is adult neurogenesis essential for olfaction? Trends in neurosciences *34*, 20-30.
Lazarini, F., Mouthon, M.A., Gheusi, G., de Chaumont, F., Olivo-Marin, J.C., Lamarque, S., Abrous, D.N., Boussin, F.D., and Lledo, P.M. (2009). Cellular and behavioral effects of cranial irradiation of the subventricular zone in adult mice. PloS one *4*, e7017.

Lazarov, O., and Marr, R.A. (2010). Neurogenesis and Alzheimer's disease: at the crossroads. Experimental neurology *223*, 267-281.
Lazic, S.E., Grote, H.E., Blakemore, C., Hannan, A.J., van Dellen, A., Phillips, W., and Barker, R.A. (2006). Neurogenesis in the R6/1 transgenic mouse model of Huntington's disease: effects of environmental enrichment. The European journal of neuroscience *23*, 1829-1838.
Le Magueresse, C., and Monyer, H. (2013). GABAergic interneurons shape the functional maturation of the cortex. Neuron *77*, 388-405.
Lehtinen, M.K., Zappaterra, M.W., Chen, X., Yang, Y.J., Hill, A.D., Lun, M., Maynard, T., Gonzalez, D., Kim, S., Ye, P.*, et al.* (2011). The cerebrospinal fluid provides a proliferative niche for neural progenitor cells. Neuron *69*, 893-905.
Lemasson, M., Saghatelyan, A., Olivo-Marin, J.C., and Lledo, P.M. (2005). Neonatal and adult neurogenesis provide two distinct populations of newborn neurons to the mouse olfactory bulb. The Journal of neuroscience : the official journal of the Society for Neuroscience *25*, 6816-6825.
Leong, S.Y., and Turnley, A.M. (2011). Regulation of adult neural precursor cell migration. Neurochemistry international *59*, 382-393.
Lepousez, G., and Lledo, P.M. (2013). Odor discrimination requires proper olfactory fast oscillations in awake mice. Neuron *80*, 1010-1024.
Lepousez, G., Valley, M.T., and Lledo, P.M. (2013). The impact of adult neurogenesis on olfactory bulb circuits and computations. Annual review of physiology *75*, 339-363.
Leventhal, C., Rafii, S., Rafii, D., Shahar, A., and Goldman, S.A. (1999). Endothelial trophic support of neuronal production and recruitment from the adult mammalian subependyma. Molecular and cellular neurosciences *13*, 450-464.
Lewis, D.A., Curley, A.A., Glausier, J.R., and Volk, D.W. (2012). Cortical parvalbumin interneurons and cognitive dysfunction in schizophrenia. Trends in neurosciences *35*, 57-67.
Li, Y.R., and Matsunami, H. (2011). Activation state of the M3 muscarinic acetylcholine receptor modulates mammalian odorant receptor signaling. Science signaling *4*, ra1.
Lim, D.A., and Alvarez-Buylla, A. (2016). The Adult Ventricular-Subventricular Zone (V-SVZ) and Olfactory Bulb (OB) Neurogenesis. Cold Spring Harbor perspectives in biology *8*.
Lim, D.A., Tramontin, A.D., Trevejo, J.M., Herrera, D.G., Garcia-Verdugo, J.M., and Alvarez-Buylla, A. (2000). Noggin antagonizes BMP signaling to create a niche for adult neurogenesis. Neuron *28*, 713-726.
Liu, J., Solway, K., Messing, R.O., and Sharp, F.R. (1998). Increased neurogenesis in the dentate gyrus after transient global ischemia in gerbils. The Journal of neuroscience : the official journal of the Society for Neuroscience *18*, 7768-7778.
Lledo, P.M., Alonso, M., and Grubb, M.S. (2006). Adult neurogenesis and functional plasticity in neuronal circuits. Nature reviews Neuroscience *7*, 179-193.
Lledo, P.M., Merkle, F.T., and Alvarez-Buylla, A. (2008). Origin and function of olfactory bulb interneuron diversity. Trends in neurosciences *31*, 392-400.
Lledo, P.M., and Saghatelyan, A. (2005). Integrating new neurons into the adult olfactory bulb: joining the network, life-death decisions, and the effects of sensory experience. Trends in neurosciences *28*, 248-254.
Lodovichi, C., Belluscio, L., and Katz, L.C. (2003). Functional topography of connections linking mirror-symmetric maps in the mouse olfactory bulb. Neuron *38*, 265-276.
Lois, C., Garcia-Verdugo, J.M., and Alvarez-Buylla, A. (1996). Chain migration of neuronal precursors. Science *271*, 978-981.
LoTurco, J.J., Owens, D.F., Heath, M.J., Davis, M.B., and Kriegstein, A.R. (1995). GABA and glutamate depolarize cortical progenitor cells and inhibit DNA synthesis. Neuron *15*, 1287-1298.
Lowe, G. (2002). Inhibition of backpropagating action potentials in mitral cell secondary dendrites. Journal of neurophysiology *88*, 64-85.
Luckasson, R., and Reeve, A. (2001). Naming, defining, and classifying in mental retardation. Mental retardation *39*, 47-52.
Luo, L. (2000). Rho GTPases in neuronal morphogenesis. Nature reviews Neuroscience *1*, 173-180.
Luo, L., Jan, L.Y., and Jan, Y.N. (1997). Rho family GTP-binding proteins in growth cone signalling. Current opinion in neurobiology *7*, 81-86.
Luo, M., and Katz, L.C. (2001). Response correlation maps of neurons in the mammalian olfactory bulb. Neuron *32*, 1165-1179.
Ma, Q.L., Yang, F., Frautschy, S.A., and Cole, G.M. (2012). PAK in Alzheimer disease, Huntington disease and X-linked mental retardation. Cellular logistics *2*, 117-125.

Machacek, M., Hodgson, L., Welch, C., Elliott, H., Pertz, O., Nalbant, P., Abell, A., Johnson, G.L., Hahn, K.M., and Danuser, G. (2009). Coordination of Rho GTPase activities during cell protrusion. Nature *461*, 99-103.
Maher, B.J., and Westbrook, G.L. (2008). Co-transmission of dopamine and GABA in periglomerular cells. Journal of neurophysiology *99*, 1559-1564.
Mandairon, N., Sultan, S., Nouvian, M., Sacquet, J., and Didier, A. (2011). Involvement of newborn neurons in olfactory associative learning? The operant or non-operant component of the task makes all the difference. The Journal of neuroscience : the official journal of the Society for Neuroscience *31*, 12455-12460.
Manent, J.B., Demarque, M., Jorquera, I., Pellegrino, C., Ben-Ari, Y., Aniksztejn, L., and Represa, A. (2005). A noncanonical release of GABA and glutamate modulates neuronal migration. The Journal of neuroscience : the official journal of the Society for Neuroscience *25*, 4755-4765.
Maric, D., Liu, Q.Y., Maric, I., Chaudry, S., Chang, Y.H., Smith, S.V., Sieghart, W., Fritschy, J.M., and Barker, J.L. (2001). GABA expression dominates neuronal lineage progression in the embryonic rat neocortex and facilitates neurite outgrowth via GABA(A) autoreceptor/Cl- channels. The Journal of neuroscience : the official journal of the Society for Neuroscience *21*, 2343-2360.
Marin, O. (2012). Interneuron dysfunction in psychiatric disorders. Nature reviews Neuroscience *13*, 107-120.
Markopoulos, F., Rokni, D., Gire, D.H., and Murthy, V.N. (2012). Functional properties of cortical feedback projections to the olfactory bulb. Neuron *76*, 1175-1188.
Marlatt, M.W., and Lucassen, P.J. (2010). Neurogenesis and Alzheimer's disease: Biology and pathophysiology in mice and men. Current Alzheimer research *7*, 113-125.
Martinez-Cue, C., Martinez, P., Rueda, N., Vidal, R., Garcia, S., Vidal, V., Corrales, A., Montero, J.A., Pazos, A., Florez, J.*, et al.* (2013). Reducing GABAA alpha5 receptor-mediated inhibition rescues functional and neuromorphological deficits in a mouse model of down syndrome. The Journal of neuroscience : the official journal of the Society for Neuroscience *33*, 3953-3966.
Martini, F.J., Valiente, M., Lopez Bendito, G., Szabo, G., Moya, F., Valdeolmillos, M., and Marin, O. (2009). Biased selection of leading process branches mediates chemotaxis during tangential neuronal migration. Development *136*, 41-50.
Martinowich, K., Hattori, D., Wu, H., Fouse, S., He, F., Hu, Y., Fan, G., and Sun, Y.E. (2003). DNA methylation-related chromatin remodeling in activity-dependent BDNF gene regulation. Science *302*, 890-893.
Marx, A., Godinez, W.J., Tsimashchuk, V., Bankhead, P., Rohr, K., and Engel, U. (2013). Xenopus cytoplasmic linker-associated protein 1 (XCLASP1) promotes axon elongation and advance of pioneer microtubules. Molecular biology of the cell *24*, 1544-1558.
Marxreiter, F., Regensburger, M., and Winkler, J. (2013). Adult neurogenesis in Parkinson's disease. Cellular and molecular life sciences : CMLS *70*, 459-473.
Matozaki, T., Nakanishi, H., and Takai, Y. (2000). Small G-protein networks: their crosstalk and signal cascades. Cellular signalling *12*, 515-524.
Mejia-Gervacio, S., Murray, K., and Lledo, P.M. (2011). NKCC1 controls GABAergic signaling and neuroblast migration in the postnatal forebrain. Neural development *6*, 4.
Menn, B., Garcia-Verdugo, J.M., Yaschine, C., Gonzalez-Perez, O., Rowitch, D., and Alvarez-Buylla, A. (2006). Origin of oligodendrocytes in the subventricular zone of the adult brain. The Journal of neuroscience : the official journal of the Society for Neuroscience *26*, 7907-7918.
Meziane, H., Khelfaoui, M., Morello, N., Hiba, B., Calcagno, E., Reibel-Foisset, S., Selloum, M., Chelly, J., Humeau, Y., Riet, F.*, et al.* (2016). Fasudil treatment in adult reverses behavioural changes and brain ventricular enlargement in Oligophrenin-1 mouse model of intellectual disability. Human molecular genetics *25*, 2314-2323.
Mirzadeh, Z., Merkle, F.T., Soriano-Navarro, M., Garcia-Verdugo, J.M., and Alvarez-Buylla, A. (2008). Neural stem cells confer unique pinwheel architecture to the ventricular surface in neurogenic regions of the adult brain. Cell stem cell *3*, 265-278.
Montani, C., Ramos-Brossier, M., Ponzoni, L., Gritti, L., Cwetsch, A.W., Braida, D., Saillour, Y., Terragni, B., Mantegazza, M., Sala, M.*, et al.* (2017). The X-Linked Intellectual Disability Protein IL1RAPL1 Regulates Dendrite Complexity. The Journal of neuroscience : the official journal of the Society for Neuroscience *37*, 6606-6627.
Moreno-Lopez, B., Romero-Grimaldi, C., Noval, J.A., Murillo-Carretero, M., Matarredona, E.R., and Estrada, C. (2004). Nitric oxide is a physiological inhibitor of neurogenesis in the adult mouse

subventricular zone and olfactory bulb. The Journal of neuroscience : the official journal of the Society for Neuroscience *24*, 85-95.
Mori, K., Kishi, K., and Ojima, H. (1983). Distribution of dendrites of mitral, displaced mitral, tufted, and granule cells in the rabbit olfactory bulb. The Journal of comparative neurology *219*, 339-355.
Mori, K., and Sakano, H. (2011). How is the olfactory map formed and interpreted in the mammalian brain? Annual review of neuroscience *34*, 467-499.
Mori, K., and Shepherd, G.M. (1994). Emerging principles of molecular signal processing by mitral/tufted cells in the olfactory bulb. Seminars in cell biology *5*, 65-74.
Murase, S., and Horwitz, A.F. (2002). Deleted in colorectal carcinoma and differentially expressed integrins mediate the directional migration of neural precursors in the rostral migratory stream. The Journal of neuroscience : the official journal of the Society for Neuroscience *22*, 3568-3579.
Nadif Kasri, N., Nakano-Kobayashi, A., Malinow, R., Li, B., and Van Aelst, L. (2009). The Rho-linked mental retardation protein oligophrenin-1 controls synapse maturation and plasticity by stabilizing AMPA receptors. Genes & development *23*, 1289-1302.
Nadif Kasri, N., Nakano-Kobayashi, A., and Van Aelst, L. (2011). Rapid synthesis of the X-linked mental retardation protein OPHN1 mediates mGluR-dependent LTD through interaction with the endocytic machinery. Neuron *72*, 300-315.
Nakano-Kobayashi, A., Kasri, N.N., Newey, S.E., and Van Aelst, L. (2009). The Rho-linked mental retardation protein OPHN1 controls synaptic vesicle endocytosis via endophilin A1. Current biology : CB *19*, 1133-1139.
Narumiya, S., Tanji, M., and Ishizaki, T. (2009). Rho signaling, ROCK and mDia1, in transformation, metastasis and invasion. Cancer metastasis reviews *28*, 65-76.
Newell-Litwa, K.A., Badoual, M., Asmussen, H., Patel, H., Whitmore, L., and Horwitz, A.R. (2015). ROCK1 and 2 differentially regulate actomyosin organization to drive cell and synaptic polarity. The Journal of cell biology *210*, 225-242.
Newey, S.E., Velamoor, V., Govek, E.E., and Van Aelst, L. (2005). Rho GTPases, dendritic structure, and mental retardation. Journal of neurobiology *64*, 58-74.
Ng, K.L., Li, J.D., Cheng, M.Y., Leslie, F.M., Lee, A.G., and Zhou, Q.Y. (2005). Dependence of olfactory bulb neurogenesis on prokineticin 2 signaling. Science *308*, 1923-1927.
Nguyen, L., Malgrange, B., Breuskin, I., Bettendorff, L., Moonen, G., Belachew, S., and Rigo, J.M. (2003). Autocrine/paracrine activation of the GABA(A) receptor inhibits the proliferation of neurogenic polysialylated neural cell adhesion molecule-positive (PSA-NCAM+) precursor cells from postnatal striatum. The Journal of neuroscience : the official journal of the Society for Neuroscience *23*, 3278-3294.
Node-Langlois, R., Muller, D., and Boda, B. (2006). Sequential implication of the mental retardation proteins ARHGEF6 and PAK3 in spine morphogenesis. Journal of cell science *119*, 4986-4993.
O'Keeffe, G.C., Tyers, P., Aarsland, D., Dalley, J.W., Barker, R.A., and Caldwell, M.A. (2009). Dopamine-induced proliferation of adult neural precursor cells in the mammalian subventricular zone is mediated through EGF. Proceedings of the National Academy of Sciences of the United States of America *106*, 8754-8759.
Obrietan, K., and van den Pol, A.N. (1999). GABAB receptor-mediated regulation of glutamate-activated calcium transients in hypothalamic and cortical neuron development. Journal of neurophysiology *82*, 94-102.
Ojima, H., Mori, K., and Kishi, K. (1984). The trajectory of mitral cell axons in the rabbit olfactory cortex revealed by intracellular HRP injection. The Journal of comparative neurology *230*, 77-87.
Ortega, F.J., Vukovic, J., Rodriguez, M.J., and Bartlett, P.F. (2014). Blockade of microglial KATP -channel abrogates suppression of inflammatory-mediated inhibition of neural precursor cells. Glia *62*, 247-258.
Ota, H., Hikita, T., Sawada, M., Nishioka, T., Matsumoto, M., Komura, M., Ohno, A., Kamiya, Y., Miyamoto, T., Asai, N.*, et al.* (2014). Speed control for neuronal migration in the postnatal brain by Gmip-mediated local inactivation of RhoA. Nature communications *5*, 4532.
Ozdinler, P.H., and Erzurumlu, R.S. (2001). Regulation of neurotrophin-induced axonal responses via Rho GTPases. The Journal of comparative neurology *438*, 377-387.
Paez-Gonzalez, P., Asrican, B., Rodriguez, E., and Kuo, C.T. (2014). Identification of distinct ChAT(+) neurons and activity-dependent control of postnatal SVZ neurogenesis. Nature neuroscience *17*, 934-942.

Pappas, G.D., Kriho, V., Liu, W.S., Tremolizzo, L., Lugli, G., and Larson, J. (2003). Immunocytochemical localization of reelin in the olfactory bulb of the heterozygous reeler mouse: an animal model for schizophrenia. Neurological research *25*, 819-830.
Paredes, M.F., James, D., Gil-Perotin, S., Kim, H., Cotter, J.A., Ng, C., Sandoval, K., Rowitch, D.H., Xu, D., McQuillen, P.S.*, et al.* (2016). Extensive migration of young neurons into the infant human frontal lobe. Science *354*.
Parras, C.M., Galli, R., Britz, O., Soares, S., Galichet, C., Battiste, J., Johnson, J.E., Nakafuku, M., Vescovi, A., and Guillemot, F. (2004). Mash1 specifies neurons and oligodendrocytes in the postnatal brain. The EMBO journal *23*, 4495-4505.
Petreanu, L., and Alvarez-Buylla, A. (2002). Maturation and death of adult-born olfactory bulb granule neurons: role of olfaction. The Journal of neuroscience : the official journal of the Society for Neuroscience *22*, 6106-6113.
Platel, J.C., Dave, K.A., Gordon, V., Lacar, B., Rubio, M.E., and Bordey, A. (2010). NMDA receptors activated by subventricular zone astrocytic glutamate are critical for neuroblast survival prior to entering a synaptic network. Neuron *65*, 859-872.
Ponti, G., Obernier, K., and Alvarez-Buylla, A. (2013). Lineage progression from stem cells to new neurons in the adult brain ventricular-subventricular zone. Cell cycle *12*, 1649-1650.
Pressler, R.T., and Strowbridge, B.W. (2006). Blanes cells mediate persistent feedforward inhibition onto granule cells in the olfactory bulb. Neuron *49*, 889-904.
Purpura, D.P. (1974). Dendritic spine "dysgenesis" and mental retardation. Science *186*, 1126-1128.
Ramakers, G.J. (2002). Rho proteins, mental retardation and the cellular basis of cognition. Trends in neurosciences *25*, 191-199.
Redolfi, N., Galla, L., Maset, A., Murru, L., Savoia, E., Zamparo, I., Gritti, A., Billuart, P., Passafaro, M., and Lodovichi, C. (2016). Oligophrenin-1 regulates number, morphology and synaptic properties of adult-born inhibitory interneurons in the olfactory bulb. Human molecular genetics *25*, 5198-5211.
Ribak, C.E., Vaughn, J.E., Saito, K., Barber, R., and Roberts, E. (1977). Glutamate decarboxylase localization in neurons of the olfactory bulb. Brain research *126*, 1-18.
Rico, B., Beggs, H.E., Schahin-Reed, D., Kimes, N., Schmidt, A., and Reichardt, L.F. (2004). Control of axonal branching and synapse formation by focal adhesion kinase. Nature neuroscience *7*, 1059-1069.
Rochefort, C., Gheusi, G., Vincent, J.D., and Lledo, P.M. (2002). Enriched odor exposure increases the number of newborn neurons in the adult olfactory bulb and improves odor memory. The Journal of neuroscience : the official journal of the Society for Neuroscience *22*, 2679-2689.
Saghatelyan, A., de Chevigny, A., Schachner, M., and Lledo, P.M. (2004). Tenascin-R mediates activity-dependent recruitment of neuroblasts in the adult mouse forebrain. Nature neuroscience *7*, 347-356.
Sailor, K.A., Schinder, A.F., and Lledo, P.M. (2017). Adult neurogenesis beyond the niche: its potential for driving brain plasticity. Current opinion in neurobiology *42*, 111-117.
San Martin, A., and Pagani, M.R. (2014). Understanding intellectual disability through RASopathies. Journal of physiology, Paris *108*, 232-239.
Sanai, N., Nguyen, T., Ihrie, R.A., Mirzadeh, Z., Tsai, H.H., Wong, M., Gupta, N., Berger, M.S., Huang, E., Garcia-Verdugo, J.M.*, et al.* (2011). Corridors of migrating neurons in the human brain and their decline during infancy. Nature *478*, 382-386.
Sanai, N., Tramontin, A.D., Quinones-Hinojosa, A., Barbaro, N.M., Gupta, N., Kunwar, S., Lawton, M.T., McDermott, M.W., Parsa, A.T., Manuel-Garcia Verdugo, J.*, et al.* (2004). Unique astrocyte ribbon in adult human brain contains neural stem cells but lacks chain migration. Nature *427*, 740-744.
Sarowar, T., Grabrucker, S., Fohr, K., Mangus, K., Eckert, M., Bockmann, J., Boeckers, T.M., and Grabrucker, A.M. (2016). Enlarged dendritic spines and pronounced neophobia in mice lacking the PSD protein RICH2. Molecular brain *9*, 28.
Sawada, M., Ohno, N., Kawaguchi, M., Huang, S.H., Hikita, T., Sakurai, Y., Bang Nguyen, H., Quynh Thai, T., Ishido, Y., Yoshida, Y.*, et al.* (2018). PlexinD1 signaling controls morphological changes and migration termination in newborn neurons. The EMBO journal *37*.
Sawamoto, K., Wichterle, H., Gonzalez-Perez, O., Cholfin, J.A., Yamada, M., Spassky, N., Murcia, N.S., Garcia-Verdugo, J.M., Marin, O., Rubenstein, J.L.*, et al.* (2006). New neurons follow the flow of cerebrospinal fluid in the adult brain. Science *311*, 629-632.

Schaar, B.T., and McConnell, S.K. (2005). Cytoskeletal coordination during neuronal migration. Proceedings of the National Academy of Sciences of the United States of America *102*, 13652-13657.
Schoppa, N.E., Kinzie, J.M., Sahara, Y., Segerson, T.P., and Westbrook, G.L. (1998). Dendrodendritic inhibition in the olfactory bulb is driven by NMDA receptors. The Journal of neuroscience : the official journal of the Society for Neuroscience *18*, 6790-6802.
Shamah, S.M., Lin, M.Z., Goldberg, J.L., Estrach, S., Sahin, M., Hu, L., Bazalakova, M., Neve, R.L., Corfas, G., Debant, A.*, et al.* (2001). EphA receptors regulate growth cone dynamics through the novel guanine nucleotide exchange factor ephexin. Cell *105*, 233-244.
Shepherd, G.M., Chen, W.R., Willhite, D., Migliore, M., and Greer, C.A. (2007). The olfactory granule cell: from classical enigma to central role in olfactory processing. Brain research reviews *55*, 373-382.
Shimozaki, K., Zhang, C.L., Suh, H., Denli, A.M., Evans, R.M., and Gage, F.H. (2012). SRY-box-containing gene 2 regulation of nuclear receptor tailless (Tlx) transcription in adult neural stem cells. The Journal of biological chemistry *287*, 5969-5978.
Shinohara, R., Thumkeo, D., Kamijo, H., Kaneko, N., Sawamoto, K., Watanabe, K., Takebayashi, H., Kiyonari, H., Ishizaki, T., Furuyashiki, T.*, et al.* (2012). A role for mDia, a Rho-regulated actin nucleator, in tangential migration of interneuron precursors. Nature neuroscience *15*, 373-380, S371-372.
Shipley, M.T., and Ennis, M. (1996). Functional organization of olfactory system. Journal of neurobiology *30*, 123-176.
Smail, S., Bahga, D., McDole, B., and Guthrie, K. (2016). Increased Olfactory Bulb BDNF Expression Does Not Rescue Deficits in Olfactory Neurogenesis in the Huntington's Disease R6/2 Mouse. Chemical senses *41*, 221-232.
Snapyan, M., Lemasson, M., Brill, M.S., Blais, M., Massouh, M., Ninkovic, J., Gravel, C., Berthod, F., Gotz, M., Barker, P.A.*, et al.* (2009). Vasculature guides migrating neuronal precursors in the adult mammalian forebrain via brain-derived neurotrophic factor signaling. The Journal of neuroscience : the official journal of the Society for Neuroscience *29*, 4172-4188.
Spiering, D., and Hodgson, L. (2011). Dynamics of the Rho-family small GTPases in actin regulation and motility. Cell adhesion & migration *5*, 170-180.
Stevenson, R.E., Abidi, F., Schwartz, C.E., Lubs, H.A., and Holmes, L.B. (2000). Holmes-Gang syndrome is allelic with XLMR-hypotonic face syndrome. American journal of medical genetics *94*, 383-385.
Stevenson, R.E., Holden, K.R., Rogers, R.C., and Schwartz, C.E. (2012). Seizures and X-linked intellectual disability. European journal of medical genetics *55*, 307-312.
Tan, J., Savigner, A., Ma, M., and Luo, M. (2010). Odor information processing by the olfactory bulb analyzed in gene-targeted mice. Neuron *65*, 912-926.
Tanaka, E., and Sabry, J. (1995). Making the connection: cytoskeletal rearrangements during growth cone guidance. Cell *83*, 171-176.
Tavazoie, M., Van der Veken, L., Silva-Vargas, V., Louissaint, M., Colonna, L., Zaidi, B., Garcia-Verdugo, J.M., and Doetsch, F. (2008). A specialized vascular niche for adult neural stem cells. Cell stem cell *3*, 279-288.
Tivodar, S., Kalemaki, K., Kounoupa, Z., Vidaki, M., Theodorakis, K., Denaxa, M., Kessaris, N., de Curtis, I., Pachnis, V., and Karagogeos, D. (2015). Rac-GTPases Regulate Microtubule Stability and Axon Growth of Cortical GABAergic Interneurons. Cerebral cortex *25*, 2370-2382.
Tolias, K.F., Duman, J.G., and Um, K. (2011). Control of synapse development and plasticity by Rho GTPase regulatory proteins. Progress in neurobiology *94*, 133-148.
Tong, C.K., Chen, J., Cebrian-Silla, A., Mirzadeh, Z., Obernier, K., Guinto, C.D., Tecott, L.H., Garcia-Verdugo, J.M., Kriegstein, A., and Alvarez-Buylla, A. (2014). Axonal control of the adult neural stem cell niche. Cell stem cell *14*, 500-511.
Tsai, J.W., Bremner, K.H., and Vallee, R.B. (2007). Dual subcellular roles for LIS1 and dynein in radial neuronal migration in live brain tissue. Nature neuroscience *10*, 970-979.
Turner, K.L., and Sontheimer, H. (2014). KCa3.1 modulates neuroblast migration along the rostral migratory stream (RMS) in vivo. Cerebral cortex *24*, 2388-2400.
Urban, N.N., and Castro, J.B. (2010). Functional polarity in neurons: what can we learn from studying an exception? Current opinion in neurobiology *20*, 538-542.

Vaghi, V., Pennucci, R., Talpo, F., Corbetta, S., Montinaro, V., Barone, C., Croci, L., Spaiardi, P., Consalez, G.G., Biella, G.*, et al.* (2014). Rac1 and rac3 GTPases control synergistically the development of cortical and hippocampal GABAergic interneurons. Cerebral cortex *24*, 1247-1258.
Valdez, C.M., Murphy, G.G., and Beg, A.A. (2016). The Rac-GAP alpha2-chimaerin regulates hippocampal dendrite and spine morphogenesis. Molecular and cellular neurosciences *75*, 14-26.
Valley, M.T., Mullen, T.R., Schultz, L.C., Sagdullaev, B.T., and Firestein, S. (2009). Ablation of mouse adult neurogenesis alters olfactory bulb structure and olfactory fear conditioning. Frontiers in neuroscience *3*, 51.
Vinay, L., and Clarac, F. (1999). Antidromic discharges of dorsal root afferents and inhibition of the lumbar monosynaptic reflex in the neonatal rat. Neuroscience *90*, 165-176.
Wachowiak, M., and Shipley, M.T. (2006). Coding and synaptic processing of sensory information in the glomerular layer of the olfactory bulb. Seminars in cell & developmental biology *17*, 411-423.
Wahl, S., Barth, H., Ciossek, T., Aktories, K., and Mueller, B.K. (2000). Ephrin-A5 induces collapse of growth cones by activating Rho and Rho kinase. The Journal of cell biology *149*, 263-270.
Wall, M.J., and Usowicz, M.M. (1997). Development of action potential-dependent and independent spontaneous GABAA receptor-mediated currents in granule cells of postnatal rat cerebellum. The European journal of neuroscience *9*, 533-548.
Wang, C., Liu, F., Liu, Y.Y., Zhao, C.H., You, Y., Wang, L., Zhang, J., Wei, B., Ma, T., Zhang, Q.*, et al.* (2011). Identification and characterization of neuroblasts in the subventricular zone and rostral migratory stream of the adult human brain. Cell research *21*, 1534-1550.
Wang, D.D., Krueger, D.D., and Bordey, A. (2003). GABA depolarizes neuronal progenitors of the postnatal subventricular zone via GABAA receptor activation. The Journal of physiology *550*, 785-800.
Whitman, M.C., and Greer, C.A. (2007). Synaptic integration of adult-generated olfactory bulb granule cells: basal axodendritic centrifugal input precedes apical dendrodendritic local circuits. The Journal of neuroscience : the official journal of the Society for Neuroscience *27*, 9951-9961.
Wilmshurst, J.M., and Ouvrier, R. (2011). Hereditary peripheral neuropathies of childhood: an overview for clinicians. Neuromuscular disorders : NMD *21*, 763-775.
Wilson, D.A., and Stevenson, R.J. (2003). Olfactory perceptual learning: the critical role of memory in odor discrimination. Neuroscience and biobehavioral reviews *27*, 307-328.
Winner, B., Cooper-Kuhn, C.M., Aigner, R., Winkler, J., and Kuhn, H.G. (2002). Long-term survival and cell death of newly generated neurons in the adult rat olfactory bulb. The European journal of neuroscience *16*, 1681-1689.
Winner, B., Kohl, Z., and Gage, F.H. (2011). Neurodegenerative disease and adult neurogenesis. The European journal of neuroscience *33*, 1139-1151.
Winner, B., and Winkler, J. (2015). Adult neurogenesis in neurodegenerative diseases. Cold Spring Harbor perspectives in biology *7*, a021287.
Wittmann, T., and Waterman-Storer, C.M. (2001). Cell motility: can Rho GTPases and microtubules point the way? Journal of cell science *114*, 3795-3803.
Wojnacki, J., Quassollo, G., Marzolo, M.P., and Caceres, A. (2014). Rho GTPases at the crossroad of signaling networks in mammals: impact of Rho-GTPases on microtubule organization and dynamics. Small GTPases *5*, e28430.
Wollman, L.B., Levine, R.B., and Fregosi, R.F. (2018). Developmental plasticity of GABAergic neurotransmission to brainstem motoneurons. The Journal of physiology.
Woo, S., and Gomez, T.M. (2006). Rac1 and RhoA promote neurite outgrowth through formation and stabilization of growth cone point contacts. The Journal of neuroscience : the official journal of the Society for Neuroscience *26*, 1418-1428.
Woolfrey, K.M., and Srivastava, D.P. (2016). Control of Dendritic Spine Morphological and Functional Plasticity by Small GTPases. Neural plasticity *2016*, 3025948.
Worth, D.C., Daly, C.N., Geraldo, S., Oozeer, F., and Gordon-Weeks, P.R. (2013). Drebrin contains a cryptic F-actin-bundling activity regulated by Cdk5 phosphorylation. The Journal of cell biology *202*, 793-806.
Xiao, B., Tu, J.C., and Worley, P.F. (2000). Homer: a link between neural activity and glutamate receptor function. Current opinion in neurobiology *10*, 370-374.
Xu, X., Miller, E.C., and Pozzo-Miller, L. (2014). Dendritic spine dysgenesis in Rett syndrome. Frontiers in neuroanatomy *8*, 97.

Yagita, Y., Sakurai, T., Tanaka, H., Kitagawa, K., Colman, D.R., and Shan, W. (2009). N-cadherin mediates interaction between precursor cells in the subventricular zone and regulates further differentiation. Journal of neuroscience research *87*, 3331-3342.
Yamaguchi, M., and Mori, K. (2005). Critical period for sensory experience-dependent survival of newly generated granule cells in the adult mouse olfactory bulb. Proceedings of the National Academy of Sciences of the United States of America *102*, 9697-9702.
Ye, J. (2000). Physiology and pharmacology of native glycine receptors in developing rat ventral tegmental area neurons. Brain research *862*, 74-82.
Yokoi, M., Mori, K., and Nakanishi, S. (1995). Refinement of odor molecule tuning by dendrodendritic synaptic inhibition in the olfactory bulb. Proceedings of the National Academy of Sciences of the United States of America *92*, 3371-3375.
Zamboni, V., Armentano, M., Saro, G., Ciraolo, E., Ghigo, A., Germena, G., Umbach, A., Valnegri, P., Passafaro, M., Carabelli, V.*, et al.* (2016). Disruption of ArhGAP15 results in hyperactive Rac1, affects the architecture and function of hippocampal inhibitory neurons and causes cognitive deficits. Scientific reports *6*, 34877.
Zamboni, V., Jones, R., Umbach, A., Ammoni, A., Passafaro, M., Hirsch, E., and Merlo, G.R. (2018). Rho GTPases in Intellectual Disability: From Genetics to Therapeutic Opportunities. International journal of molecular sciences *19*.
Zanni, G., Saillour, Y., Nagara, M., Billuart, P., Castelnau, L., Moraine, C., Faivre, L., Bertini, E., Durr, A., Guichet, A.*, et al.* (2005). Oligophrenin 1 mutations frequently cause X-linked mental retardation with cerebellar hypoplasia. Neurology *65*, 1364-1369.
Zheng, W., Nowakowski, R.S., and Vaccarino, F.M. (2004). Fibroblast growth factor 2 is required for maintaining the neural stem cell pool in the mouse brain subventricular zone. Developmental neuroscience *26*, 181-196.
Zigova, T., Pencea, V., Wiegand, S.J., and Luskin, M.B. (1998). Intraventricular administration of BDNF increases the number of newly generated neurons in the adult olfactory bulb. Molecular and cellular neurosciences *11*, 234-245.